Escola de Camins
Escola Tècnica Superior d'Enginyeria de Camins, Canals i Ports
UPC BARCELONATECH

TREBALL FINAL DE MÀSTER

Assessing the impact of local emission abatement measures on ozone levels in Catalonia

Treball realitzat per:
Paula Camps Pla

Dirigit per:
Marc Guevara Vilardell
María Gonçalves Ageitos

Màster en:
Enginyeria Ambiental

Barcelona, 26 de setembre de 2023

Departament d'Enginyeria de Projectes i de la Construcció

Acknowledgements

I would like to acknowledge Marc Guevara and María Gonçalves for their support and for providing me the opportunity to be involved in this enriching project at the Barcelona Supercomputing Center. I deeply appreciate their guidance throughout the development of this master's thesis.

I would also like to extend my acknowledgements to the Earth Sciences Department of BSC, and particularly the Atmospheric Composition research group (AC-BSC). It is inspiring to be surrounded by such professional people. Especially, I would like to express my gratitude to Oriol, Carlos, Hervé, Angie, Dene, Roger, Kevin, Miriam and Carles for their valuable feedback and support.

The results obtained under this master's thesis have contributed to two national on-going projects of the AC-BSC research group. The first one has the objective of supporting the Spanish Ministry for the Ecological Transition and the Demographic Challenge to develop the scientific basis for the design of a national O_3 plan, while the second one is developed under the "Proyectos I+D+I Retos Investigación" program and investigates the impact of Barcelona's urban mobility plans on local and regional air quality levels.

Earth Sciences Department | BSC Barcelona Supercomputing Center Centro Nacional de Supercomputación

Resum

L'ozó troposfèric (O_3) és un contaminant atmosfèric secundari complex que afecta la salut humana, la biodiversitat, els cultius i les infraestructures. Es crea principalment per la interacció de la llum solar amb els òxids de nitrogen (NO_x) i la química en la que intervenen compostos orgànics volàtils (COVs). La contaminació per O_3 és habitual a Espanya a causa de les freqüents condicions anticiclòniques i les altes temperatures que n'afavoreixen la producció. Concretament, Catalunya inclou dues de les zones espanyoles més afectades per aquest contaminant: les regions del nord de l'Àrea Metropolitana de Barcelona (AMB; *i.e.*, la Plana de Vic i el Montseny) i el Camp de Tarragona, on se superen sistemàticament els llindars legals establerts per la Directiva Europea de Qualitat de l'Aire (2008/50/CE) i els nivells recomanats definits per l'Organització Mundial de la Salut (OMS).

Aquest estudi té com a objectiu avaluar les tendències i els nivells actuals d'O_3 registrats a Catalunya i identificar-ne les causes principals, així com quantificar l'impacte del Programa Nacional de Control de la Contaminació Atmosfèrica (PNCCA) i del Pla de Mobilitat Urbana (PMU) de Barcelona sobre les concentracions d'O_3, combinant l'ús d'observacions i de tècniques de modelització numèrica.

Les concentracions d'O_3 mesurades entre el 2000 i el 2021 no mostren una clara tendència a la baixa, amb l'excepció dels anys 2020 i 2021, en què es van registrar nivells inusualment baixos a causa de l'impacte de les restriccions de mobilitat durant la pandèmia de COVID-19 sobre les emissions antropogèniques globals i locals. Exceptuant aquests dos anys, les concentracions d'O_3 s'han mantingut força constants malgrat la important reducció de les emissions de precursors de NO_x i COV a Catalunya (-51% i -38%, respectivament), observant-se els nivells més alts d'O_3 durant els anys amb majors anomalies de la temperatura mitjana estival. Els llindars d'O_3 establerts per la legislació europea i l'OMS s'han superat de forma persistent, especialment a les zones rurals situades a sotavent de les principals zones emissores de precursors d'O_3 (*i.e.*, l'AMB i Tarragona). En canvi, els nivells d'O_3 a zones urbanes i industrials són generalment inferiors a causa del consum d'O_3 per reaccions amb el monòxid de nitrogen (NO) i els COVs.

Per quantificar l'impacte dels plans de reducció d'emissions PNCCA i PMU, utilitzem els resultats numèrics del sistema de modelització de la qualitat de l'aire CALIOPE, desenvolupat i gestionat pel grup de Composició Atmosfèrica del Barcelona Supercomputing Center (AC-BSC). Els experiments de modelització inclouen dos escenaris de reducció d'emissions (PE_PNCCA i PE_BCN_UMP) i els seus escenaris base respectius (BE1 i BE2), que consideren les emissions en una situació de normalitat (*business-as-usual*, en anglès). Analitzem els efectes d'aquests dos escenaris sobre els nivells d'O_3 durant els mesos d'abril a setembre de 2019, coincidint amb l'època de màximes concentracions d'aquest contaminant, i durant episodis específics d'O_3 identificats. Els resultats permeten identificar el nombre de superacions dels límits establerts per la normativa europea i les recomanacions de l'OMS que s'haurien evitat amb els escenaris de reducció d'emissions PE_PNCCA i PE_BCN_UMP.

Segons els resultats de la modelització, els escenaris de reducció d'emissions reduirien un -27% (PE_PNCCA) i un -2% (PE_BCN_UMP) el nombre de superacions del valor objectiu d'O_3 per a la protecció de la salut humana (120 $\mu g/m^3$). A més, considerant únicament els episodis d'O_3 del 2019 reproduïts correctament pel model, en l'escenari PE_PNCCA tots s'haurien evitat. Per al PE_BCN_UMP, que només inclou canvis en les emissions de la ciutat de Barcelona i

principalment en el transport per carretera local, les mesures no serien suficients per evitar tots els episodis d'O_3, però sí que suposarien una reducció de la freqüència i severitat dels episodis clàssics que afecten la Plana de Vic i el Montseny. Tot i això, en ambdós escenaris se seguiria superant el llindar de 100 µg/m^3 corresponent a les Directrius de l'OMS en el 100% de totes les estacions de monitorització de Catalunya. Així, per garantir uns nivells de qualitat de l'aire adequats, cal un esforç més gran a escala local, però també a escala global, a causa de la rellevant contribució de l'O_3 importat a la Península Ibèrica.

Resumen

El ozono troposférico (O_3) es un contaminante atmosférico secundario complejo que afecta a la salud humana, la biodiversidad, los cultivos y las infraestructuras. Se crea principalmente por la interacción de la luz solar con los óxidos de nitrógeno (NO_x) y la química en la que intervienen compuestos orgánicos volátiles (COVs). La contaminación por O_3 es habitual en España debido a las frecuentes condiciones anticiclónicas y las altas temperaturas que favorecen su producción. Concretamente, Cataluña incluye dos de las zonas españolas más afectadas por este contaminante: las regiones ubicadas al norte del Área Metropolitana de Barcelona (AMB; *i.e.*, la Plana de Vic y el Montseny) y el Camp de Tarragona, donde se superan sistemáticamente los umbrales legales establecidos por la Directiva Europea de Calidad del Aire (2008/50/CE) y los niveles recomendados definidos por la Organización Mundial de la Salud (OMS).

Este estudio tiene como objetivo evaluar las tendencias y los niveles actuales de O_3 registrados en Cataluña e identificar sus causas principales, así como cuantificar el impacto del Programa Nacional de Control de la Contaminación Atmosférica (PNCCA) y del Plan de Movilidad Urbana (PMU) de Barcelona sobre las concentraciones de O_3, combinando el uso de observaciones y técnicas de modelización numérica.

Las concentraciones de O_3 medidas entre 2000 y 2021 no muestran una clara tendencia a la baja, a excepción de los años 2020 y 2021, en los que se registraron niveles inusualmente bajos debido al impacto de las restricciones de movilidad durante la pandemia de COVID-19 sobre las emisiones antropogénicas globales y locales. Exceptuando estos dos años, las concentraciones de O_3 se han mantenido bastante constantes a pesar de la importante reducción de las emisiones de precursores de NO_x y COV en Cataluña (-51% y -38%, respectivamente), observándose los mayores niveles de O_3 durante los años con anomalías más altas de la temperatura media estival. Los umbrales de O_3 establecidos por la legislación europea y la OMS se han superado de forma persistente, especialmente en las zonas rurales situadas a sotavento de las principales zonas emisoras de precursores de O_3 (*i.e.,* el AMB y Tarragona). En cambio, los niveles de O_3 en zonas urbanas e industriales son generalmente inferiores debido al consumo de O_3 por reacciones con monóxido de nitrógeno (NO) y COVs.

Para cuantificar el impacto de los planes de reducción de emisiones PNCCA y PMU, utilizamos los resultados numéricos del sistema de modelización de la calidad del aire CALIOPE, desarrollado y gestionado por el grupo de Composición Atmosférica del Barcelona Supercomputing Center (AC-BSC). Los experimentos de modelización incluyen dos escenarios de reducción de emisiones (PE_PNCCA y PE_BCN_UMP) y sus respectivos escenarios base (BE1 y BE2), que consideran las emisiones en una situación de normalidad (*business-as-usual*, en inglés). Analizamos los efectos de estos dos escenarios sobre los niveles de O_3 durante los meses de abril a septiembre de 2019, coincidiendo con la época de máximas concentraciones de este contaminante, y durante episodios específicos de O_3 identificados. Los resultados permiten identificar el número de superaciones de los límites establecidos por la normativa europea y las recomendaciones de la OMS que se habrían evitado con los escenarios de reducción de emisiones PE_PNCCA y PE_BCN_UMP.

Según los resultados de la modelización, los escenarios de reducción de emisiones reducirían un -27% (PE_PNCCA) y un -2% (PE_BCN_UMP) el número de superaciones del valor objetivo de O_3 para la protección de la salud humana (120 µg/m^3). Además, considerando únicamente los

episodios de O_3 de 2019 reproducidos correctamente por el modelo, todos ellos se habrían evitado en el escenario PE_PNCCA. Para el PE_BCN_UMP, que sólo incluye cambios en las emisiones de la ciudad de Barcelona y principalmente en el transporte por carretera local, las medidas no serían suficientes para evitar todos los episodios de O_3, pero sí supondrían una reducción de la frecuencia y severidad de los episodios clásicos que afectan a la Plana de Vic y al Montseny. No obstante, en ambos escenarios, se seguiría superando el umbral de 100 $\mu g/m^3$ correspondiente a las Directrices de la OMS en el 100% de todas las estaciones de monitoreo de Cataluña. Así, para garantizar unos niveles de calidad del aire adecuados, es necesario un mayor esfuerzo a escala local, pero también a escala global, debido a la relevante contribución del O_3 importado en la Península Ibérica.

Abstract

Tropospheric ozone (O_3) is a complex secondary air pollutant that affects human health, biodiversity, crops and infrastructures. It is mainly created by the interaction of sunlight with nitrogen oxides (NO_x) and chemistry involving volatile organic compounds (VOCs). O_3 pollution is prevalent in Spain due to frequent anticyclonic conditions and high temperatures that enhance its production. Specifically, Catalonia includes two main O_3 Spanish hotspots: the northern regions of the Barcelona Metropolitan Area (BMA; i.e., Plana de Vic and Montseny) and Camp de Tarragona, where the legal thresholds established by the European Air Quality Directive (2008/50/EC) and recommended levels defined by the World Health Organisation (WHO) are systematically exceeded.

This study has the objective of assessing the trends and current O_3 levels measured in Catalonia and identifying its main causes, as well as quantifying the impact of the Spanish National Air Pollution Control Programme (PNCCA) and the Barcelona Urban Mobility Plan (UMP) on O_3 concentrations, combining the use of observations and numerical modelling techniques.

Concentrations of O_3 measured between 2000 and 2021 do not show a clear downward trend except for the years 2020 and 2021, when unusually low levels were recorded due to the impact of COVID-19 mobility restrictions on global-to-local anthropogenic emissions. Apart from these two years, O_3 concentrations have remained rather unaltered despite the significant reduction of NO_x and VOC precursor emissions in Catalonia (-51% and -38%, respectively), the largest O_3 levels being observed during the years with the highest summer mean temperature anomalies. The O_3 thresholds established by the European legislation and WHO have been persistently exceeded, especially in rural areas located downwind of the main O_3 precursor emitting areas (i.e., the BMA and Tarragona). O_3 levels in urban and industrial areas are usually lower due to the consumption of O_3 through titration by nitrogen monoxide (NO) and ozonolysis of VOCs.

To quantify the impact of the PNCCA and UMP emission abatement plans, we make use of the numerical outputs from the CALIOPE air quality modelling system, developed and maintained by the Atmospheric Composition group of the Barcelona Supercomputing Center (AC-BSC). The modelling experiments include two emission abatement scenarios (PE_PNCCA and PE_BCN_UMP) and their respective base case scenarios (BE1 and BE2), which consider emissions in a business-as-usual situation. We analyse the effects of these two scenarios on O_3 levels during April-September 2019, coinciding with the O_3 peak season, and during specific O_3 episodes that were identified. The results allow identifying the number of exceedances of the limits established by the European legislation and WHO that would have been avoided with the PE_PNCCA and PE_BCN_UMP emission abatement scenarios.

According to the modelling results, the emission abatement scenarios would reduce -27% (PE_PNCCA) and -2% (PE_BCN_UMP) the number of exceedances of the O_3 target value for the protection of human health (120 $\mu g/m^3$). Furthermore, only considering the 2019 O_3 episodes correctly reproduced by the model, all of them would have been avoided under the PE_PNCCA scenario. For PE_BCN_UMP, which only tackles emissions from Barcelona city, the measures would not be sufficient to avoid all O_3 episodes, but it would lead to a reduction in the frequency and severity of the classic episodes affecting Plana de Vic and Montseny. Nevertheless, the WHO Guidelines threshold of 100 $\mu g/m^3$ would still be exceeded in 100% of all the reporting stations

in Catalonia, both for PE_PNCCA and PE_BCN_UMP. Therefore, to ensure proper air quality levels, further efforts must be undertaken locally but also on a global scale, owing to the relevant contribution of imported O_3 in the Iberian Peninsula.

List of abbreviations

AC-BSC: Atmospheric Composition group of the Barcelona Supercomputing Center

BE1: base case emission scenario 1 considered in the PNCCA modelling exercise

BE1: base case emission scenario 2 considered in the Barcelona UMP modelling exercise

BMA: Barcelona Metropolitan Area

BSC: Barcelona Supercomputing Center

BVOCs: biogenic volatile organic compounds

CALIOPE: CALIdad del aire Operacional Para España air quality forecasting system

EEA: European Environment Agency

EF: emission factor

EMEP: European Monitoring and Evaluation Programme

MITECO: Ministerio para la Transición Ecológica y el Reto Demográfico

MONARCH: Multiscale Online Non-hydrostatic Atmosphere Chemistry modelling system

NMVOCs: non-methane volatile organic compounds

NO: nitrogen monoxide or nitrogen oxide

NO_2: nitrogen dioxide

NO_x: nitrogen oxides

O_3: ozone

O_3^h: hourly concentration for ozone

O_3^d: daily mean concentration for ozone

O_3^{d8max}: maximum daily 8-hour mean concentration for ozone

O_3^{d1max}: maximum daily 1-hour concentration for ozone

PE_PNCCA: emission abatement scenario based on PNCCA

PE_BCN_UMP: emission abatement scenario based on the Barcelona UMP

PNCCA: Programa Nacional de Control de la Contaminación Atmosférica

PNIEC: Plan Nacional Integrado de Energía y Clima

SNAP: Selected Nomenclature for reporting of Air Pollutants

UMP: Urban Mobility Plan of Barcelona (2019-2024)

VOCs: volatile organic compounds

WHO: World Health Organisation

XEMA: Xarxa d'Estacions Meteorològiques Automàtiques

Index

1. Introduction

Air pollution is the biggest environmental risk to human health in the European Union (EU) and a major cause of premature death and disease (European Environment Agency; EEA, 2023a). According to the World Health Organisation (WHO, 2022), almost the entire global population (99%) breathe air that threatens their health, with low- and middle-income countries suffering from the highest exposures.

Tropospheric ozone (O_3) is one of the key air quality pollutants (Querol et al., 2016) that affects human health, biodiversity, crops and infrastructures (Fleming et al., 2018, and references therein). O_3 is associated with both short- and long-term respiratory and cardiovascular diseases (e.g., asthma, reduced lung function, damaged lung tissue, coronary heart disease, heart failure and stroke) and in 2019 worldwide exposure to O_3 was estimated to contribute to approximately 365,000 deaths and 6.2 million disability-adjusted life years (DALYs) (Malashock et al., 2022). Furthermore, O_3 air pollution is likely to continue to worsen, especially in low- and middle-income nations, driven by both increased emissions and climate change.

O_3 is a secondary pollutant, which means that it is not directly emitted by pollution sources and is formed when other pollutants react in the atmosphere. The formation processes of O_3 are interdependent and complex, and their reaction and production rates are not linear. A major part of O_3 is created by chemical reactions between nitrogen oxides (NO_x) and volatile organic compounds (VOCs) from both anthropogenic and biogenic sources in the presence of sunlight (*hv*, see reaction R1 in Figure 1). As a result, there is no O_3 production at night and its levels are usually highest at midday on summer days. However, O_3 concentrations are reduced through the process of NO_x titration, which consists of the removal of O_3 through reaction with nitrogen monoxide (NO) or nitrogen dioxide (NO_2) ($NO + O_3 \rightarrow NO_2 + O_2$ or $NO_2 + O_3 \rightarrow NO_3 + O_2$; see respective reactions R2 and R3 in Figure 1). This process can happen both at daytime and nighttime, in the immediate vicinity of very large emissions of NO_x (e.g., large cities) (Gorrochategui et al., 2022). The process of O_3 formation is also driven by other precursors such as methane (CH_4) and carbon monoxide (CO) (Massagué et al., 2022). Presently, several studies are being conducted on the implication of the observed increases in global CH_4 concentrations on O_3 levels (Turnock et al., 2018).

Figure 1. Reactions involved in O_3 formation and destruction in the troposphere at nighttime and daytime. R1, R2 and R3 indicate the main reactions: O_3 formation from NO_x and VOCs (R1), and O_3 suppression through NO_x titration (R2 and R3). From Gorrochategui et al., (2022).

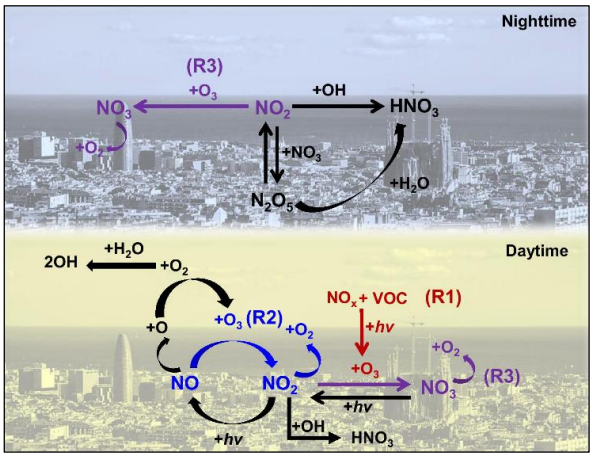

On the other hand, the O_3 formation rate is strongly affected by the NO_x:VOC ratio (Massagué et al., 2022). For instance, in highly polluted urban areas, O_3 production is usually VOC-limited (high NO_x concentrations), therefore, the O_3 levels rise with decreased NO_x concentrations and increased VOCs. In contrast, rural areas located downwind of urban and suburban regions tend to be NO_x-limited since biogenic VOCs emissions are usually higher and NO_x concentrations are low. Thus, the O_3 levels rise with increasing NO_x, and only small changes occur with increases in VOCs levels (Badia et al., 2023).

Variations in O_3 concentrations at a given location are determined by multiple factors, such as geographic characteristics, prevailing meteorology, and the proximity and distribution of precursor sources (Massagué et al., 2022). Meteorological stagnation, high temperatures, high solar radiation and low precipitation enhance O_3 formation (Pay et al., 2019). Furthermore, O_3 contributions can be local, regional, hemispheric or stratospheric (Massagué et al., 2022). In the Iberian Peninsula, the contribution of imported O_3 is particularly dominant (46-68% of the daily mean O_3 concentration) as a result of the accumulation and recirculation of pollutants over the Mediterranean (Pay et al., 2019).

The European Air Quality Directive (2008/50/EC) is the current mandatory regulation on air pollution and has been transposed into the legislation of all the European Union Member States. It establishes the following air quality objectives for O_3 (Table 1): (i) a human health target value fixed at 120 μg/m^3 (120^{d8max}) for the maximum daily 8-hour mean concentration (O_3^{d8max}), not to be exceeded on more than 25 days per year, averaged over 3 years; (ii) an alert hourly threshold of 240 μg/m^3 (240^{h}); and (iii) an information hourly threshold of 180 μg/m^3 (180^{h}).

On the other hand, the WHO guidelines provide two more severe recommended thresholds (Table 1): (i) an 8-hour threshold fixed at 100 μg/m^3 for the O_3^{d8max} (100^{d8max}), not to be exceeded more than 3-4 days per year (we have considered 3 days to be as restrictive as possible), and (ii) a peak season threshold of 60 μg/m^3 ($60^{peak\ season}$) for the peak season concentration, which is the average of the O_3^{d8max} in the six consecutive months with the highest six-month running-average O_3 concentration, never to be exceeded (WHO, 2021).

Furthermore, in October 2022, the European Commission tabled a proposal for a revision of the Air Quality Directive, expecting to set air quality standards for 2030 that are more closely aligned with the WHO's recommendations (Table 1). Therefore, they suggest (i) a target value of 120 μg/m^3 (120^{d8max}), not to be exceeded on more than 18 days per year, averaged over 3 years; and (ii) a long-term objective for the same metric (120^{d8max}), not to be exceeded on more than 3 days per year (European Parliamentary Research Service, 2023).

Table 1. Objectives and guidelines for the protection of human health regarding O_3.

	O_3 metric	Averaging period	Threshold	Maximum number of allowed occurrences
Directive 2008/50/EC	Human health target value (120^{d8max})	Maximum daily 8-hour mean averaged over 3 years	120 µg/m^3	25 days per year
	Alert threshold (240^{h})	Hourly	240 µg/m^3	-
	Information threshold (180^{h})	Hourly	180 µg/m^3	-
WHO guidelines (2021)	8-hour threshold (100^{d8max})	Maximum daily 8-hour mean	100 µg/m^3	3-4 days per year
	Peak season threshold ($60^{peak\ season}$)	Average of maximum daily 8-hour mean in the six consecutive months with the highest six-month running-average O_3 concentration	60 µg/m^3	0
Directive 2008/50/EC revision	Human health target value 120^{d8max}	Maximum daily 8-hour mean averaged over 3 years	120 µg/m^3	18 days per year
	Long-term objective 120^{d8max}	Maximum daily 8-hour mean averaged over 3 years	120 µg/m^3	3 days per year

To monitor and assess compliance with the mentioned thresholds, a large number of air quality stations exist throughout Europe. As shown in Figure 2, the levels of O_3 registered in these stations indicate that the Southern European regions, and especially the Mediterranean Basin, are the most exposed to O_3 pollution in Europe, with Spain and several other countries regularly exceeding the 120^{d8max} threshold (Massagué et al., 2022). This is mainly due to frequent anticyclonic conditions with clear skies during summer, leading to high insolation and temperatures, therefore, photochemical production of O_3 is favoured. Regional emissions of pollutants, high biogenic VOCs' (BVOCs) emissions in spring and summer, and the existence of particular orographic features that help stagnation-recirculation episodes also contribute to O_3 high levels (Massagué et al., 2019). Furthermore, the geographic location of the Mediterranean Basin makes it a receptor of the long-range transport of pollution from Europe, Asia and even North America (Pay et al., 2019).

Figure 2. 93.2 percentile of O_3^{d8max} [µg/m^3] at air quality stations in Europe in 2022 (preliminary data) (EEA, 2023b). This percentile corresponds to the mean 26th highest value. Therefore, exceeding the 120 µg/m^3 threshold is statistically equivalent to surpassing the 25-day limit set by European legislation.

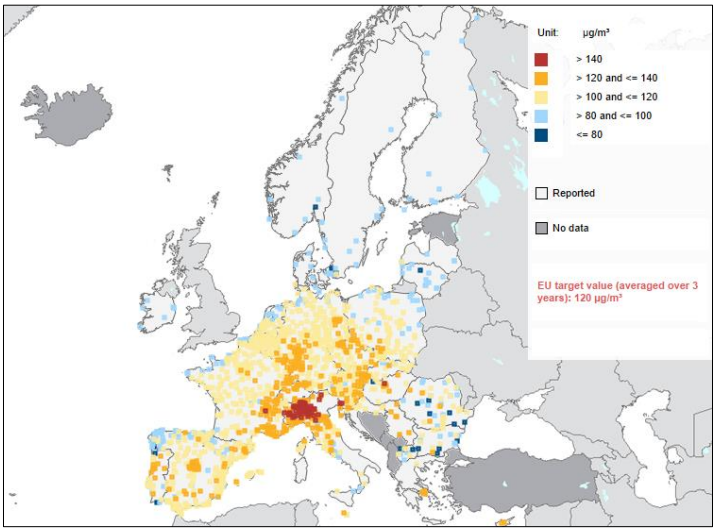

Two of the largest and longstanding O_3 Spanish hotspots identified by the MITECO (2023a) are located in Catalonia: the northern regions of the Barcelona Metropolitan Area (BMA), followed at some distance by Camp de Tarragona. The BMA is a highly industrialised and dense urban agglomeration, whereas the city of Tarragona is surrounded by two of the major chemical and petrochemical industrial complexes in Spain. Local urban and industrial O_3 emissions in the BMA and Tarragona, together with the high background levels due to regional transport, contribute significantly to the generation of O_3 episodes in areas downwind of the emission sources, such as Plana de Vic or the northern region of Tarragona (Querol et al., 2016).

To minimise the exposure of the population to high levels of atmospheric pollution, the Spanish government published in 2019 the first National Air Pollution Control Programme (*Programa Nacional de Control de la Contaminación Atmosférica,* PNCCA; MITECO, 2019). The PNCCA defines strategic objectives and actions from 2020 onwards, aligned with national air quality policies and the National Energy and Climate Plan (*Plan Nacional Integrado de Energía y Clima*, PNIEC; MITECO, 2020).

At the local level, 3 years ago the Barcelona city council began to design and implement a series of traffic management policies as part of the latest Urban Mobility Plan (2019-2024) (*Pla de Mobilitat Urbana 2019-2014, UMP*; Ajuntament de Barcelona, 2022), which include the implementation of superblocks and a low emissions zone to reduce the number of cars circulating throughout the city and improve local air quality levels. In addition, the Port of Barcelona has started a process of electrification of the docks with a 2030 horizon in the framework of the NEXIGEN project (Port de Barcelona, 2022).

While these measures have the objective of reducing emissions and air pollution levels, assessing the impact they may have on O_3 is quite complex to determine since: (i) O_3 formation depends on complex nonlinear chemical reactions between many precursors, mainly NO_x and VOCs (Petetin et al., 2023); (ii) imported O_3 has a significant contribution on O_3 levels in the Iberian Peninsula (Pay et al., 2019); and (iii) O_3 precursors are mainly emitted far from the sites where O_3 exceedances occur (Badia et al., 2023). In this context, the use of air quality numeric models in combination with monitoring data becomes essential to analyse the impacts of different strategies and measures aimed at reducing anthropogenic emissions and improving air quality (Soret et al., 2022). Furthermore, the proposed revision of the Air Quality Directive establishes the use of modelling applications as mandatory in zones where the target value for O_3 is exceeded for both air quality assessment and planning (European Parliamentary Research Service, 2023).

2. Objectives

The main objective of this study is to **assess the trends of measured O_3 levels in Catalonia and quantify the impact of Spanish national and Barcelona's local emission abatement plans on its concentrations, combining the use of observations and numerical modelling techniques**.

To achieve the main objective of the project, three specific objectives are defined:

- To analyse the evolution and trends of observed O_3 levels in Catalonia in the last two decades (2000 to 2021), comparing them with the threshold and recommendation levels established by European legislation and WHO guidelines, respectively, and identify the main hotspots. Considering that O_3 levels depend on multiple factors, such as precursor emissions and meteorological conditions, the analysis also includes the evolution of NO_x and NMVOC anthropogenic emissions and temperature.
- To assess the performance of a numerical air quality system to model surface O_3 concentrations over Catalonia and reproduce specific O_3 episodes. For this purpose, modelling outputs are compared against the monitoring data from the official air quality stations measuring O_3 concentrations in Catalonia from April to September 2019, when the O_3 levels are at their maximum.
- To quantify the expected impact of the Spanish National Air Pollution Control Programme (PNCCA) and the Barcelona Urban Mobility Plan (UMP) on O_3 levels over Catalonia making use of air quality modelling results. The resulting O_3 concentrations are used to discuss the level of compliance that monitoring stations in Catalonia would have in terms of current legal and recommended thresholds.

This document is structured as follows: Section 3 includes a description of the methodology of this master's thesis. Section 4 provides a summary of the trends of emission precursors, temperature and O_3 levels in Catalonia during 2000-2021. Section 5 evaluates the performance of the numerical air quality system, while Section 6 presents and discusses the results of modelling the impact of the emission abatement scenarios on O_3 levels. Section 7 conducts a sustainability analysis. Finally, Section 8 highlights the main results and conclusions of this study.

3. Methodology

3.1. Framework of the master's thesis

This work is conducted in the context of the Atmospheric Composition research group (AC-BSC) of the Department of Earth Sciences of the BSC. This group works to better understand and predict the spatiotemporal variations of atmospheric pollutants along with their effects on weather, climate and air quality. They have strong expertise in emissions and air quality modelling at the Barcelona, Spain, Europe and global scales. The AC-BSC group develops and maintains the CALIOPE mesoscale air quality modelling system (*CALIdad del aire Operacional Para España*; www.bsc.es/caliope; Soret et al., 2022 and references therein) and the High-Elective Resolution Modelling Emission System version 3 (HERMESv3; Guevara et al., 2019, 2020), which is the emission core of the CALIOPE system. Both numerical models, which are run, implemented and executed in the MareNostrum 4 supercomputer (https://www.bsc.es/es/marenostrum/marenostrum), are used in the framework of this master's thesis and are described in Sections 3.5.1 and 3.6, respectively.

3.2. Characterisation of the evolution of O_3 precursor emissions in Catalonia

To characterise the evolution of O_3 precursor emissions over the 2000-2021 period (Section 4.1), we will use the official NO_x and NMVOC annual emissions of Catalonia provided by the MITECO in the framework of the Spanish Emission Inventory System (MITECO, 2023b). They classify the emissions data according to the official SNAP nomenclature (Selected Nomenclature for Air Pollution), which allows the distribution of emissions according to sectors, subsectors and activities. Based on the analysis of these data and the information provided in the official Air Pollutant Emission Inventory Reports (MITECO, 2023c), we will describe the evolution of annual NO_x and NMVOC emissions and identify the underlying causes that led to these trends, in total and by relevant sectors.

In this analysis, we will not account for natural emissions, as only anthropogenic sources are of concern here. Furthermore, some SNAP groups will not be considered: group 08 04 (Maritime activities), as they are mainly occurring at sea, and groups 08 05 03 (National air cruise traffic, > 1000 m) and 08 05 04 (International air cruise traffic, > 1000 m), since emissions from airplanes flying at such altitudes practically do not affect surface O_3 levels.

3.3. Analysis of the meteorological drivers of O_3 formation in Catalonia

O_3 levels are affected by several meteorological variables, mainly temperature. High temperatures and solar radiation enhance the photochemical reactions involved in O_3 formation (Pay et al., 2019, and references therein), as previously stated. Therefore, in Section 4.2, we will analyse the evolution of temperature in Catalonia from 2000 to 2021 to identify whether the years with the highest temperatures correspond to those with the highest O_3 levels. For this purpose, we will use multiple annual climate reports published by Servei Meteorològic de Catalunya.

In addition to temperature, wind and pressures also affect O_3 levels but they are more significant during specific O_3 episodes and lose relevance when analysing annual trends. O_3 episodes occur when ground-level concentrations exceed threshold values set by the European Air Quality Directive (Table 1). We will study winds and pressures during these events in Section S.3 in

Supplementary Material, which includes a characterisation of the O_3 episodes that occurred in 2019. In this case, we will use maps of wind speed and direction at the automatic meteorological stations of the XEMA network (*Xarxa d'Estacions Meteorològiques Automàtiques*) from Servei Meteorològic de Catalunya (2023b). We will also use maps of the 500hPa geopotential height provided by the Global Forecast System of the United States weather service available at Wetterzentrale (2023). The 500hPa geopotential height is the vertical coordinate referenced to Earth's mean sea level where the air pressure is constant and equal to 500hPa. Higher geopotential heights usually correspond to areas of anticyclones, whereas lower geopotential heights to areas of depressions (Copernicus Climate Change Service, 2022). This is relevant since anticyclonic conditions enhance O_3 production.

3.4. Analysis of measured O_3 concentrations in Catalonia

To characterise the evolution of O_3 concentrations over the 2000-2021 period (Section 4.3), we will use measurements of the EEA AQ e-Reporting (EEA, 2023d) and EEA AirBase (EEA, 2023e), which are centralised databases that include official air quality data provided by the EU Member States. In the present work, we will use O_3 data from the EEA AirBase from 2000 to 2011 and the EEA AQ e-Reporting from 2012 to 2021, as the EEA changed the reporting framework.

These data are available through the BSC's internal Globally Harmonised Observational Surface Treatment (GHOST) system, which is an initiative developed in the AC-BSC research group. The GHOST project harmonizes global surface atmospheric observations to facilitate quality-assured comparison between observations and models within the atmospheric chemistry community (Bowdalo et al., 2023).

In the present work, we will process the 2000-2021 hourly O_3 concentrations in each air quality station obtained through the GHOST system with R programming language (R Core Team, 2021). From these data, we will calculate the O_3 metrics that are used to define legal thresholds and recommendations set up by the European Air Quality Directive and WHO, respectively: hourly (O_3^h), daily mean (O_3^d), maximum daily 8-hour mean (O_3^{d8max}) and maximum daily 1-hour (O_3^{d1max}) concentrations. We will use these data in multiple parts of this master's thesis: (i) in the characterisation of the evolution of O_3 concentrations over the 2000-2021 period (Section 4.3); (ii) in the evaluation of the performance of the numerical air quality model for the base case scenarios from April to September 2019 (Section 5), since we will compare modelling outputs against the monitoring data in the air quality stations; and (iii) in the quantification of the impact of the emission abatement scenarios on O_3 concentrations at the air quality stations (Section 6.3.2) to calculate the estimated O_3 observations for the scenarios in the monitoring sites.

During the 2000-2021 period, there were a total of 82 air quality stations measuring O_3, although most of them were not operational during the entire study period. In 2019, which is the reference year considered in Sections 5 and 6, the available monitoring sites were 50. In this study, we will follow the EEA (2023c) classification of air quality stations according to multiple criteria. On the one hand, depending on the distribution or density of buildings around the sampling point, stations are classified as urban, suburban or rural. On the other hand, depending on the predominant emission sources, they are classified as traffic, industrial or background stations. This distinction is relevant since the spatial representativeness of the station measurements is closely linked to their classification.

Furthermore, the Air Quality Directive establishes that the territory must be divided into air quality zones to facilitate the air quality assessment. These are homogeneous areas in terms of climatology, orography, population density, and industrial and traffic emissions volume. In the present study, we will consider this distinction and we will include the boundaries corresponding to the 14 air quality zones of Catalonia in the maps shown throughout this document. For this purpose, we will use the file published in ShapeFile format (i.e., digital vector storage format for storing geographic location and associated attribute information) by the Generalitat de Catalunya (2022), which contains the coordinates of the air quality zone boundaries.

3.5. Evaluation of the numerical air quality system and quantification of the impact of the emission abatement scenarios

To quantify the impact of emission abatement scenarios prior to their implementation, it is essential to use air quality numeric models in combination with monitoring data. In the present work, we will post-process, evaluate and analyse the numerical outputs from two air quality modelling exercises that were conducted by the AC-BSC research group using the CALIOPE air quality modelling system, which we describe in Section 3.5.1. The two exercises included the execution of the CALIOPE system under two emission abatement scenarios (based on the PNCCA and the UMP) and their respective base case scenarios, which consider emissions in a business-as-usual situation. The definition of the emission scenarios and execution of the CALIOPE system are beyond the scope of this study, since the time needed for the system to produce all the results would have required much more time than the usual six months devoted to conducting a final master's thesis.

To perform the post-processing and analysis of the numerical outputs of the model and the O_3 observations, we will get acquainted with the data formats typically used in earth system models (i.e., Network Common Data Form; NetCDF), as well as with the R programming language to automatically and agilely conduct the processing, among others. Most of the graphs and maps included in this study are produced using RStudio (RStudio Team, 2020), which is an open-source integrated development environment for working on the R programming language.

The study period considered in Sections 5 and 6 (April-September 2019, further details in Section 5) is shorter than the 2000-2021 period we assume for the analysis of O_3 trends. This is because as the study period gets longer, more time and computational resources are required.

In the following sections, we describe the CALIOPE air quality modelling system, and the tools and statistics used in the evaluation of the model.

3.5.1. The CALIOPE air quality modelling system

The CALIOPE system is implemented in the MareNostrum 4 supercomputer and integrates the Weather Research and Forecasting – Advanced Research Weather meteorological model (WRF-ARW) (Skamarock and Klemp, 2008), the Community Multiscale Air Quality Modelling System (CMAQ) (Byun and Schere, 2006) as a chemical transport model, and the HERMESv3 as the emission core of the system (Guevara et al., 2019, 2020).

The CALIOPE system works with a temporal resolution of 1h and with a horizontal resolution that varies according to the working domain. CALIOPE is run over three nested domains including Europe at a 12km × 12km horizontal resolution (EU-12km), the Iberian Peninsula at

4km × 4km (IP-4km) and the Catalonian domain, including Barcelona, at 1km × 1km (CAT-1km) (Figure 3). The results analysed in the present work correspond to the modelling outputs obtained for the 4km x 4km Iberian Peninsula and 1km x 1km Catalonia domains. The CALIOPE system has been evaluated and used in the framework of multiple air quality assessment studies (e.g., Pay et al., 2012; Soret et al., 2014; Pay et al., 2019; Soret et al., 2022 and references therein).

Figure 3. Modular structure of the CALIOPE air quality modelling system and model output example in each domain (BSC, 2023).

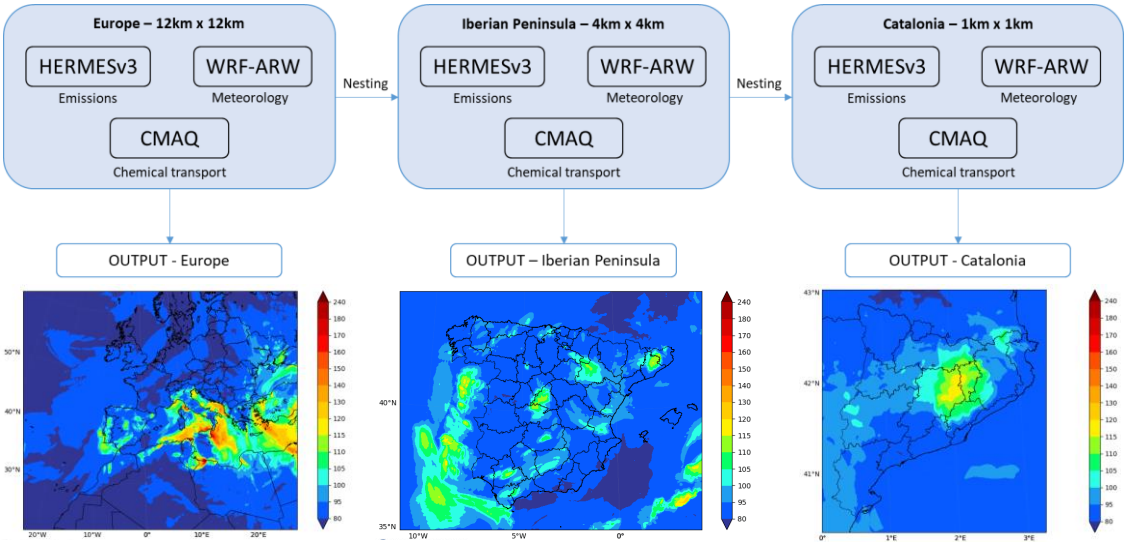

3.5.2. Evaluation of the model

The model outputs consist of hourly O_3 concentrations for each individual cell in the considered domain. The Providentia tool, which is developed in the BSC, interpolates these data to each station to be able to compare the modelling outputs against the monitoring data from the official air quality stations measuring O_3 concentrations in Catalonia (provided by the GHOST system). We will also use the Providentia tool for applying the criteria of the European Air Quality Directive regarding the required proportion of valid data for aggregating O_3 concentrations and calculating statistical parameters (e.g., 75% representativeness in the O_3^{d8max}).

In Section 5, we will use multiple statistics to assess the performance of CALIOPE in the base case emission scenarios. These are as follows: (i) mean bias (MB), which measures the average difference between the modelled and the observed values; (ii) normalized mean bias (nMB), which uses the observation average to normalise the mean bias; (iii) root mean square error (RMSE), which measures the standard deviation of the differences between the modelled and the observed values; (iv) normalised root mean square error (nRMSE), which uses the observation average to normalise the root mean square error; and (v) Pearson correlation coefficient (PCC), which refers to the extent to which the modelled and the observed values have a linear relationship with each other (Copernicus Atmosphere Monitoring Service, 2022). Equation 1-Equation 5 include the definition of these statistics (M and O are the predicted and observed concentrations, respectively, and n corresponds to the number of observations).

Equation 1. Definition of mean bias (MB).

$$MB = \frac{1}{N} \cdot \sum_{i=1}^{N} (M_i - O_i)$$

Equation 2. Definition of normalised mean bias (nMB).

$$nMB = \frac{\sum_{i=1}^{N} (M_i - O_i)}{\sum_{i=1}^{N} O_i}$$

Equation 3. Definition of root mean square error (RMSE).

$$RMSE = \sqrt{\frac{1}{N} \cdot \sum_{i=1}^{N} (M_i - O_i)^2}$$

Equation 4. Definition of normalised root mean square error (nRMSE).

$$nRMSE = \frac{\sqrt{\frac{1}{N} \cdot \sum_{i=1}^{N} (M_i - O_i)^2}}{\sum_{i=1}^{N} O_i}$$

Equation 5. Definition of Pearson correlation coefficient (PCC).

$$PCC = \frac{\sum_{i=1}^{N} (M_i - \bar{M}) \cdot (O_i - \bar{O})}{\sqrt{\sum_{i=1}^{N} (M_i - \bar{M})^2} \cdot \sqrt{\sum_{i=1}^{N} (O_i - \bar{O})^2}}$$

3.6. Emission modelling exercise

To gain some knowledge on how to work with numerical models in a supercomputing environment, we will run four emission simulations using the bottom-up module of HERMESv3 model. With this modelling exercise, we will be able to quantify the impact of the emission abatement scenarios on NO_x and NMVOC anthropogenic emissions over Catalonia (Section 6.2).

The HERMESv3 system is an open source, parallel and stand-alone multi-scale atmospheric emission modelling framework that calculates gaseous and aerosol emissions for use in atmospheric chemistry models. Specifically, the bottom-up module computes high spatial (e.g., road link, point source) and temporal (i.e., hourly) resolution anthropogenic emissions using state-of-the-art calculation methods that couples local activity and emission factors with meteorological data (Guevara et al., 2020). This system estimates emissions for the main criteria pollutants and greenhouse gases, but in our emission modelling exercise we will only consider NO_x and NMVOCs emissions for being O_3 precursors.

4. Trends of emission precursors, temperature and O_3 levels in Catalonia (2000-2021)

The main objective of this section is to characterise the evolution and trends of O_3 precursor emissions (NO_x and NMVOC), temperature and O_3 levels in Catalonia from 2000 to 2021, as well as to identify the main O_3 hotspots in the region.

4.1. NO_x and NMVOC anthropogenic emissions

Figure 4 and Figure 5 show the evolution of the official annual anthropogenic emissions of the main O_3 precursors (NO_x and NMVOC) disaggregated by sectors in Catalonia from 2000 to 2021 (MITECO, 2023b).

Figure 4. Evolution of annual NO_x anthropogenic emissions [tonnes] disaggregated by SNAP sectors in Catalonia from 2000 to 2021 (MITECO, 2023b).

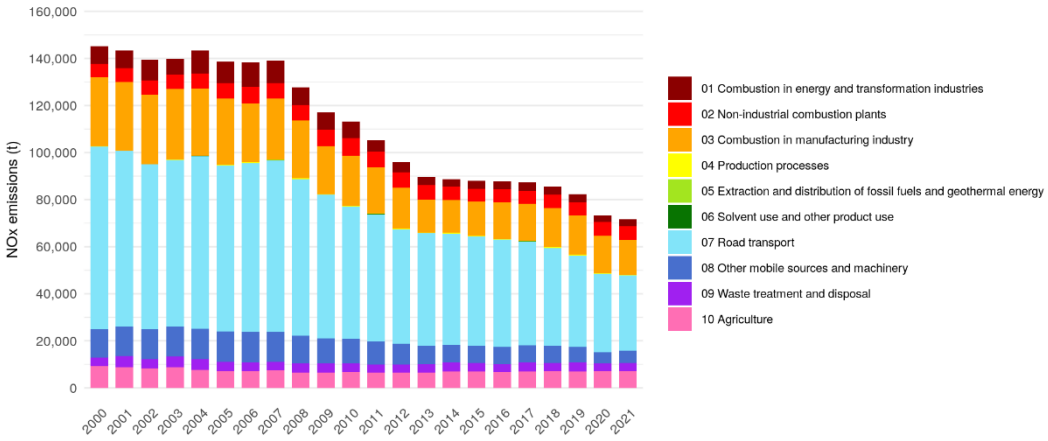

According to Figure 4, NO_x emissions have decreased by -50.7% in the last two decades, from 145,299 tonnes in 2000 to 71,638 tonnes in 2021, with almost all sectors experiencing reductions. The period with the greatest reductions in total NO_x emissions is between 2007 and 2013, due to the 2008-2014 economic recession in Spain. On the other hand, after a stable period, it is also noteworthy the -10.9% reduction in NO_x emissions in 2020 compared to the preceding year, especially in the case of road transport, as a result of the mobility restrictions associated with the COVID-19 pandemic (MITECO, 2023c).

The main emitting sector is road transport, with a contribution to total NO_x emissions of around 50%, mainly due to the private car and heavy-duty vehicles. Nevertheless, over the last two decades, this sector has reduced its NO_x emissions by -58.8%. The sharp decline between 2007 and 2013 stemmed from the aforementioned economic crisis, coupled with technological advances resulting from the introduction of EURO emission standards in passenger cars and in heavy-duty vehicles and buses (MITECO, 2023c). The increasingly stringent EURO standards define the acceptable limits for exhaust emissions of NO_x, VOC, particulate matter (PM) and carbon monoxide (CO) for new vehicles sold in the European Union and the European Economic Area Member States and the United Kingdom.

The second sector with the highest NO_x emissions is combustion in the manufacturing industry, contributing around 20% to the total. In this case, the reduction between 2000 and 2021 was -49.3%, primarily due to the progressive introduction of abatement techniques imposed by

Directive 1/2008, concerning integrated pollution prevention and control, and Directive 2010/75/EU on Industrial Emissions.

Figure 5. Evolution of annual NMVOC anthropogenic emissions [tonnes] disaggregated by SNAP sectors in Catalonia from 2000 to 2021 (MITECO, 2023b).

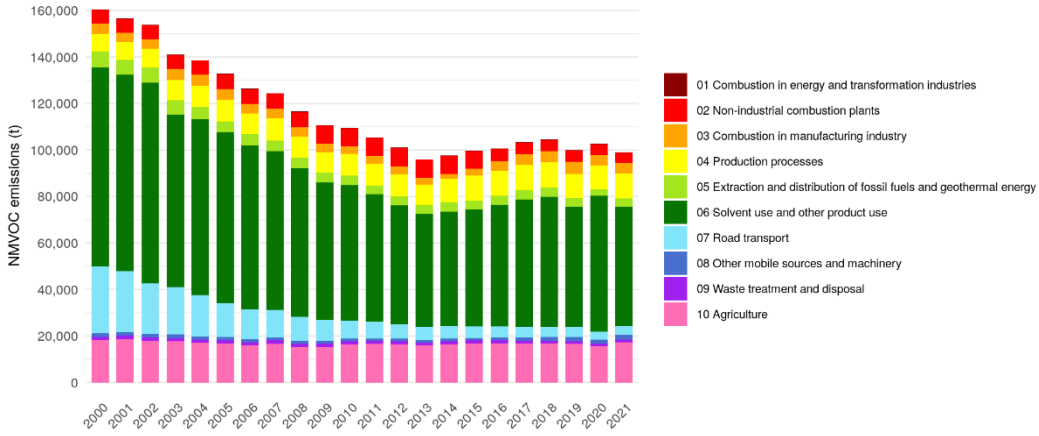

According to Figure 5, NMVOC emissions have also decreased (-38.3%) over the last two decades, from 160,440 tonnes in 2000 to 99,002 tonnes in 2021. In this case, the main contributor (about 50% of the total) is the sector related to the use of solvents and other products, with the associated emissions declining by -40% between 2000 and 2021. The drop since 2002 is a result of different regulations on paintings and painting installations (Royal Decree 117/2003 and Royal Decree 227/2006, transposition of Directives 1999/13/EC and 2004/42/CE, respectively). Moreover, the economic downturn also had a noticeable effect on paint consumption. The downward trend stopped in 2013, and a slight upward tendency in emissions, with minor fluctuations, has been observed since then. The peak in 2020 compared to the surrounding years was primarily due to an increase in the use of hand sanitizers and other solvent-containing products, as a result of the COVID-19 pandemic (MITECO, 2023c).

It is also worth noting the reduction (by -87% between 2000 and 2021) of NMVOC emissions from road transport, especially in the early years of the time series, owing to the introduction of the EURO standards for road vehicles and to the shift towards a diesel predominant car fleet in Spain (MITECO, 2023c). On the other hand, another significant contributor is the agriculture sector, mainly due to manure management in terms of nitrogen compounds. Emissions of NMVOCs from this sector have remained considerably stable over the last two decades.

4.2. Temperature

High temperatures and solar radiation are essential to trigger the photochemical reactions responsible for the generation of O_3 (Pay et al., 2019, and references therein). Therefore, temperature is the meteorological variable that most affects O_3 mean levels. Here, we analyse the evolution of temperature in Catalonia from 2000 to 2021 to subsequently identify whether the years with the highest temperatures correspond to those with the highest O_3 levels.

Figure 6 shows the evolution of the annual mean temperature anomaly in Catalonia for the period 1950-2021 with respect to the reference period 1961-1990. Here, we show a longer time period than the studied to highlight the increase in the average air temperature in Catalonia, as is occurring globally, due to the rise in atmospheric concentrations of greenhouse gases (Servei

Meteorològic de Catalunya, 2022a). This is relevant as in the expected climate change scenario, global warming will lead to increased O_3 formation (EEA, 2020).

Figure 6. Evolution of the annual mean temperature anomaly [ºC] in Catalonia for the period 1950-2021 with respect to the reference period 1961-1990 (in blue, negative anomalies; in red, positive anomalies). The black curve corresponds to a 13-member Gaussian filter (Servei Meteorològic de Catalunya, 2022b).

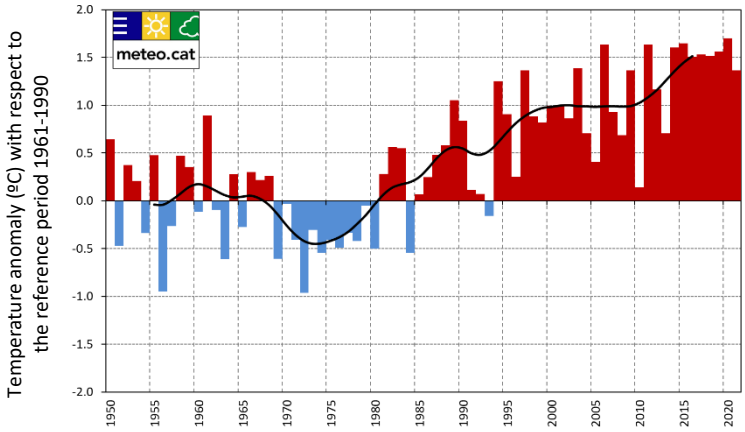

In the 2000-2021 period, a positive annual mean temperature anomaly was recorded each year (Figure 6). As shown in the graph, 2020 was the warmest year in Catalonia since 1950, with an average temperature anomaly of +1.7 ºC with respect to the reference period. Nevertheless, such a high annual mean temperature anomaly does not directly convert 2020 into a candidate for being one of the years with the highest O_3 levels (further details in Section 4.3.1.3), since the contribution to this high anomaly came not so much from the summer, which is usually when the highest levels of O_3 are recorded, but from the winter and spring, as shown in Figure 7 (Servei Meteorològic de Catalunya, 2021a). Furthermore, in 2020 there was an absence of general heat waves in Catalonia (Servei Meteorològic de Catalunya, 2021c).

Figure 7. Spatial distribution by season of the mean temperature anomaly [ºC] in Catalonia in 2020, with respect to the 1961-1990 reference period (Servei Meteorològic de Catalunya, 2023a).

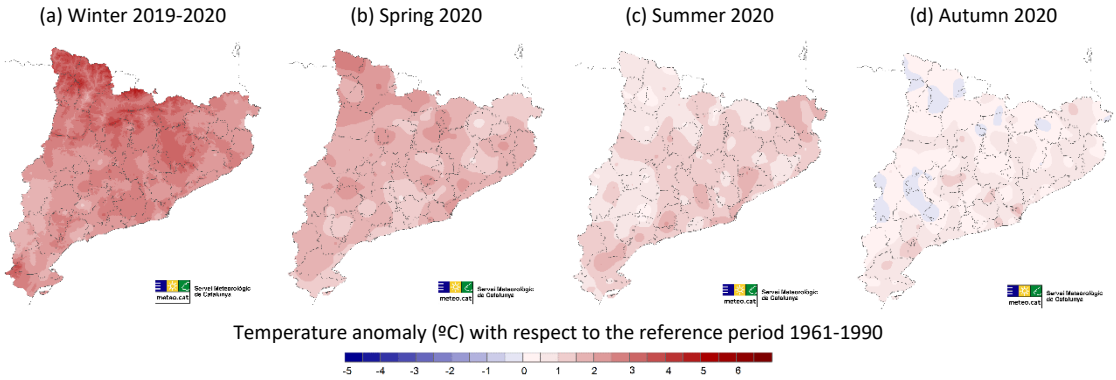

Apart from 2020, the years 2006, 2011, 2014 and 2015 were noteworthy for significant anomalies (around +1.6 ºC). On the other hand, 2010 stands out as the year in the analysed time series with the lowest anomaly (Figure 6), albeit still positive. Nevertheless, the summer of 2010 had a positive anomaly in mean temperature of +1.2 ºC, and there were some heat episodes in August and July (Servei Meteorològic de Catalunya, 2011).

It is also worth analysing the evolution of the summer mean temperature anomalies (Figure 8), as the O_3 peak season occurs mainly during this season (June, July, August and September). As

shown in the graph above, the hottest summer in the period 1950-2021 occurred in 2003, reaching an anomaly of +3.7 ºC with respect to the reference period. The second and third positions are occupied by the summers of 2017, 2015 and 2019, with anomalies of approximately +2.6, +2.5 and +2.3 ºC respectively.

Figure 8. Evolution of the summer mean temperature anomaly [ºC] in Catalonia for the period 1950-2021, with respect to the reference period 1961-1990 (in blue, negative anomalies; in red, positive anomalies). The black curve corresponds to a 13-member Gaussian filter (Servei Meteorològic de Catalunya, 2022a).

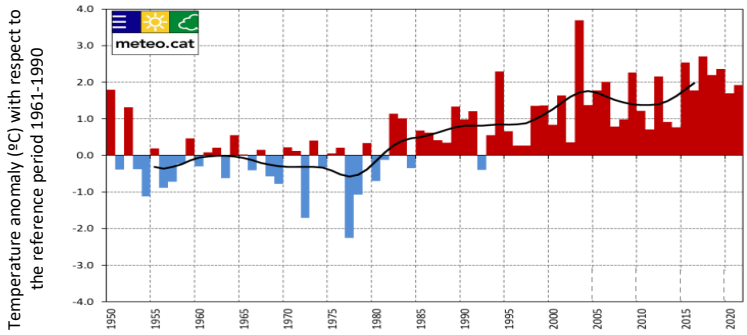

4.3. O_3 levels

In this section, we perform an analysis of the evolution of the O_3 levels in Catalonia during the last two decades (2000-2021). For this purpose, the observations from the official air quality stations are compared with the European legislation and the WHO guidelines (Table 1). Figure 9 shows the 14 air quality zones of Catalonia, which were considered in the present analysis, in addition to the 82 O_3 measuring stations available from 2000 to 2021, according to the classification mentioned in Section 3.4. Note that some stations practically overlap because, over the years, some stations have been relocated within the same municipality, and therefore the station reference has changed.

Figure 9. Air quality zones and O_3 measuring stations available from 2000 to 2021 in Catalonia. The different symbols and colours indicate the type of station (i.e., square for urban; triangle for suburban; circle for rural; blue for background; red for industrial and purple for traffic).

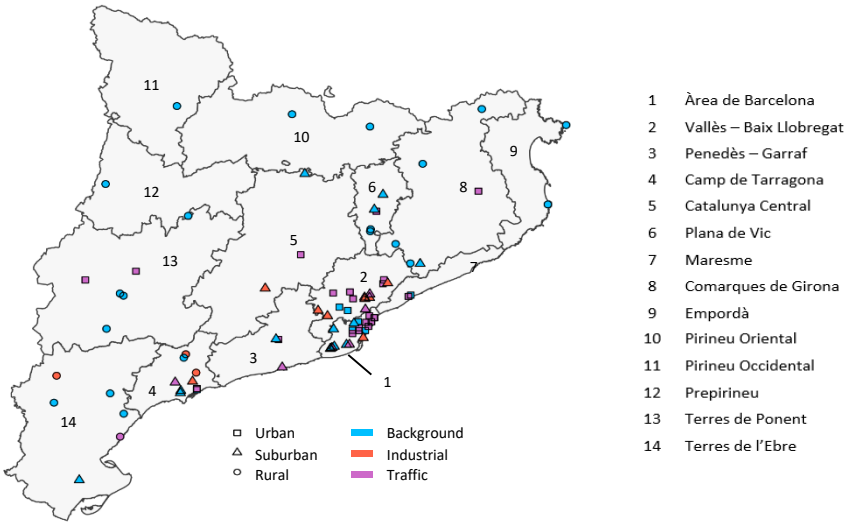

Figure 10 shows the evolution of the number of available stations measuring O_3 levels in Catalonia according to the different types of station. Note that the total number of stations

fluctuates from 2000 to 2021, which is due to the following reasons: (i) not all of the air quality stations were operational during the entire study period; and (ii) between 2014 and 2017 there was a lack of observations at some stations, which may be due to the loss of data by the EEA in the process of switching to the new reporting system. The graphs below evidence that the data loss problem is particularly apparent in industrial and traffic stations. Despite all this, we have not excluded any stations from the analysis because there are few measuring points covering the entire time series.

Figure 10. Evolution of the number of available stations measuring O_3 levels in Catalonia from 2000 to 2021 according to the different types of station (rural, suburban, urban; background, industrial, traffic).

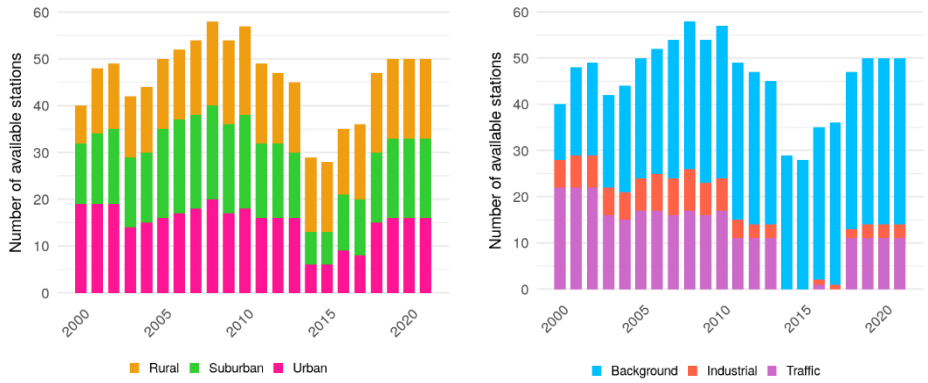

4.3.1. O_3 levels compared to the European Air Quality Directive thresholds

4.3.1.1. Alert threshold (240^h)

According to the European Air Quality Directive (2008/50/EC), the alert threshold (240 µg/m^3) is the level beyond which a brief exposure poses a risk to human health affecting the population as a whole and requiring immediate action. Figure 11 shows the evolution of the total number of exceedances of this threshold per year from 2000 to 2021. The most outstanding years are 2003, with 6 exceedances at 5 air quality stations, and 2019, with 8 exceedances at 7 stations. Both 2003 and 2019 were identified previously in Section 4.2 in the set of years from 1950-2021 with the highest summer mean temperature anomaly. Furthermore, in both cases, all exceedances except one in 2019 coincide temporally with the principal heat episodes that occurred in the corresponding year (Servei Meteorològic de Catalunya, 2021b and 2013). This exception, which occurred in Tarragona, will be further analysed in Section 5.2.3.

Figure 11. Evolution of the total number of exceedances (hours) of the alert threshold included in the European standards for O_3 (240 µg/m^3) per year from 2000 to 2021 (in orange). The secondary axis contains the number of available air quality stations measuring O_3 each year in Catalonia (in blue).

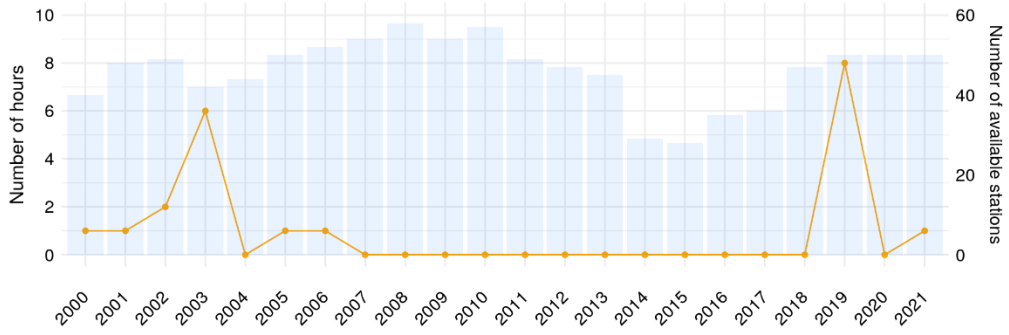

Figure 12 shows the air quality stations affected by the exceedances reported in Figure 11. The most affected air quality zones are Camp de Tarragona, the southern part of Comarques de Girona (Montseny area), Plana de Vic, a station of Penedès-Garraf and Àrea de Barcelona. Camp de Tarragona, Plana de Vic and Montseny are some of the main Spanish O_3 hotspots identified by the MITECO (2023a). Figure 13 locates them on the map and shows the main topographic features of these areas.

Figure 12. Total number of exceedances (hours) of the alert threshold included in the European standards for O_3 (240 µg/m^3) at each air quality station in Catalonia during the period 2000-2021. The grey boundaries correspond to air quality zones.

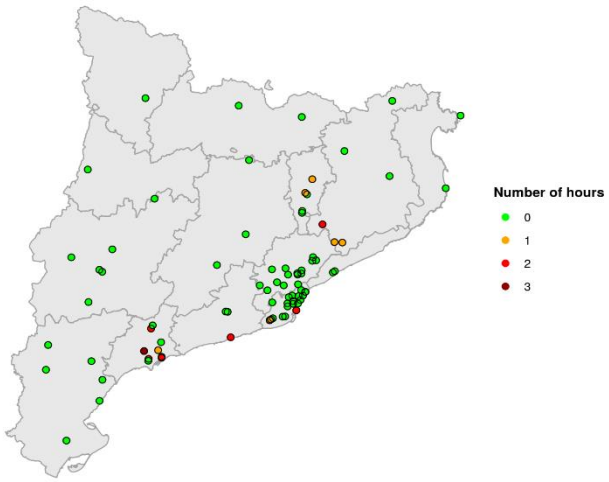

Figure 13. Location and main topographic features of the principal O_3 hotspots of Catalonia (Plana de Vic, Montseny and Camp de Tarragona, in blue). In yellow, the air quality stations in these three regions; in orange, the main emitting areas of O_3 precursors in Catalonia. Adapted from Massagué et al. (2019).

Plana de Vic and Montseny are located downwind of the BMA (Figure 13), the most industrialised and dense urban agglomeration of Catalonia. The urban plume of the BMA, especially from morning traffic rush hours (Jaén, 2020), is driven inland by the combined southeast and southern sea-valley-mountain breeze winds. It crosses the coastal and pre-coastal

Catalan Ranges, where the Montseny area is located, until reaching an intra-mountain plain, where the cities of Tona, Vic and Manlleu lay down. The complex topography of the area protects Plana de Vic from Atlantic advections and continental air masses, but also hinders the dispersion of pollutants. Moreover, the valleys of the two main rivers in the area (Llobregat and Besòs) play an important role in the creation of air-flow patterns: the Congost River is a tributary of the Besòs River and its valley connects the Pre-coastal Depression with Plana de Vic, whereas the Llobregat River valley favours the transport of the BMA plume towards the Manresa area, although this region is not as critical as Plana de Vic in terms of O_3 levels (Massagué et al., 2019).

On the other hand, Camp de Tarragona (Figure 13) includes the city and port of Tarragona and two of the major chemical and petrochemical industrial complexes in Spain. In this case, a meteorological and orographic scenario similar to the one described for Barcelona is responsible for the transport of industrial and urban plumes towards the north and northwest and high O_3 episodes are recorded inland (Querol et al., 2016).

Apart from these three principal O_3 hotspots, Figure 12 showed other air quality zones with exceedances of the alert threshold during the 2000-2021 period (i.e., Penedès-Garraf and Àrea de Barcelona). First, the zone of Penedès-Garraf is not mentioned in recent research as an O_3 hotspot in Catalonia. Nevertheless, as we will see in Figure 16 (Section 4.3.1.3), this is an area in which there have been many exceedances of the 120^{d8max} threshold throughout the analysed period, especially from 2000 to 2010 in Vilanova i la Geltrú. According to Ortega et al. (2006), the power plant in Cubelles and the presence of the sea breeze could lead to O_3 episodes downwind (i.e., Vilanova i la Geltrú). The power plant completely ceased its activity in 2015, and from 2010 onwards it only operated during periods of peak energy demand (Agència Catalana de Notícies, 2015). Since then, exceedances of the 120^{d8max} threshold in the area have considerably decreased.

Àrea de Barcelona is not a typical area for O_3 episodes, since as it is an urban and highly industrialised area, the ozonolysis of VOCs (i.e., oxidation of alkenes with O_3 to form alcohols, aldehydes, ketones or carboxylic acids) and titration by NO consume a lot of the O_3 (Massagué et al., 2022). Nevertheless, the two 120^{d8max} threshold exceedances in the station called *Barcelona (Ciutat Vella – Escullera)*, which is located in the Barcelona Port (see the red dot in Figure 12) could be due, among other factors, to O_3 fumigation: O_3 and its precursors can be trapped in stacked layers formed along the coast and return to land the following day (Jaén, 2020). As we will see in Figure 16, this station has exceeded the 120^{d8max} threshold several times in the analysed period. On the other hand, the alert threshold exceedance that occurred in Gavà in 2019 (see the orange dot in Figure 12) will be further studied in Section 5.2.1.

4.3.1.2. Information threshold (180^{h})

The European Air Quality Directive (2008/50/EC) defines the information threshold as the level beyond which a brief exposure poses a risk to the health of particularly sensitive sections of the population and which requires immediate and appropriate information. Figure 14 shows the evolution of the total number of exceedances of this threshold per year from 2000 to 2021. This limit is obviously exceeded more frequently than the alert threshold as it is lower. The trend over the last two decades is not clear: it might seem to be slightly downward, but there are still recent years, such as 2015 and 2019, with more than 110 exceedances of the information threshold.

Figure 14. Evolution of the total number of exceedances (hours) of the information threshold included in the European standards for O_3 (180 µg/m^3) per year from 2000 to 2021 (in orange). The secondary axis contains the number of available air quality stations measuring O_3 each year in Catalonia (in blue).

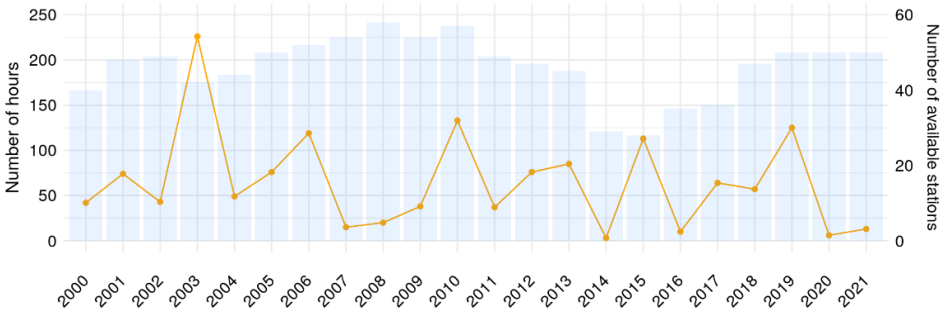

The most outstanding year was again 2003, with 226 exceedances distributed among 23 stations, and many of them coincided temporally with the main heat episodes of that period. Other years with a high number of exceedances were 2006, 2010, 2015 and 2019. The latter two, along with 2003, were listed in Section 4.2 among the years in the analysed period with the highest summer mean temperature anomaly. 2006 was also highlighted as one of the years with the highest annual mean temperature anomaly.

On the other hand, we mentioned in Section 4.2 that 2010 was the coldest year in the last two decades, but according to Figure 14, this is one of the years with the highest number of exceedances of the 180^h threshold. This is partly because high temperatures were recorded in June and July 2010 in different parts of Catalonia, which coincided with the majority of these exceedances. Nevertheless, there are other factors that lead to high O_3 levels apart from temperature, such as winds, pressures or O_3 precursor emissions, among others.

Figure 15 shows the evolution of the total number of exceedances of the information threshold (180^h) per year from 2000 to 2021. As expected, Plana de Vic is the air quality zone with the highest number of exceedances of this threshold in the period 2000-2021. Specifically, this limit was surpassed 625 times there, accounting for 43.9% of the total exceedances in Catalonia. The air quality stations located in the north of Plana de Vic also have a high number of total exceedances: Bellver de Cerdanya (65 hours), Santa Pau (61), Pardines (44) and Berga (41). Other authors, such as Massagué et al. (2019) and Jaén (2020), have already reported high O_3 levels at these stations, which usually receive the remnant of the pollution plume coming from BMA.

Camp de Tarragona is the second air quality zone with the highest exceedances of the 180^h threshold (178 hours in total), corresponding to 12.5 % of the total exceedances in Catalonia from 2000 to 2021. The most affected air quality stations in this area are the two located in Alcover (see the red dots in Camp de Tarragona in Figure 15). O_3 levels in this rural zone are usually higher than in the other urban and suburban stations of Camp de Tarragona. This is due to the wind regimes blowing from the sea (from south to north), as wind transports NO_2 and VOCs from the urban and industrial areas. As mentioned above, there is a major petrochemical complex in this area and chemical industries and oil refineries are known emission sources of VOCs. In addition, the presence of mountains in Alcover does not allow the dispersion of O_3 (Rovira et al., 2021).

Finally, another air quality station with a high number of exceedances (47 hours) of the information threshold is Cap de Creus (Figure 15). This is discussed in more detail in Section 4.3.1.3, as Figure 16 provides a better understanding of the situation in that area.

Figure 15. Total number of exceedances (hours) of the the information threshold included in the European standards for O_3 (180 µg/m^3) at each air quality station in Catalonia during the period 2000-2021. The grey boundaries correspond to air quality zones.

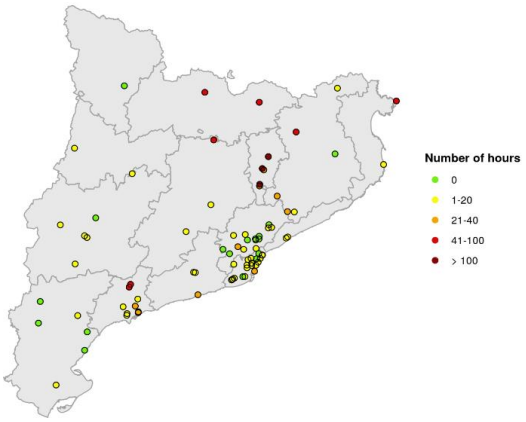

4.3.1.3. Target value for the protection of human health (120^{d8max})

According to the Air Quality Directive (2008/50/CE), a target value is a level fixed to avoid, prevent or reduce harmful effects on human health and/or the environment as a whole, which must be attained where possible over a given period. The O_3^{d8max} may not exceed the 120^{d8max} target value on more than 25 days per calendar year averaged over three years. To facilitate the assessment, in this section, we perform an annual analysis instead of considering the 3-year average.

Figure 16 shows the number of days per year exceeding the 120^{d8max} target value at each air quality station in 2000, 2003, 2019 and 2021. The complete series of graphs for the period 2000-2021 is available in Supplementary Material (Figure S.1), as only the extremes of the period and two representative years are shown here (2003 and 2019, since they were the two years in the study period with the highest number of 240^h exceedances, according to Section 4.3.1.1).

The complete series of graphs shows that in each year of the period 2000-2021, the threshold of 25 days was surpassed by several stations, except 2020, when the O_3 levels decreased and any station exceeded it. At the opposite end of the spectrum was 2006, with 19 stations over the 25-day limit. As mentioned previously, this was one of the years in the analysed period with the highest annual mean temperature anomaly.

The majority of the stations that exceed the 25-day limit in Figure 16 correspond to the most affected air quality zones already mentioned in Sections 4.3.1.1 and 4.3.1.2. However, other stations outside these zones also have more than 25 exceedances, such as those in Cap de Creus, Montsec and Els Torms. They are remote rural background stations, which typically have high daily O_3 average concentrations as they are less affected by NO titration during the night due to their considerable distance to urban and industrial areas (Massagué et al., 2019).

One of the most affected rural background stations is the one located in Cap de Creus. This is the station with the highest number of annual exceedances of the 120^{d8max} threshold (82 days in 2000, according to Figure 16a). The number of exceedances in Cap de Creus was extremely

high in the early years of the time series, albeit decreasing significantly throughout the analysed period, especially from 2006 onwards. This could be due to pollution from the large urban and industrialised area of the Gulf of Lion, especially from Marseille, and from the major shipping routes passing relatively close to Cap de Creus. Similar assumptions have been made for particulate matter (Escudero et al., 2007).

Figure 16. Number of days exceeding the 120^{d8max} target value for the protection of human health at the air quality stations in Catalonia in 2000, 2003, 2019 and 2021. The red vertical line shows the 25-day limit set in the Air Quality Directive.

Figure 17 and Figure 18 show the 93.2 percentile of O_3^{d8max} per station type. This percentile corresponds to the mean 26th highest value. Therefore, exceeding the 120 µg/m^3 threshold is statistically equivalent to surpassing the 25-day limit set by European legislation. On the other hand, in these graphs, it is relevant to show the number of air quality stations available each year, especially in Figure 18, as there is missing data from 2014 to 2017 for industrial and traffic stations. As previously mentioned, these were the most affected by the data loss problem.

According to Figure 17, the 93.2 percentile of O_3^{d8max} is higher at rural stations, followed by suburban and urban sites, as expected. According to the EEA (2020), urban stations, which are

usually located in areas of high NO_x emissions, have lower O_3 levels due to O_3 titration reaction with the emitted NO to form NO_2 and O_2. In contrast, in rural areas, the nocturnal consumption of O_3 (if occurring) is much less pronounced, therefore, O_3 levels tend to be higher (Massagué et al., 2022).

Figure 17. 93.2 percentile of O_3^{d8max} [µg/m^3] for rural, suburban and urban stations in Catalonia from 2000 to 2021. The grey horizontal line shows the 120^{d8max} target value for the protection of human health set in the European Air Quality Directive. The secondary axis contains the number of total available air quality stations measuring O_3 each year in Catalonia (in blue).

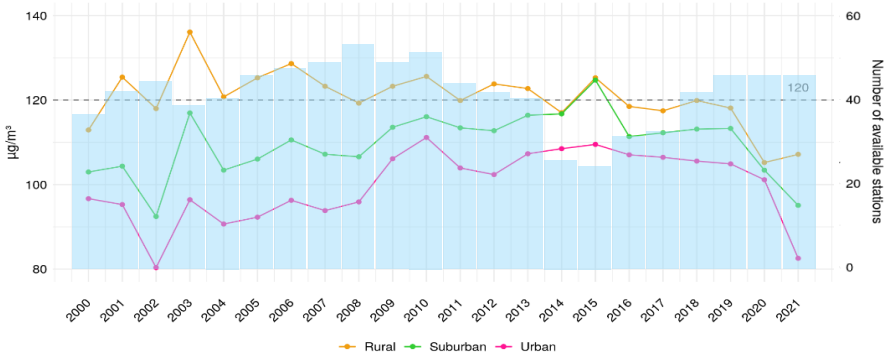

Throughout the analysed period, the 93.2 percentile in urban sites remains significantly below the 120 µg/m^3 limit established by the Directive, but it seems to be slightly increasing across the years (Figure 17). Regarding suburban stations, the threshold is only surpassed in 2015, in which high exceedances of the alert and information levels have already been observed. In this type of station, there is also an upward trend throughout the analysed period. In contrast, the average concentrations for rural stations are generally above the 120^{d8max} limit until 2016, and it seems to be moderately decreasing over the 2000-2021 period.

This seems to be in line with the results of Sicard (2021) and Sicard et al. (2020): they noted a general decrease in O_3 concentrations since the early 2000s in European rural areas, which are usually representative of background levels. This can be attributed to the reduction in O_3-precursor emissions, mainly due to the implementation of stringent vehicle emission standards, the use of exhaust gases abatement techniques and the progress in the storage and distribution of solvents. Nevertheless, these reductions in the precursors were not sufficient to shift from VOC-limited to NO_x-limited regime (defined in Section 1) in the cities, thereby leading to an overall increase in O_3 concentrations in urban environments as NO_x emissions have been reduced.

Furthermore, Figure 17 shows a general decrease in the 93.2 percentile for all three types of station in 2020 and 2021. This overall reduction is due to several reasons. The first one is related to meteorological factors: in the summers of 2020 and 2021, temperatures were not especially high. Although 2020 was the warmest year in Catalonia since 1950, as seen in Section 4.2, the summer mean temperature anomaly was relatively low and there was an absence of general heat waves in Catalonia (Servei Meteorològic de Catalunya, 2021c). The second reason is related to the decrease in O_3 precursor emissions in June-July 2020 associated with the -20% reduction of urban vehicles in almost all cities of Spain, the absence of cruise ships and greatly reduced airport traffic, all in the context of the COVID-19 restrictions. In 2021, the situation was similar to 2020: still with vehicle reduction of -7%, and maintaining the overall reduction of cruise ships and very low airport traffic (MITECO, 2023a). In the same line, at the Northern Hemisphere level,

free tropospheric O_3 decreased in 2020 and 2021 likely due to decreases in emitted pollutants due to reduced human activities, including lockdowns during the COVID-19 pandemic (Ziemke et al., 2022).

Figure 17 also shows a more pronounced reduction in the 2020 93.2 percentile in rural sites than in urban environments. This difference might be due to distinct regimes in these areas: in NO_x-limited environments, which are typical of rural areas, O_3 levels decrease with reductions in NO_x, such as those seen in 2020 (Badia et al., 2023). In contrast, in VOC-limited regimes, which tend to be associated with urban areas, the O_3 levels increase when NO_x decreases. On this basis, we would expect the 93.2 percentile to increase in 2020 in urban areas compared to previous years, but this is not the case as it decreases moderately (Figure 17). This might be due to differing VOCs- or NO_x-limiting regimes among the urban areas or differences in the relative balance between NO titration and VOCs ozonolysis decrease versus O_3 formation decreases (Querol et al., 2021).

On the other hand, Figure 18 shows that industrial and traffic sites are below the 120 µg/m^3 limit throughout the 2000-2021 period, although industrial stations have generally higher levels. In contrast, background sites have the highest values and exceed the Directive limit in several cases, highlighting 2003. As expected, the values recorded in the traffic sites are the lowest because these stations tend to be highly affected by NO titration and the ozonolysis of VOCs from traffic emissions (Massagué et al., 2022), as opposed to the background sites. The difference between traffic and industrial stations might be because the latter generally have lower NO_x levels (Figure S.2 in Supplementary Material), therefore, in industrial areas O_3 titration by NO is weaker than in urban sites.

Figure 18. 93.2 percentile of O_3^{d8max} [µg/m^3] for background, industrial and traffic stations in Catalonia from 2000 to 2021. The grey horizontal line shows the 120^{d8max} target value for the protection of human health set in the European Air Quality Directive. The secondary axis contains the number of total available air quality stations measuring O_3 each year in Catalonia (in blue).

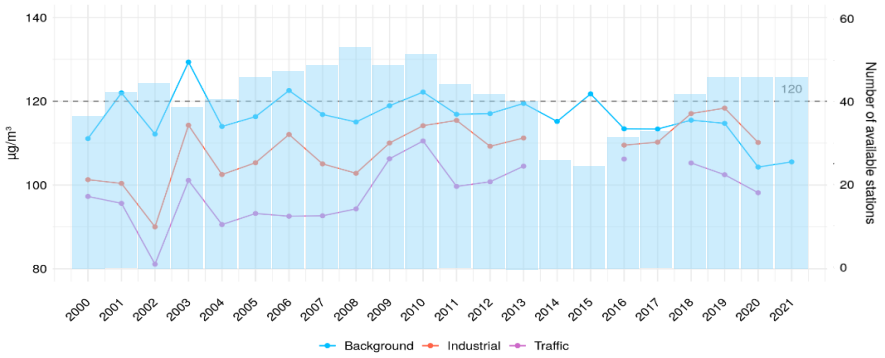

Figure 18 also shows a slightly decreasing trend of the 93.2 percentile at background stations over the analysed period, whereas at industrial and traffic sites the tendency is upward. This may be related to the general downward trend in NO_x levels (Figure S.2 in Supplementary Material) and differences in the VOC-NO_x regime: background areas tend to be NO_x-limited (Valverde et al., 2016), whereas the majority of industrial and traffic sites might be VOC-limited as they have higher NO_x levels compared to VOCs.

4.3.2. O_3 levels compared to the WHO recommendations

As previously mentioned in Section 1, the WHO recommendations establish two thresholds for O_3. One of them (100^{d8max}) is related to short-term exposure, as the thresholds established in the European legislation, whereas the other refers to long-term exposure ($60^{peak\ season}$), as it considers a six-month average as the reference period.

Figure 19 and Figure 20 show that the majority of stations in Catalonia systematically exceeded both thresholds during 2019, 2020 and 2021 (> 3 exceedance days in Figure 19; > 60 µg/m^3 in Figure 20). This also applies to the rest of the years of the entire time series (Figure S.3 and Figure S.4 in Supplementary Material). Therefore, O_3 poses a significant health problem for the inhabitants of Catalonia, both in terms of chronic and episodic exposure.

Figure 19. Number of days per year exceeding the WHO recommended 100^{d8max} threshold at each air quality station in Catalonia in 2019, 2020 and 2021. Note that 3 days is the limit set in the WHO guidelines.

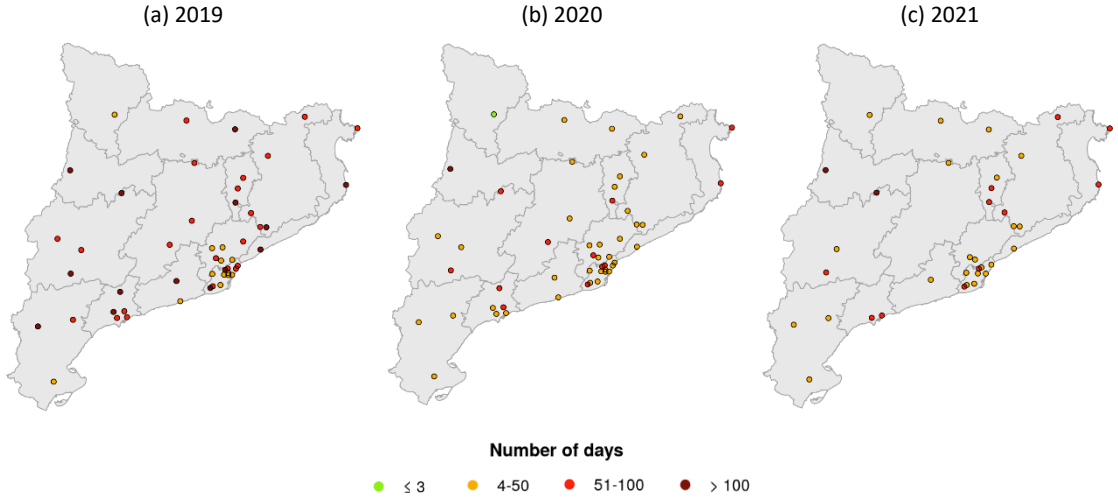

Figure 20. Peak season O_3 concentration [µg/m^3] at each air quality station in Catalonia in 2019, 2020 and 2021. Note that 60 µg/m^3 is the peak season threshold set in the WHO guidelines ($60^{peak\ season}$).

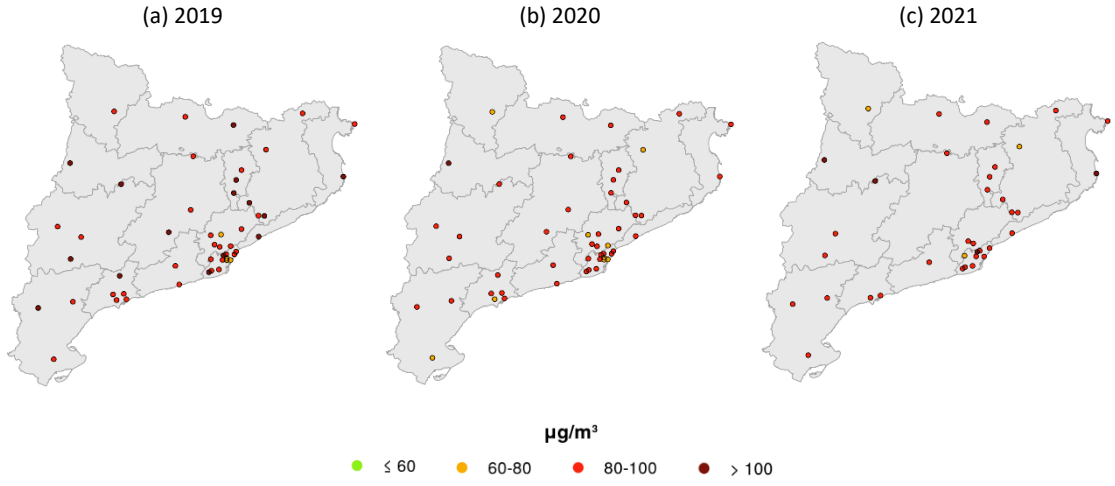

5. Evaluation of CALIOPE for the base case emission scenarios

In this section, we assess the performance of the CALIOPE air quality modelling system (described in Section 3.5.1) to represent surface O_3 concentrations in Catalonia. For this purpose, we compare the modelling outputs against the monitoring data from the official air quality stations measuring O_3 concentrations in Catalonia from April to September 2019. It is necessary to evaluate the model to be able to rely on it when subsequently quantifying the impact of the emission abatement scenarios on O_3 levels.

Here, we consider the modelling results of two base case scenarios (BE1 and BE2) for the IP-4km and CAT-1km CALIOPE domains (further details in Section 3.5.1), respectively, which account for emissions in a business-as-usual situation from April to September 2019. In Section 6, we will use these scenarios as a reference for the quantification of the two emission abatement scenarios based on the PNCCA and the UMP, respectively. The air quality simulations of the PNCCA were done considering the IP-4km working domain as the scope of the runs is national, whereas the simulations related to the UMP focus on the CAT-1km since the spatial coverage is limited to Barcelona and downwind areas.

The year 2019 was selected as the reference year for the modelling exercise as it is the most recent year with available data unaffected by the COVID-19 restrictions and the associated emission decreases. Furthermore, it is the year with the highest exceedances of the alert threshold in the 2000-2021 period (Figure 11). Figure 21 shows the evolution of mean O_3^{d8max} levels at the 50 available measuring points of Catalonia in 2019 per station type (rural, suburban and urban). This graph clearly depicts the annual cycle of O_3 levels, which are higher in spring and summer, especially from April to September, coinciding with the months with the highest solar radiation. It is during these months that occur most of the exceedances of the 120^{d8max} and 100^{d8max} limits established in the European Directive and the WHO guidelines, respectively. Therefore, it is reasonable to choose April-September as the study period.

Figure 21. Mean O_3^{d8max} levels [µg/m^3] for rural, suburban and urban air quality stations from Catalonia in 2019. The grey horizontal lines show the 120^{d8max} and 100^{d8max} limits established in the European Directive and the WHO guidelines, respectively.

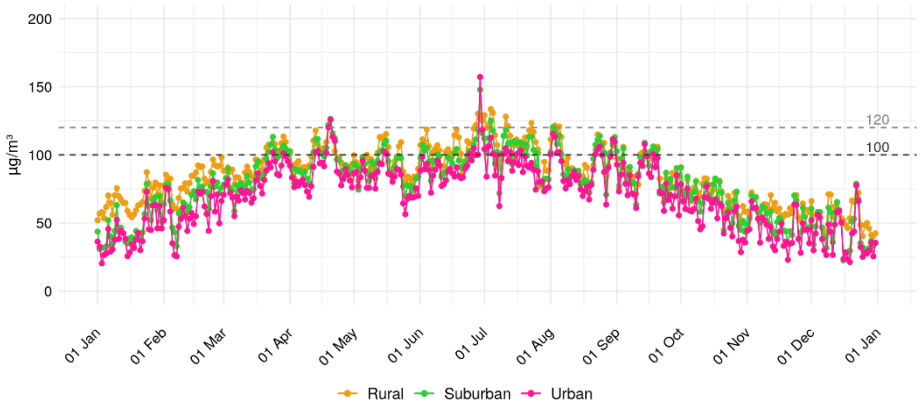

The modelling results obtained with CALIOPE are compared against observed concentrations averaged per type of station (i.e., urban, suburban and rural). We also perform a more detailed evaluation (i.e., at the station level) for the three O_3 episodes that occurred during the period of study to understand the behaviour of the model in the most critical situations.

5.1. General evaluation of the model

Table 2 summarises the statistics (described in Section 3.5.2) obtained when comparing the model outputs for the BE1 and BE2 scenarios with the O_3 concentrations measured at the air quality stations in Catalonia. The statistics were estimated for four different temporal scales, including: O_3^h, O_3^d, O_3^{d8max} and O_3^{d1max} (described in Section 3.4). Both base case scenarios show similar behaviour, characterised by a larger positive nMB at O_3^h and O_3^d scales than at O_3^{d8max} and O_3^{d1max}. On the other hand, in both scenarios, the nRMSE takes values of around 20% at O_3^{d8max} and O_3^{d1max} scales, 40% at O_3^d scale and 50% at O_3^h scale. The PCC is around 0.6-0.7 in all cases, so the O_3 temporal variability is reasonably well reproduced.

Table 2. Evaluation of the model for BE1 and BE2 scenarios over April-September 2019 for the 50 available air quality stations in 2019, at different temporal scales: O_3^h, O_3^d, O_3^{d8max} and O_3^{d1max}. The statistics are MB [µg/m^3], nMB [%], RMSE [µg/m^3], nRMSE [%] and PCC. N is the number of observations.

Scenario	Temporal scale	MB [µg/m^3]	nMB [%]	RMSE [µg/m^3]	nRMSE [%]	PCC	N
BE1	O_3^h	26.08	37.97	34.99	50.94	0.67	219600
BE1	O_3^d	26.16	38.10	30.13	43.88	0.62	9150
BE1	O_3^{d8max}	16.95	18.00	22.80	24.21	0.62	9150
BE1	O_3^{d1max}	14.34	13.88	22.72	21.99	0.62	9150
BE2	O_3^h	22.40	32.61	32.29	47.01	0.67	219600
BE2	O_3^d	22.47	32.73	27.00	39.33	0.61	9150
BE2	O_3^{d8max}	12.45	13.23	20.37	21.63	0.61	9150
BE2	O_3^{d1max}	9.65	9.35	20.72	20.06	0.61	9150

The general overestimation in the modelled concentrations is an already known characteristic of the CMAQ model and is mainly attributed to the underestimation of O_3 titration by NO, which may lead to this considerable overprediction of low O_3 at night seen in Figure 22 (Guevara et al., 2014). This is the reason why nMB and nRMSE have higher values on the temporal scales that include night-time values (O_3^h and O_3^d) than those that only consider daytime values (O_3^{d8max} and O_3^{d1max}). Nevertheless, since O_3 peaks occur at daytime, these overestimations of O_3 levels at night are not as relevant.

Based on the results in Table 2, it may seem that the Barcelona UMP modelling exercise (BE2) has a better performance than the PNCCA (BE1), as it generally shows a lower mean bias and root mean square error. Nevertheless, when analysing specific O_3 episodes and stations, the behaviour of the model in BE2 is not always better than that of BE1, as we show in Section 5.2. These dissimilarities between the two simulations may be due to differences in model resolution (4km x 4km in PNCCA compared to 1km x 1km in Barcelona UMP) or in emissions (the Barcelona UMP modelling exercise accounts for more accurate emissions in Barcelona city).

Figure 22 includes the daily cycle of observed and modelled O_3^h mean concentrations. Specifically, Figure 22c shows that the above-mentioned characteristic of the CMAQ model on the underestimation of O_3 titration by NO is more significant at urban stations as they are located near large point sources. It is in these areas that O_3 titration is more pronounced due to higher levels of NO and NO_2. For this reason, urban sites have larger nMB than rural areas (e.g.,

at O_3^{d8max} scale, 26% and 22% at urban stations against 12% and 7% at rural stations, for BE1 and BE2, respectively, according to Table S.1 in Supplementary Material). Rural stations are the ones in which the discrepancy between modelled and observed concentrations is the lowest, since O_3 titration is weaker there, especially during the day. The higher overestimation of O_3 levels at urban sites can also be observed in Figure 23, Figure 24, Figure 25 and Figure 26, which show the weekly and the April-September cycles of observed and modelled O_3^h and O_3^{d8max} mean concentrations. As expected, the difference between modelled and observed concentrations is lower in O_3^{d8max} (Figure 24 and Figure 26) than in O_3^h (Figure 23 and Figure 25) in all the station types, since the O_3^{d8max} does not consider night-time values, which are more overestimated, as previously mentioned.

Figure 22. Daily cycle of observed (in black) and modelled (BE1 in blue and BE2 in pink) O_3^h mean concentrations [µg/m^3] from April to September 2019 for rural, suburban and urban stations.

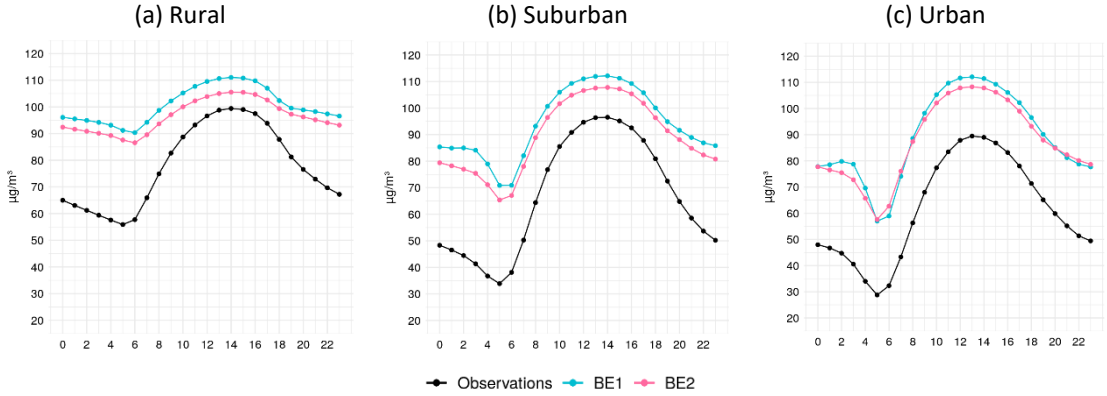

On a weekly basis, both O_3^h (Figure 23) and O_3^{d8max} (Figure 24) mean concentrations are considerably steady at rural stations, whereas at suburban and especially at urban sites the "weekend effect" is noticeable (Adame et al., 2014). This phenomenon usually occurs in urban areas, under VOC-limited conditions, where a reduction in NO_x emissions from road traffic on weekends leads to a lower O_3 titration by NO and, therefore, to higher O_3 concentrations. In contrast, at rural stations, which are less affected by traffic emissions and tend to be NO_x-limited systems, this effect is not observed (Sicard et al., 2020). In general, it seems that the model reproduces this phenomenon more accurately in the Barcelona UMP simulation (BE2), probably because it has a better spatial resolution than the PNCCA simulation (BE1).

Figure 23. Weekly cycle of observed (in black) and modelled (BE1 in blue and BE2 in pink) O_3^h mean concentrations [µg/m^3] from April to September 2019 for rural, suburban and urban stations.

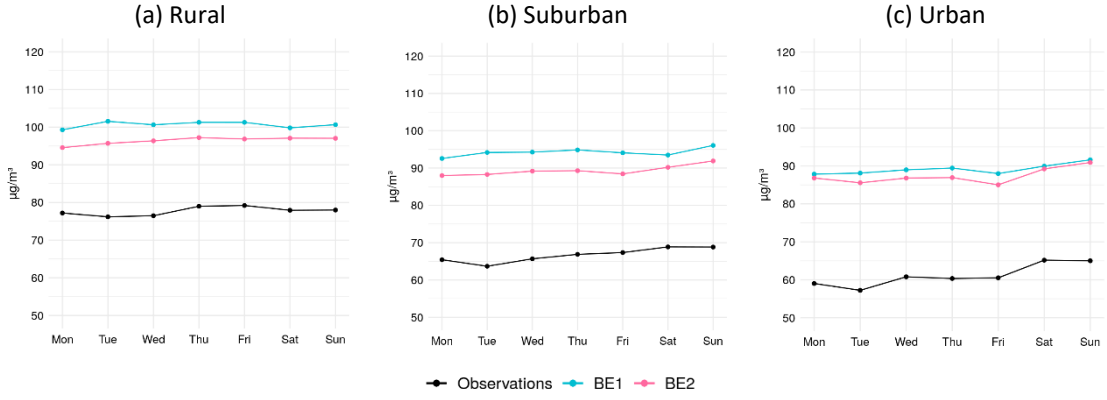

Figure 24. Weekly cycle of observed (in black) and modelled (BE1 in blue and BE2 in pink) O_3^{d8max} mean concentrations [µg/m^3] from April to September 2019 for rural, suburban and urban stations.

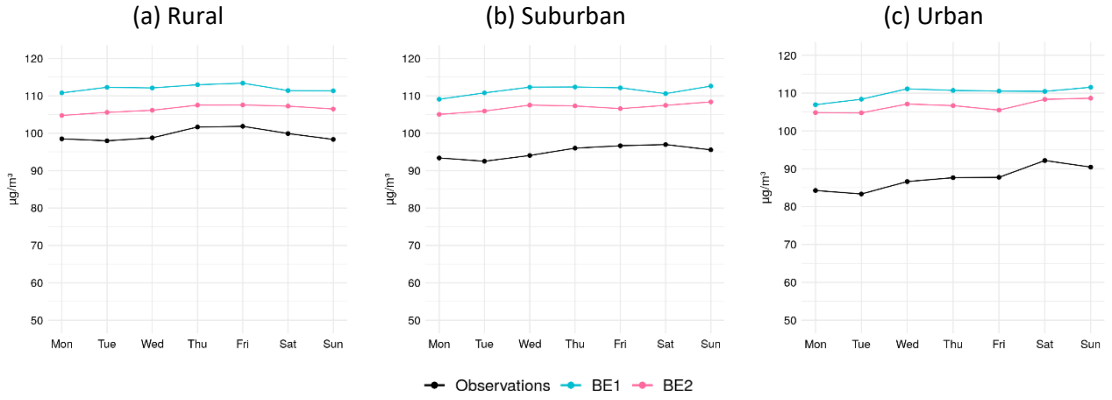

Regarding monthly averages, Figure 25 and Figure 26 show a considerably consistent correlation of O_3 seasonality: both modelled and observed mean concentrations follow a similar trend, either for O_3^h and O_3^{d8max}. The highest levels are generally found in June and July, and the lowest in September. This is in line with the results of the study of Massagué et al. (2019) for the 2005-2017 period: they found that most of the exceedances of the information threshold (180^h) occurred in June and July. We might expect the highest levels to occur in August, as temperatures are usually higher in this month compared with June. Nevertheless, industrial and traffic activity decreases in August, resulting in lower concentrations of precursors and, therefore, reduced O_3 levels.

Figure 25. April-September cycle of observed (in black) and modelled (BE1 in blue and BE2 in pink) O_3^h mean concentrations [µg/m^3] in 2019 for rural, suburban and urban stations.

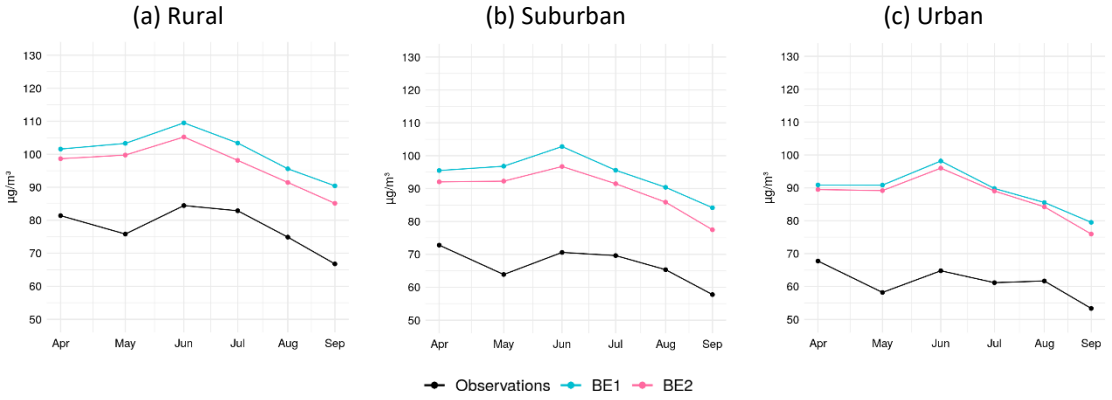

Figure 26. April-September cycle of observed (in black) and modelled (BE1 in blue and BE2 in pink) O_3^{d8max} mean concentrations [µg/m^3] in 2019 for rural, suburban and urban stations.

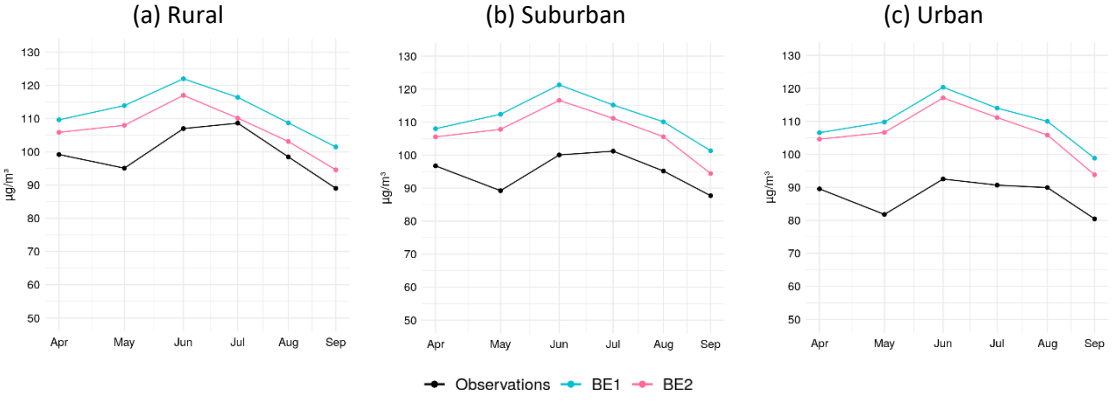

Overall, despite the overestimation of O_3 levels at night and at urban stations, the model performs reasonably well, especially during the day and at rural and suburban stations, which are the times and sites in which O_3 levels are the highest, as seen in previous sections. Therefore, the performance of the CALIOPE modelling system on average terms appears sufficiently good for applying it in the two modelling exercises considered in this study.

5.2. Evaluation of the model during O_3 episodes

In this section, we assess the model performance in the stations that registered the O_3 episodes that occurred in 2019. O_3 episodes occur when ground-level concentrations exceed threshold values set by the European Air Quality Directive (Table 1). In this study, we consider the alert threshold (240^h) for the identification of episodes. It is essential to analyse the behaviour of CALIOPE during these events to be able to rely on the model when quantifying the impact of emission reduction scenarios on O_3 episodes.

During 2019, there were a total of three O_3 episodes: Episode A (28-29 June), Episode B (23 July) and Episode C (18 September). In Supplementary Material (Section S.3), we provide a characterisation of these episodes, including a meteorological analysis. Table 3 summarises the exceedances of the alert threshold recorded from April to September 2019. In addition, we also analyse some stations that registered information threshold exceedances (summarised in Table 4) during these episodes to further understand each event. Note that in this work we use the Coordinated Universal Time (UTC). Therefore, the local official time in Spain is UTC +2 in summer and UTC +1 in winter.

Table 3. List of exceedances of the alert threshold (240^h) recorded from April to September 2019: episode, date, station and O_3 observed concentrations [$\mu g/m^3$].

Episode	Date	Station	O_3 observed concentrations [$\mu g/m^3$]
A	28 June 12h UTC	Sant Celoni	245.04
	28 June 13h UTC	Santa Maria de Palautordera	248.04
	28 June 13h UTC	Montseny	250.05
	28 June 14h UTC	Montseny	263.05
	29 June 14h UTC	Gavà	242.04
B	23 July 13h UTC	Vic	243.04
	23 July 14h UTC	Manlleu	240.04
C	18 September 11h UTC	Tarragona	248.04

Table 4. List of exceedances of the information threshold (180^h) during Episodes A, B and C which have been considered in the model assessment: episode, date and station. Note that O_3 observed concentrations are not provided here because the 180^h threshold was surpassed continuously in each station.

Episode	Date	Station
A	28 June	Tona
		Vic
		Manlleu
B	23 July	Tona
C	18 September	Vila-seca

In the following sections, we show the O_3^h modelled and observed concentrations for each episode in the affected stations, although we use the O_3^{d8max} scale to calculate the relative difference between the modelled and observed values, as it is more representative of the O_3 concentrations during the entire day.

5.2.1. Episode A (28-29 June)

Figure 27 and Figure 28 show the most representative hours of Episode A (Figure S.8 and Figure S.10 in Supplementary Material represent the rest of the episode). They include the O_3 concentration values predicted by the model in BE1 and BE2 (shaded colour) and those measured by the air quality stations (coloured dots). Specifically, they show how the breeze transported O_3 and its precursors mainly originated in the BMA inland, following the Besòs-Congost pathway (28 June; Figure 27) or the Llobregat pathway (29 June; Figure 28), as detailed in Section S.3.1 in Supplementary Material.

On 28 June (Figure 27), exceedances of the alert threshold were recorded in Sant Celoni, Santa Maria de Palautordera and Montseny, but the O_3 plume also affected Plana de Vic, leading to subsequent information threshold exceedances in Tona, Vic and Manlleu. In this case, the modelled O_3 plume (both for BE1 and BE2) agrees reasonably well with the observed concentrations at the stations, either temporally or spatially, as the shaded colours generally correspond to the colours of the dots.

On 29 June (Figure 28), an alert threshold exceedance was recorded in Gavà. Nevertheless, although the model detected that an episode was occurring, it located the O_3 peaks further to the northeast compared to the observations, both for BE1 and BE2. This might be due to inaccurate reproduction of the meteorology.

Figure 27. Observed and modelled O_3 concentrations [µg/m^3] in Catalonia for 28 June from 12h to 15h UTC (top: BE1; bottom: BE2). The shaded contour plot shows modelled values while the coloured dots correspond to the air quality station measurements.

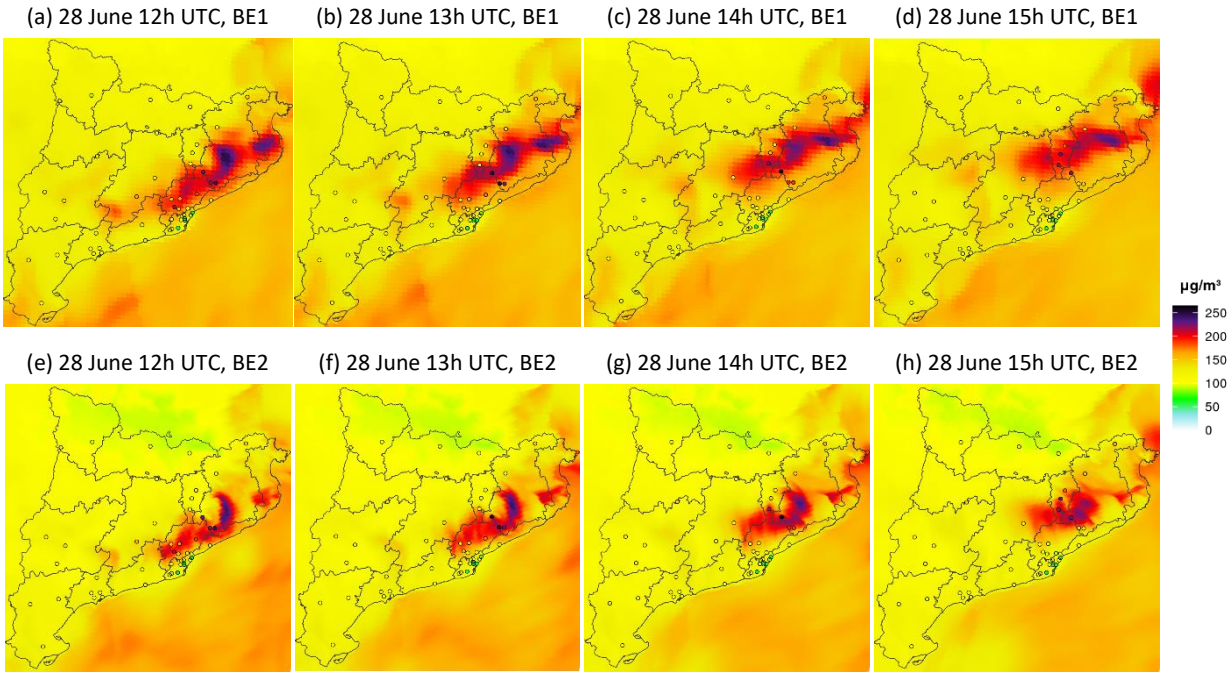

Figure 28. Observed and modelled O_3 concentrations [µg/m^3] in Catalonia for 29 June from 12h to 15h UTC (top: BE1; bottom: BE2). The shaded contour plot shows modelled values while the coloured dots correspond to the air quality station measurements.

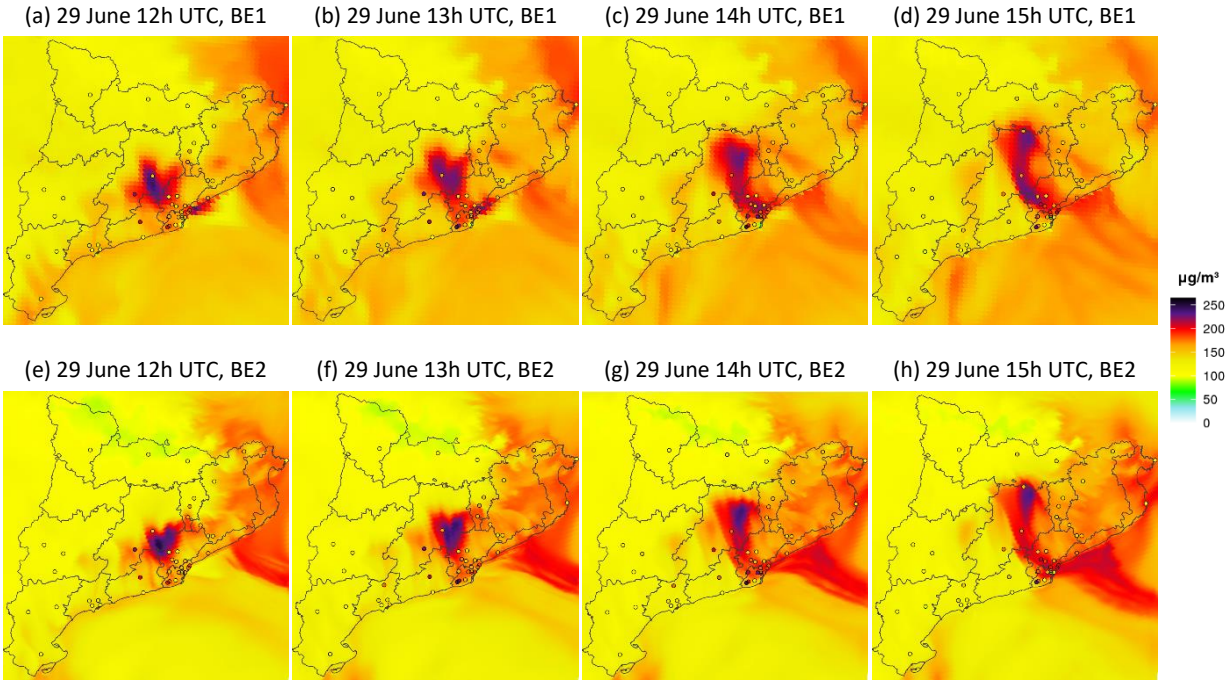

Figure 29 shows the observed and modelled concentrations at each station at O_3^h scale for the BE1 and BE2 scenarios, whereas Table 5 quantifies the difference between the modelled and the observed values at O_3^{d8max} scale.

Figure 29. Observed (in black) and modelled (BE1 in blue and BE2 in pink) O_3^h concentrations [µg/m^3] for the affected stations in Episode A from 24 June to 8 July. The grey horizontal lines show the 240^h alert threshold and the 180^h information threshold established in the European Directive.

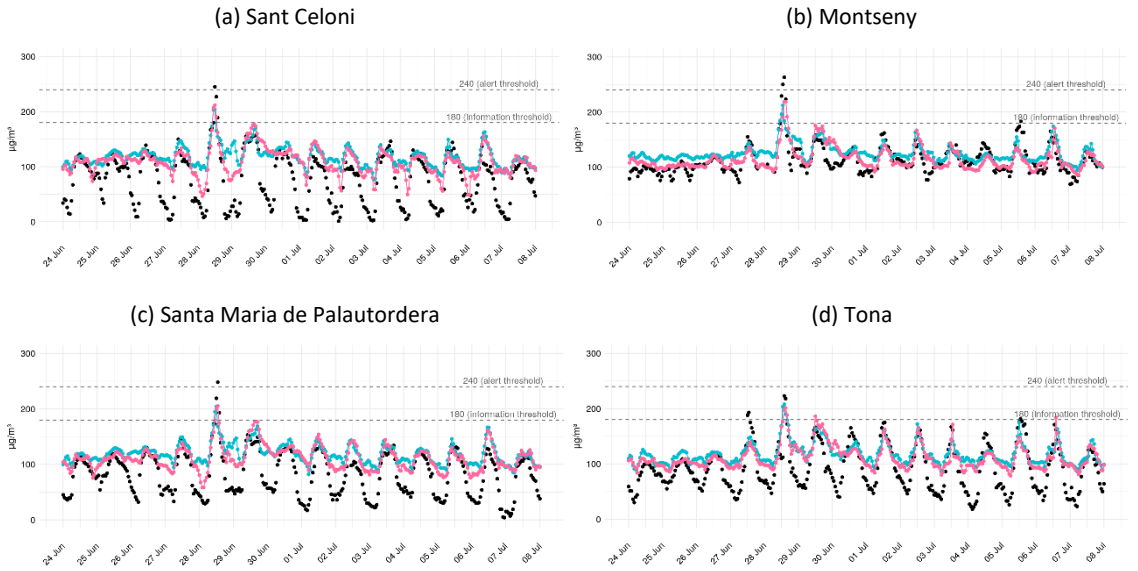

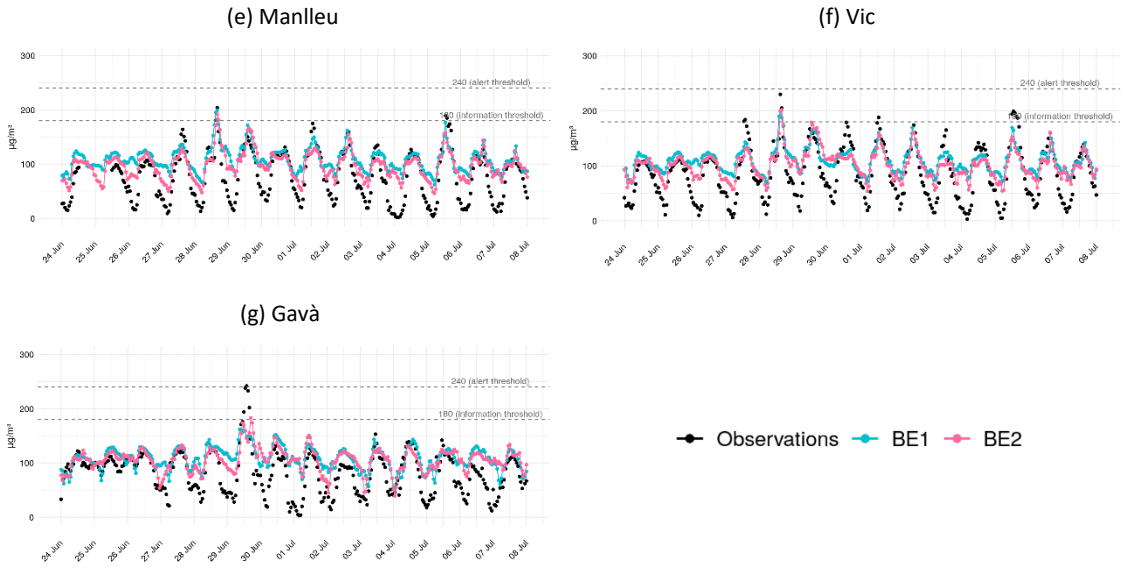

Table 5. Evaluation of the model for BE1 and BE2 scenarios compared to observations at the most affected stations during Episode A (28-29 June), at O_3^{d8max} scale. The statistics are MB [µg/m³] and nMB [%].

		Observations	BE1			BE2		
		Observed O_3^{d8max} concentration [µg/m³]	Modelled O_3^{d8max} concentration [µg/m³]	MB [µg/m³]	nMB [%]	Modelled O_3^{d8max} concentration [µg/m³]	MB [µg/m³]	nMB [%]
Alert threshold exceedances (240^h)								
28 June	Sant Celoni	181.66	169.72	-11.94	-6.57	167.71	-13.94	-7.68
	Montseny	199.66	180.45	-19.21	-9.62	181.88	-17.78	-8.90
	Santa Maria de Palautordera	176.66	169.42	-7.24	-4.10	167.86	-8.79	-4.98
29 June	Gavà	200.04	156.63	-43.40	-21.70	162.48	-37.56	-18.78
Information threshold exceedances (180^h)								
28 June	Tona	155.15	177.77	+22.61	+14.57	169.99	+14.83	+9.56
	Vic	153.28	162.79	+9.51	+6.20	153.62	+0.34	+0.22
	Manlleu	140.28	161.74	+21.46	+15.30	154.96	+14.68	+10.47

On 28 June, according to Figure 29 a-c, the model predicted the episode in the Montseny area reasonably well, although it slightly underestimated the peak in all cases (between -9.62% and -4.10% for BE1, and between -8.90% and -4.98% for BE2, at O_3^{d8max} scale, as shown in Table 5). On the other hand, the model correctly predicted the maximum O_3^h value in Plana de Vic (Figure 29 d-f), especially in Manlleu, although slightly overestimating the O_3^{d8max} concentration (between +6.20% and +15.30% for BE1, and between +0.22% and +10.47% for BE2, according to Table 5). Overall, on 28 June, the model predicted reasonably well the observed concentrations in terms of magnitude (both for BE1 and BE2). The underestimation of the peaks is in line with the general performance of CMAQ model, which has difficulties in capturing the high O_3 peaks (Petetin et al., 2023).

In contrast, on 29 June, the model predicted an increase in O_3 concentrations in Gavà (Figure 29 g) but the underestimation of the peak in this case was more significant, as it located the episode further to the northeast for both scenarios, as we already mentioned. For O_3^{d8max},

the relative difference between the modelled and the observed values was -21.70% for BE1 and -18.78% for BE2 (Table 5).

Figure 29 clearly illustrates the characteristic of the CMAQ model mentioned in Section 5.1 concerning the underestimation of O_3 titration by NO and, therefore, the overestimation of O_3 levels at night. Nevertheless, night O_3 concentrations at Montseny station are high compared to the other stations. This station is located at 693 m of altitude, compared to the 145 m or 460 m of Sant Celoni and Manlleu stations, respectively. This indicates that the station in Montseny may be measuring background O_3 concentrations remaining in high altitudes due to sea breeze circulation (Jaén et al., 2021b).

5.2.2. Episode B (23 July)

Episode B occurred on 23 July and mainly affected Plana de Vic, where the alert threshold was exceeded (Vic and Manlleu). We also include the station of Tona in the assessment because the information threshold was exceeded there and the alert threshold was nearly surpassed.

Figure 30 and Figure S.9 in Supplementary Material show how the O_3 plume moves inland over time towards Plana de Vic, affecting first the southernmost station located in Tona, closely followed by Vic and eventually Manlleu, situated further north. In this case, the modelled O_3 concentrations are in close agreement with the observed concentrations for both scenarios.

Figure 30. Observed and modelled O_3 concentrations [µg/m^3] in Catalonia for 23 July from 12h to 15h UTC (top: BE1; bottom: BE2). The shaded contour plot shows modelled values while the coloured dots correspond to the air quality station measurements.

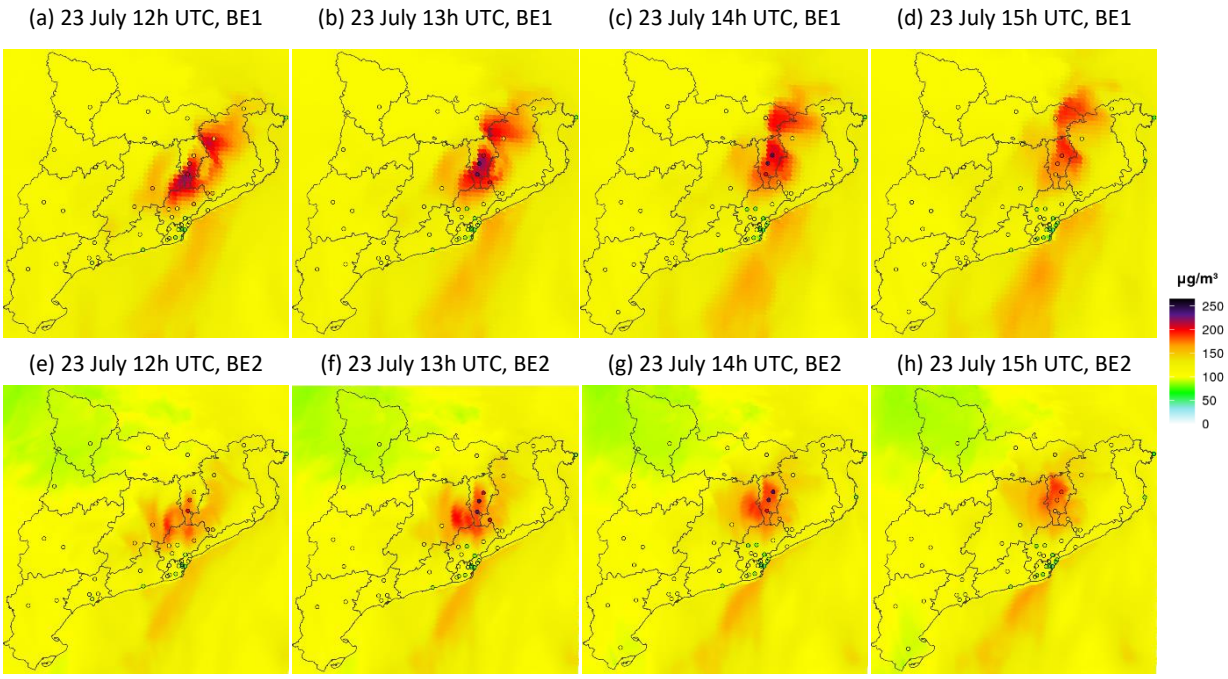

This is the episode that was better predicted by the model, either in terms of location, time and magnitude, according to Figure 30, Figure 31 and Table 6, especially for the BE1 scenario. In this case, the relative difference between modelled and observed values for O_3^{d8max} ranges from -2.10% to +4.00% (Table 6). On the other hand, in the BE2 scenario, the model slightly underestimated the peak, although the relative differences were not significantly high (between -6.30% and -9.16%, at O_3^{d8max} scale, according to Table 6). This is an example of what we already

mentioned in Section 5.1: although at a global level it seems that the model performs better in the BE2 scenario than in BE1, for some specific O_3 episodes such as this one, the model has better results in the BE1 scenario. This may be due to differences in model resolution, meteorology or emissions.

Figure 31. Observed (in black) and modelled (BE1 in blue and BE2 in pink) O_3^h concentrations [µg/m^3] for the affected stations in Episode B from 19 to 28 July. The grey horizontal lines show the 240^h alert threshold and the 180^h information threshold established in the European Directive.

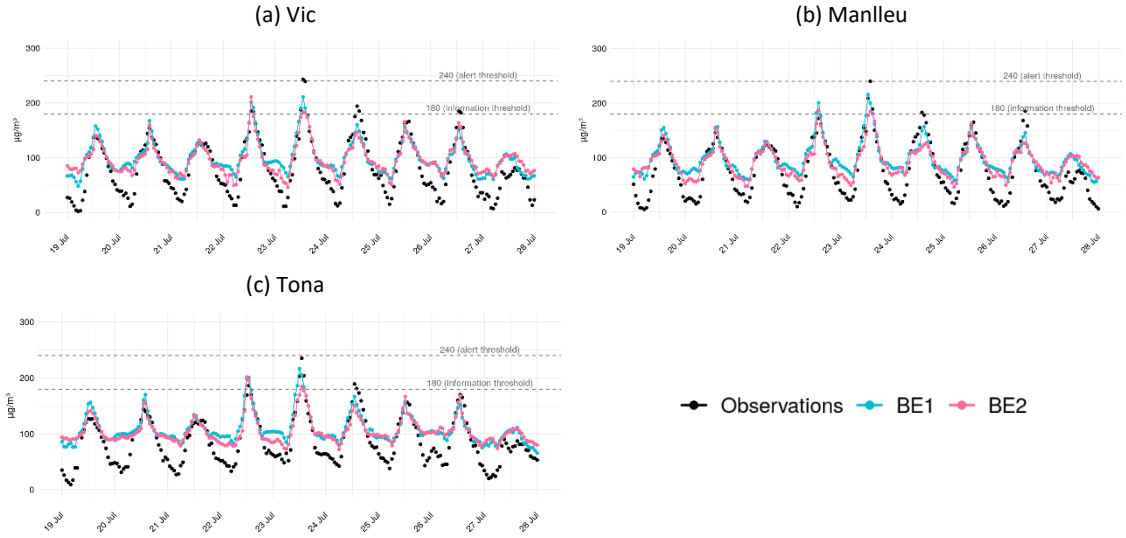

Table 6. Evaluation of the model for BE1 and BE2 scenarios compared to observations at the most affected stations during Episode B (23 July), at O_3^{d8max} scale. The statistics are MB [µg/m^3] and nMB [%].

		Observations	**BE1**			**BE2**		
		Observed O_3^{d8max} concentration [µg/m^3]	Modelled O_3^{d8max} concentration [µg/m^3]	MB [µg/m^3]	nMB [%]	Modelled O_3^{d8max} concentration [µg/m^3]	MB [µg/m^3]	nMB [%]
Alert threshold exceedances (240^h)								
23 July	Vic	174.66	170.99	-3.67	-2.10	159.04	-15.62	-8.94
	Manlleu	169.66	170.39	+0.73	+0.43	154.12	-15.54	-9.16
Information threshold exceedances (180^h)								
23 July	Tona	169.78	176.58	+6.80	+4.00	159.09	-10.69	-6.30

5.2.3. Episode C (18 September)

Episode C occurred exclusively in the southern part of Camp de Tarragona air quality zone, and the alert threshold was only exceeded in the city of Tarragona on 18 September, although the information threshold was also surpassed on the same day in Vila-seca. This was a rather particular episode because, in addition to being located in a specific and limited area (both stations are near the coastline), the alert threshold was exceeded at 11 h UTC, whereas O_3 peaks usually occur a few hours later when solar radiation is at its highest.

We provide further explanation of this unusual event in Supplementary Material (Section S.3.2), but it was probably caused due to a combination of different causes: (i) the usual high levels of O_3 precursors in this area resulting from the petrochemical complex and the urban agglomeration; (ii) the existence of meteorological stagnation and relatively high temperatures (Servei Meteorològic de Catalunya, 2023b) that enhanced O_3 formation and (iii) a possible

breeze blockage that caused air masses that had been accumulating overnight over the Mediterranean, loaded with NO_x and O_3, to return to land on the morning of 18 September when the sea breeze direction shifted.

Figure 32 and Figure 33 show that the model was not capable of reproducing this episode, neither in BE1 nor BE2 scenarios. The relative difference between the modelled and the observed values at O_3^{d8max} is considerably important (e.g., -30.62% and -32.64% for BE1 and BE2, respectively, according to Table 7). This might be because the model did not properly reproduce the meteorological conditions, i.e., the stagnation situation and the breeze blockage.

Figure 32. Observed and modelled O_3 concentrations [µg/m^3] in Catalonia for 18 September from 10h to 13h UTC (top: BE1; bottom: BE2). The shaded contour plot shows modelled values while the coloured dots correspond to the air quality station measurements.

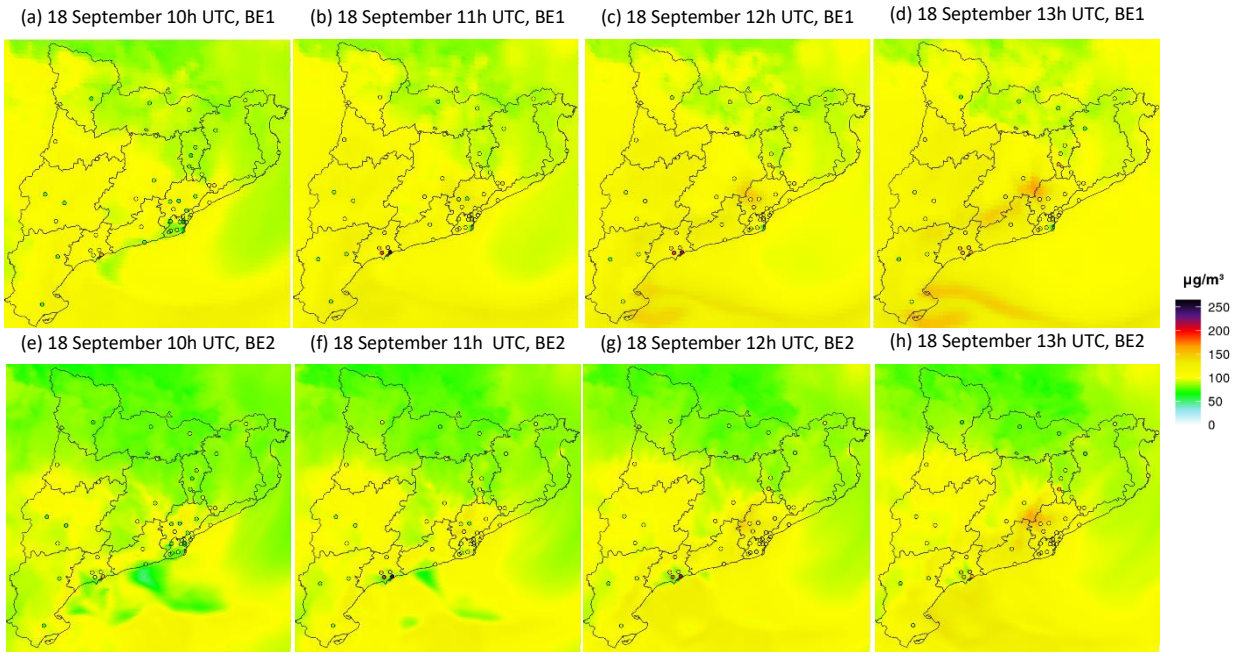

Figure 33. Observed (in black) and modelled (BE1 in blue and BE2 in pink) O_3^h concentrations [µg/m^3] for the affected stations in Episode C from 13 to 22 September. The grey horizontal lines show the 240^h alert threshold and the 180^h information threshold established in the European Directive.

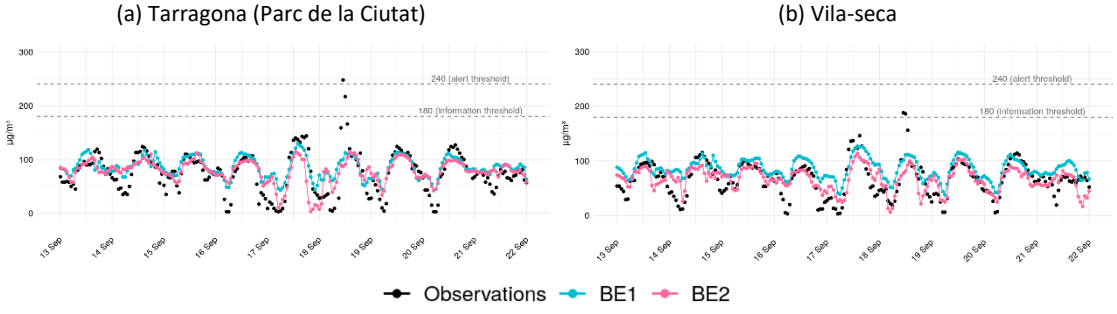

Table 7. Evaluation of the model for BE1 and BE2 scenarios compared to observations at the most affected stations during Episode C (18 September), at O_3^{d8max} scale. The statistics are MB [µg/m^3] and nMB [%].

		Observations	**BE1**			**BE2**		
		Observed O_3^{d8max} concentration [µg/m^3]	Modelled O_3^{d8max} concentration [µg/m^3]	MB [µg/m^3]	nMB [%]	Modelled O_3^{d8max} concentration [µg/m^3]	MB [µg/m^3]	nMB [%]
Alert threshold exceedances (240^h)								
18 September	Tarragona	153.53	106.52	-47.01	-30.62	103.42	-50.11	-32.64
Information threshold exceedances (180^h)								
18 September	Vila-seca	123.02	105.71	-17.32	-14.08	84.63	-38.39	-31.20

6. Quantification of the impact of the emission abatement scenarios

The main objective here is to quantify the impact of two emission abatement scenarios based on national and local programs, including the Air Pollution Control Programme emission scenario (PE_PNCCA) and the Barcelona Urban Mobility Plan (PE_BCN_UMP), in comparison with the base case emission scenarios (BE1 and BE2), which are assumed as a reference. Table 8 summarises the four scenarios considered in this study and their abbreviations.

Table 8. Summary of the base case scenarios and the emission abatement scenarios considered in this study.

Scenario	Abbreviation
Base case emission scenario 1 for the PNCCA modelling exercise (IP-4km)	BE1
Emission abatement scenario based on PNCCA (IP-4km)	PE_PNCCA
Base case emission scenario 2 for the Barcelona UMP modelling exercise (CAT-1km)	BE2
Emission abatement scenario based on the Barcelona UMP (CAT-1km)	PE_BCN_UMP

This section is structured as follows: first, in Section 6.1, we provide a description of the two emission abatement scenarios. As previously mentioned, the definition of the emission scenarios and execution of the CALIOPE system are beyond the scope of this study. In Section 6.2, we analyse the numerical outputs of the four emission simulations that we executed in the framework of this study using the HERMESv3 model to quantify the impact of the PE_PNCCA and PE_BCN_UMP scenarios on NO_x and NMVOC primary anthropogenic emissions over Catalonia. In Section 6.3, we quantify the impact of the emission abatement scenarios on O_3 levels during April-September, whereas in Section 6.4 we discuss the impact of both scenarios on the three O_3 episodes that occurred in 2019.

6.1. Description of the emission abatement scenarios

6.1.1. National Air Pollution Control Programme emission scenario (PE_PNCCA)

The emission scenario PE_PNCCA includes the measures and policies reported in the National Energy and Climate Plan (Plan Nacional Integrado de Energía y Clima, PNIEC; MITECO, 2020) and the National Air Pollution Control Programme (Programa Nacional de Control de la Contaminación Atmosférica, PNCCA; MITECO, 2019) of the MITECO and to be implemented before 2030. This emission scenario is compared with the BE1 base case emission scenario.

The emissions of the PE_PNCCA scenario were calculated by the AC-BSC research group using HERMESv3, as described in Petetin et al. (2023). Emissions estimated for the BE1 scenarios were scaled using specific adjustment factors (AFs) that vary per sector and pollutant. These AFs were estimated using the official Spanish emission projections reported under the agreement on the Long-Range Transboundary Air Pollution (LRTAP; United Nations Economic Commission for Europe, 1979), which include the expected impacts from the implementation of the PNIEC and the PNCCA.

Table 9 shows NO_x and NMVOC emissions for the years 2019 and 2030 according to official MITECO projections, in addition to the associated relative differences and the estimated AF for each sector. These are the reference years considered in the BE1 and PE_PNCCA scenarios, respectively. Emissions were scaled for those sectors with a higher contribution to total NO_x

(61%) and NMVOC (56%) emissions (energy industry, manufacturing industry, road transport, solvent use, maritime traffic and solvent use).

The overall relative changes of total NO_x and NMVOC anthropogenic emissions over Spain comparing the PE_PNCCA to the BE1 are -37.0% and -4.9%, respectively (Petetin et al., 2023). The most significant NO_x emission changes between 2019 and 2030, according to Table 9, are those related to the transport sector (-60.8% for road transport and -43.1% for national shipping) and the energy and manufacturing industries (-30%). For road transport, the reductions are mainly related to the expected implementation of low emission zones in all municipalities with more than 50000 inhabitants, while in the case of the energy and manufacturing industries, the reductions are attributable to the foreseeable combined effect of the virtual extinction of coal use and the further decrease in the consumption of oil-based fuels for power generation (PNCCA; MITECO, 2019).

Table 9. NO_x and NMVOC annual emissions (E, kt/year) for 2019 and 2030 (according to official MITECO projections), associated relative differences between 2030 and 2019 emission levels (RD, %) and adjustment factors (AF) per sector. Adapted from Petetin et al. (2023).

NFR code: Sector	NO_x				NMVOC			
	E (2019) [kt/year]	E (2030) [kt/year]	RD (%)	AF [unitless]	E (2019) [kt/year]	E (2030) [kt/year]	RD (%)	AF [unitless]
1A1: Energy industry	55.6	38.9	-30.0	0.70	10.3	12.9	+25.2	1.26
1A2: Manufacturing industry	110.8	76.8	-30.7	0.69	20.8	21.4	+2.9	1.03
1A3b: Road transport	211.2	82.7	-60.8	0.39	20.2	23.2	+14.9	1.15
1A3d: National shipping*	40.8	23.2	-43.1	0.57	1.8	1.4	-22.2	0.75
2D: Use of solvents	0.1	0.1	0.0	1.00	257.6	244.5	-5.1	0.95

*National shipping accounts for only 10% of total shipping.

Regarding NMVOC, the most important variation is the +25.2% increase in emissions from the energy industry sector (Table 9). This is mainly related to the expected increase in electricity production from biomass, which has a significantly higher NMVOC emission factor in comparison with other fuels such as natural gas or coal (EMEP/EEA, 2019). Another considerable relative change is the one concerning NMVOC emissions from the road transport sector (+14.9%), which is due to the expected higher proportion of petrol vehicles compared to diesel cars in the coming years (PNCCA; MITECO, 2019), and the NMVOC emission factors (EF) for the latter are approximately one order of magnitude lower than the ones reported for petrol cars (EMEP/EEA, 2019). Furthermore, it is also assumed that in the following years, there will be an increase in the number of motorbikes and mopeds in the vehicle fleet, both of which also present large NMVOC emission factors (EMEP/EEA, 2019).

6.1.2. Barcelona Urban Mobility Plan emission scenario (PE_BCN_UMP)

The emission scenario PE_BCN_UMP considers a set of traffic restriction measures included in the latest Urban Mobility Plan presented by the City Council of Barcelona, which aims at reducing on-road traffic emissions and thus improving air quality through the renewal and reduction of private motorised transport in the city.

These traffic management strategies include the application of (I) a low emission zone to accelerate the renewal of the circulating vehicle fleet, (II) a superblock system consisting of the

traffic pacification of various streets within an area comprised of several blocks, and (III) a set of tactical urban planning actions, which reduce the space that private transport has on specific streets of the city. Overall, these measures are expected to reduce the number of private vehicles in the city by -25% (Rodriguez-Rey et al., 2022).

Furthermore, this emission abatement scenario also accounts for the electrification of the docks of the Port of Barcelona in the framework of the NEXIGEN project (Port de Barcelona, 2022), which is expected to reduce emissions from hoteling activities by -38% (Rodriguez-Rey et al., 2023). In this scenario, we also assumed that this electrification will be extended to the docks of the Port of Tarragona.

6.2. Impact of the emission abatement scenarios on NO_x and NMVOC anthropogenic emissions over Catalonia

This section includes the analysis of the results obtained in the emission modelling exercise that has been conducted as part of this study. We run four simulations, one per scenario, over the 1km x 1km Catalonia domain from April to September 2019. Using the HERMESv3 model (described in Section 3.6), we estimated the differences in NO_x and NMVOC anthropogenic emissions between the two sets of emission abatement and base case scenarios. The obtained results are summarised in Table 10 and Table 11. Figure 34 and Figure 35 show the spatial distribution of NO_x and NMVOC emissions in each scenario, in addition to the relative differences between the abatement (PE_PNCCA and PE_BCN_UMP) and the base case scenarios (BE1 and BE2).

Table 10. NO_x monthly emissions (E, t/month) for the base case (BE1 and BE2) and the abatement scenarios (PE_PNCCA and PE_BCN_UMP) over Catalonia from April to September 2019 and the absolute (t) and relative differences (RD, %) among scenarios.

	April	May	June	July	August	September	TOTAL
E(BE1) [t/month]	6265.55	6540.02	6649.02	7374.09	6973.73	7685.24	**41487.64**
E(PE_PNCCA) [t/month]	3988.68	4146.17	4277.36	4657.16	4328.52	5344.70	**26742.59**
E(PE_PNCCA-BE1) [t/month]	-2276.87	-2393.85	-2371.65	-2716.93	-2645.21	-2340.54	**-14745.05**
Relative difference [%]	**-36.34**	**-36.60**	**-35.67**	**-36.84**	**-37.93**	**-30.46**	**-35.54**
E (BE2) [t/month]	6102.52	6288.54	6155.77	6654.65	6205.33	6894.18	**38300.99**
E (PE_BCN_UMP) [t/month]	5919.50	6088.70	5973.91	6475.09	6073.25	6719.56	**37250.00**
E(PE_BCN_UMP-BE2) [t/month]	-183.02	-199.84	-181.86	-179.56	-132.09	-174.62	**-1050.99**
Relative difference [%]	**-3.00**	**-3.18**	**-2.95**	**-2.70**	**-2.13**	**-2.53**	**-2.74**

Table 11. NMVOC monthly emissions (E, t/month) for the base case (BE1 and BE2) and the abatement scenarios (PE_PNCCA and PE_BCN_UMP) over Catalonia from April to September 2019 and the absolute (t) and relative differences (RD, %) among scenarios.

	April	May	June	July	August	September	TOTAL
E (BE1) [t/month]	7754.78	7711.90	7636.69	7664.58	7373.11	7707.55	**45848.61**
E (PE_PNCCA) [t/month]	7416.32	7367.21	7311.21	7355.28	7091.32	7388.14	**43929.49**
E(PE_PNCCA-BE1) [t/month]	-338.46	-344.69	-325.48	-309.29	-281.78	-319.42	**-1919.12**
Relative difference [%]	**-4.36**	**-4.47**	**-4.26**	**-4.04**	**-3.82**	**-4.14**	**-4.19**
E (BE_2) [t/month]	7802.96	7753.91	7652.76	7663.77	7364.60	7699.96	**45937.96**
E (PE_BCN_UMP) [t/month]	7753.89	7700.42	7604.31	7616.07	7329.50	7653.43	**45657.62**
E(PE_BCN_UMP-BE2) [t/month]	-49.07	-53.49	-48.45	-47.70	-35.10	-46.52	**-280.34**
Relative difference [%]	**-0.63**	**-0.69**	**-0.63**	**-0.62**	**-0.48**	**-0.60**	**-0.61**

Compared to the respective base case scenarios, the overall relative changes of total NO_x anthropogenic emissions over Catalonia are -35.54% for PE_PNCCA and -2.74% for PE_BCN_UMP (Table 10). For NMVOC emissions, these rates are -4.19% and -0.61%, respectively (Table 11). NO_x and NMVOC emissions are largely reduced in the PE_PNCCA than in the PE_BCN_UMP, as the latter only reduces emissions in the city of Barcelona, and mainly from local road transport, whereas the PE_PNCCA measures impact over all the study domain and several sources. Nevertheless, the city of Barcelona is one of the main hotspots of NO_x and NMVOC in Catalonia, according to Figure 34 a-b and Figure 35 a-b. Thus, the emission reductions achieved through the PE_BCN_UMP should not be downplayed.

The aforementioned percentages show that, in both sets of scenarios, the reduction of NMVOCs between the PE and the BE is very limited when compared to NO_x. In the case of PE_PNCCA, one of the reasons justifying this difference is the fact that in three of the sectors considered in Table 9, NMVOC emissions are assumed to increase against BE1, whereas in the case of NO_x, the majority of the sectors are expected to reduce emissions from 2019 and 2030. Furthermore, the use of solvents sector, which is the largest NMVOC emitter, is expected to reduce its emissions only -5.1%. On the other hand, in the second set of scenarios (BE2 and PE_BCN_UMP), NMVOC emission reductions are even smaller because the proposed measures in the emission abatement scenario only affect the road transport and shipping sectors, which have a limited contribution to overall NMVOC emissions in Catalonia (Figure 5).

It is observed that the total emissions reported in BE1 and BE2 are not exactly the same, the differences being larger for NO_x (41487.64 t in BE1 versus 38300.99 t in BE2). This is because in the first set of scenarios (BE1 and PE_PNCCA), traffic emissions were estimated using HERMESv3, while in the second set (BE2 and PE_BCN_UMP), road transport emissions for the city of Barcelona were estimated making use of a tailor-made coupling system between HERMESv3 and a macroscopic traffic model to be able to simulate the actions related to the Barcelona Urban Mobility Plan (Rodriguez-Rey et al., 2021). This traffic model is based on the detailed multimodal transport model Barcelona Virtual Mobility Lab and its domain comprises the First Crown of the Metropolitan Area of Barcelona plus a large extension including its access highways. Thus, considering that this traffic model tackles the road transport sector in the main NO_x emitting area of Catalonia, and that NO_x emissions related to the road transport sector are higher than those of NMVOC, it is in NO_x that the difference in emissions is most pronounced depending on whether or not the traffic model is applied.

On a monthly basis, both sets of simulated scenarios follow a similar pattern: in the BEs and consequently in the PEs, NO_x emissions increase between April and September, with two peaks in July and September, and a trough in August. In contrast, NMVOC emissions remain reasonably stable, although in August they also decrease significantly (according to Table 10 and Table 11). This decline in emissions of both pollutants in August results from the substantial drop in industrial activity and on-road transport, especially in Barcelona.

September stands out as the month with the highest NO_x emissions, especially in rural areas, which is due to the seasonality assumed for agricultural machinery, with emissions from tractors and rotavators starting to increase in September and reaching their maximum in November. Since, in both PEs, emissions from the agricultural machinery sector are not modified, the

increase of NO_x emissions from this sector in September leads to lower relative differences between PEs and BEs during this month.

Figure 34. Spatial distribution of NO_x (left) and NMVOC (right) emissions [t/year] for the base case scenario BE1 and the emission abatement scenario PE_PNCCA over Catalonia from April to September 2019, and the relative differences among PE_PNCCA and BE1 (RD, %).

(a) NO_x emissions, BE1 [t/year]

(b) NMVOC emissions, BE1 [t/year]

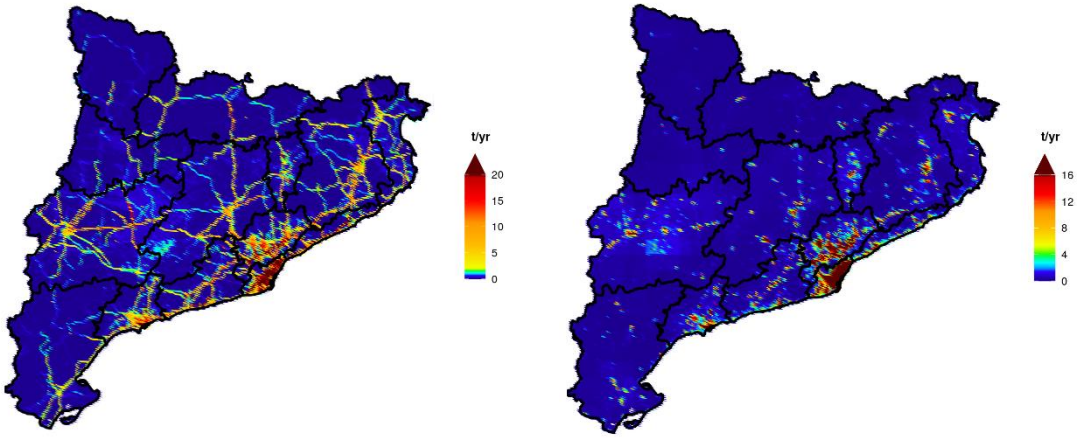

(c) NO_x emissions, PE_PNCCA [t/year]

(d) NMVOC emissions, PE_PNCCA [t/year]

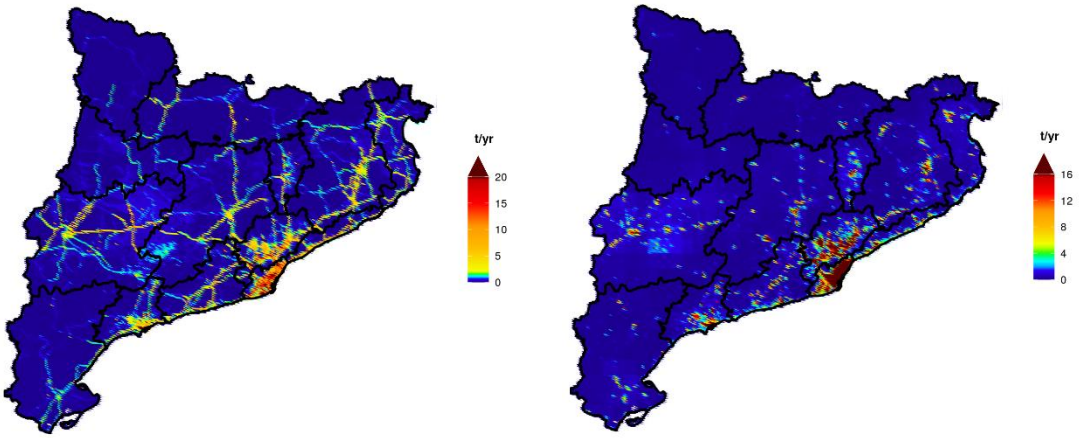

(e) NO_x emissions, RD [%]

(f) NMVOC emissions, RD [%]

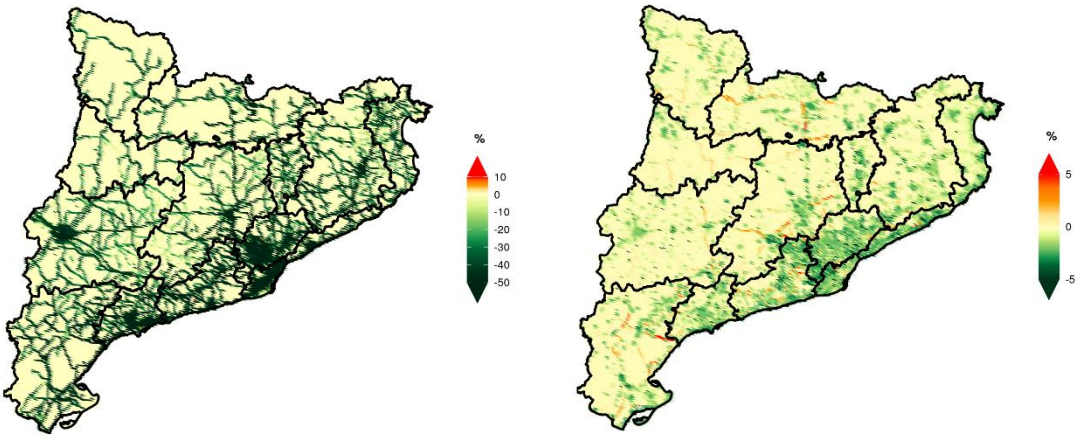

Figure 35. Spatial distribution of NO_x (left) and NMVOC (right) emissions [t/year] for the base case scenario BE2 and the emission abatement scenario PE_BCN_UMP over Catalonia from April to September 2019, and the relative differences among PE_BCN_UMP and BE2 (RD, %).

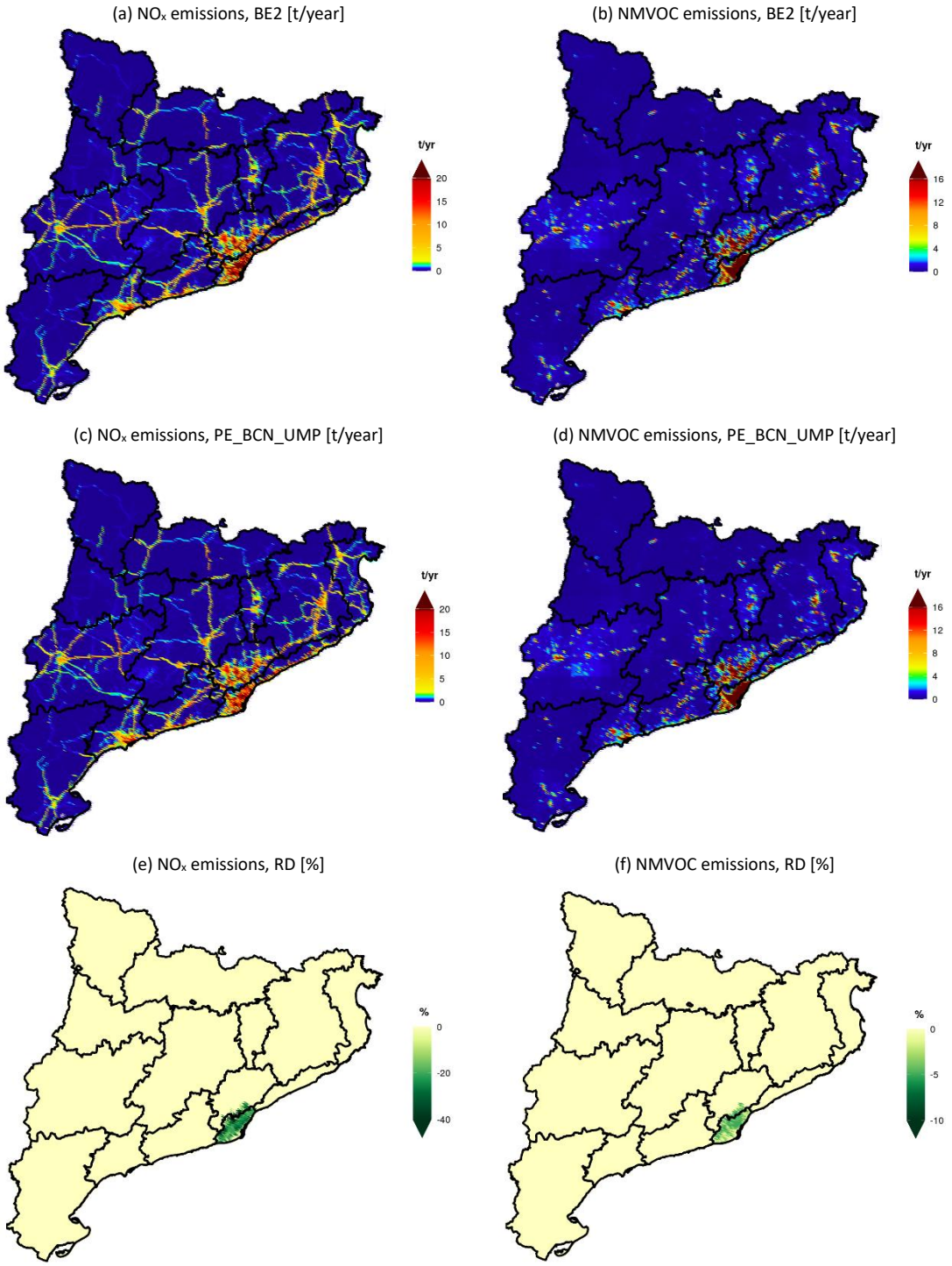

In terms of spatial distribution, Figure 34a and Figure 35a show that the BMA is the largest emitter of NO_x in Catalonia. Other cities such as Tarragona, Girona and Lleida also stand out, in addition to the main roads, which are clearly marked on the maps. In the case of NMVOC, emissions are more concentrated around urban areas due to the domestic use of solvents, especially in Barcelona, although other important cities of Catalonia also emerge in the maps (Figure 34b and Figure 35b).

It is precisely in the areas with the highest emissions that the largest reductions in the PE_PNCCA against BE1 occur, as shown in Figure 34e-f: NO_x emissions are expected to decrease around -50% in the BMA and in Tarragona, Lleida and Girona cities. In addition, Figure 34e shows a noticeable reduction in NO_x emissions on most of the main roads. On the other hand, the largest decreases (around -5%) in NMVOC emissions would occur in the most populated areas, where the use of solvents is predominant and where the decrease in NMVOC emissions associated with this sector is expected to be most noticeable. On the contrary, in rural areas, a slight increase in the NMVOC emissions related to the PE_PNCCA scenario is observed (in reddish colours in Figure 34f). This owes to the fact that in these areas the emissions related to the use of solvents sector are minor, hence NMVOC emissions from road transport, which are expected to increase in the following years, predominate.

Regarding PE_BCN_UMP against BE2, the reductions in NO_x (Figure 35e) and NMVOC (Figure 35f) emissions are focused in Air Quality Zone 1, predictably, since this is the target area of these scenarios. Specifically, according to the PE_BCN_UMP, NO_x emissions would be reduced on average by around -23% in this area, whereas the average reduction in terms of NMVOC would be around -3%. Nevertheless, when considering the entire Catalonia (Table 10 and Table 11), these relative differences diminish because the emission reductions only occur in a specific area.

6.3. Impact of the emission abatement scenarios on O_3 concentrations

6.3.1. O_3^{d8max} concentrations over Catalonia

Figure 36 shows the impact of the emission abatement scenarios on gridded mean O_3^{d8max} levels between April and September 2019 compared to the BEs, while Table 12 indicates the mean, minimum and maximum differences between PEs and BEs across the entire domain.

Figure 36. Differences between gridded mean O_3^{d8max} levels [µg/m^3] estimated in the abatement (PE) and base case (BE) scenarios (April-September 2019).

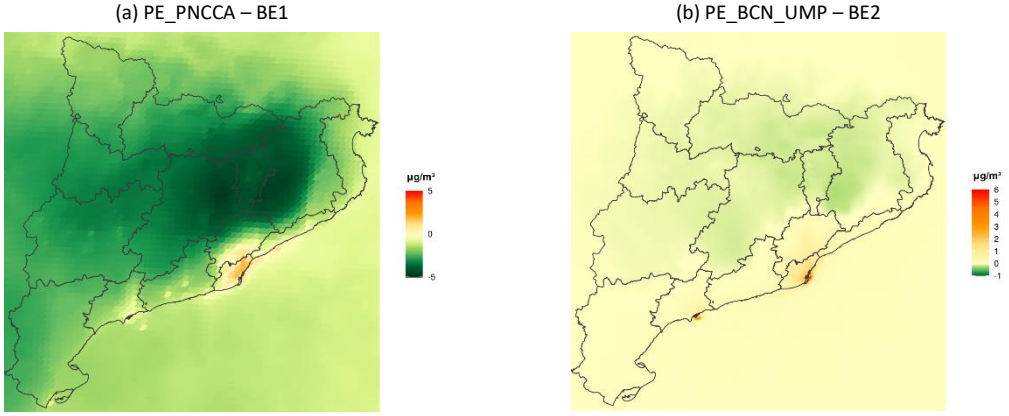

Table 12. Mean, minimum and maximum differences between gridded mean O_3^{d8max} levels [µg/m^3] estimated in the abatement (PE) and base case (BE) scenarios (April-September 2019).

	Metric	PE_PNCCA – BE1 [µg/m^3]	PE_BCN_UMP – BE2 [µg/m^3]
O_3^{d8max}	Mean	-0.95	-0.03
	Minimum	-5.07	-0.27
	Maximum	+4.08	+5.64

Concerning the PE_PNCCA scenario, the mean difference of O_3^{d8max} against BE1 is -0.95 µg/m^3, whereas the minimum and maximum values are -5.07 and +4.08 µg/m^3, respectively (Table 12). On average, O_3^{d8max} levels are reduced in most of Catalonia with respect to the BE1 scenario, but slightly increased in the BMA (Figure 36a). The highest reductions (between -4 and -5 µg/m^3) are located in inland Catalonia, mainly in the air quality zones of Catalunya Central, Plana de Vic and Comarques de Girona.

An average increase of +3 µg/m^3 in O_3^{d8max} is found in the BMA (Figure 36a). This effect is linked to the decrease of NO_x levels in a VOCs-limited environment such as Barcelona, which leads to rising O_3 concentrations (Tobías et al., 2020). In the city of Tarragona, the increases in O_3^{d8max} levels between PE_PNCCA and BE1 are lower: about +0.5 or +1 µg/m^3. This area, although it has high NO_x concentrations, also has significant levels of NMVOC associated with the petrochemical industrial complexes. Therefore, despite being an urban area, Tarragona is not as VOC-limited as Barcelona, thus reductions in NO_x levels lead to lower increases in O_3.

In contrast, in the second set of scenarios, the mean reduction in O_3^{d8max} levels of the PE_BCN_UMP against the BE2 in all Catalonia is -0.03 µg/m^3, while the minimum and maximum values are -0.27 and +5.64 µg/m^3, respectively (Table 12). The PE_BCN_UMP scenario would also lead to slight reductions (up to -0.27 µg/m^3) in O_3^{d8max} levels in some of the most problematic regions of Catalonia in terms of O_3 episodes: Comarques de Girona, Plana de Vic, Catalunya Central and part of Pirineu Oriental. Nevertheless, as expected, the overall reduction is more moderate compared to the PE_PNCCA scenario.

On the other hand, similarly to the PE_PNCCA, O_3^{d8max} mean levels would increase between +4 and +5 µg/m^3 in some areas of the city of Barcelona (Figure 36b) due to the effect of VOCs-limited environments mentioned before. Figure 36b also shows increases around +3 µg/m^3 in the Tarragona port area, as the electrification of the Tarragona port docks was included in the PE_BCN_UMP scenario.

Overall, the reported reductions are modest compared to the typical O_3 levels reported in Section 4.3. This is in part because the imported O_3 is the largest contributor to the ground-level O_3 concentration in the Iberian Peninsula, accounting for 46-68% of the daily mean O_3 concentration during exceedances of the 120^{d8max} target value for the protection of human health (Pay et al., 2019). Thus, the margin for reducing mean O_3 concentrations locally is highly limited and is confined mainly to O_3 episodes. Indeed, Massagué et al. (2019) found that most of the days in the period 2005-2017 in which the O_3 information threshold of 180 µg/m^3 was surpassed in Plana de Vic, the exceedance occurred when an additional local contribution was added to the regional external O_3 and the surface fumigation from the mid-troposphere high-O_3 upper layers arising from the concatenation of the vertical recirculation of air masses: O_3 supply by the channelling of the BMA pollution plume towards Vic through the Besòs-Congost rivers valley. Therefore, O_3 episodes require a more detailed analysis that we develop in Section 6.4 to quantify the impact of the emission abatement scenarios in these particular events.

6.3.2. O_3^{d8max} and O_3^{d1max} concentrations at air quality stations

In this section, we estimate the O_3 concentrations that the air quality stations would have measured under the emission abatement scenarios.

To perform this exercise, we followed the same approach as proposed by Petetin et al. (2023). In their work, the authors note that the CMAQ model represents reasonably well the spatio-temporal variability of O_3 concentrations but has more difficulties in capturing the high O_3 peaks, as seen in Section 5.2. This behaviour is unfortunately widespread in most air quality models (Im et al., 2015). Consequently, the direct exploitation of simulated absolute O_3 concentrations does not usually enable a proper investigation of exceedances of high O_3 thresholds, especially when they occur relatively infrequently. To partly address this limitation, it is assumed that the relative response of the model to the emissions reductions is correct, or at least less biased. This assumption is challenging to assess, and may be too strong in some situations, but remains a pre-requisite in any emission scenario analysis.

In view of this, to estimate the values that the stations would have measured under the emission abatement scenarios (Obs_Δ_PE in Figure 37), we applied the modelled relative difference of O_3 levels between the PEs and the BEs (Δ in Figure 37) to the concentrations registered at the air quality stations (Obs in Figure 37). We calculated Obs_Δ_PE and Δ for both sets of scenarios according to Equation 6 and Equation 7.

Figure 37. Approach used to calculate the estimated O_3 observations for the emission abatement scenarios (Obs_Δ_PE).

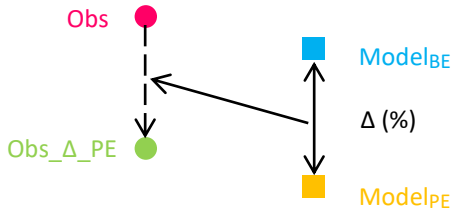

Where:

Obs: base case measured O_3 observations [µg/m^3]
Obs_Δ_PE: estimated O_3 observations for the emission abatement scenarios [µg/m^3]
Model$_{PE}$: modelled O_3 levels in the PE scenario [µg/m^3]
Model$_{BE}$: modelled O_3 levels in the BE scenario [µg/m^3]
Δ: relative difference of modelled O_3 levels between the PE scenario and the BE scenario [%]

Equation 6. Calculation of the relative difference of modelled O_3 levels between the PE scenario and the BE scenario (Δ).

$$\Delta\,[\%] = \frac{Model_{PE} - Model_{BE}}{Model_{BE}} \cdot 100$$

Equation 7. Calculation of the estimated O_3 observations for the emission abatement scenarios (Obs_Δ_PE).

$$Obs\_\Delta\_PE\left[\frac{\mu g}{m^3}\right] = Obs \cdot \left(1 + \frac{\Delta}{100}\right)$$

We implemented this approach for the analysis of O_3^{d8max} and O_3^{d1max} concentrations. We did not consider hourly values (O_3^h) because, as mentioned in Section 5.1, the CMAQ model has difficulties in reproducing low O_3 at night due to a problem in modelling O_3 titration by NO (Guevara et al., 2014). Due to this limitation, some hourly modelled concentrations are so small that a minor change between the BE and the PE leads to large relative increases and, therefore, to unrealistically high O_3^h concentrations.

Figure 38 shows the absolute difference between the estimated O_3 observations for the abatement scenarios following the strategy described before (designated as Obs_Δ_PE_PNCCA and Obs_Δ_PE_BCN_UMP) and the base case measured observations (referred to as Obs) per air quality station for the period April to September. On the other hand, Section S.4 in Supplementary Material includes the evolution of these differences throughout the study period and per station type.

Figure 38. Mean absolute difference [µg/m^3] between the estimated O_3^{d8max} and O_3^{d1max} observations for the abatement scenarios (PE_PNCCA and PE_BCN_UMP) and the O_3^{d8max} and O_3^{d1max} base case measured observations per air quality station from April to September 2019. The different symbols indicate the type of station (i.e., square for urban; triangle for suburban and circle for rural).

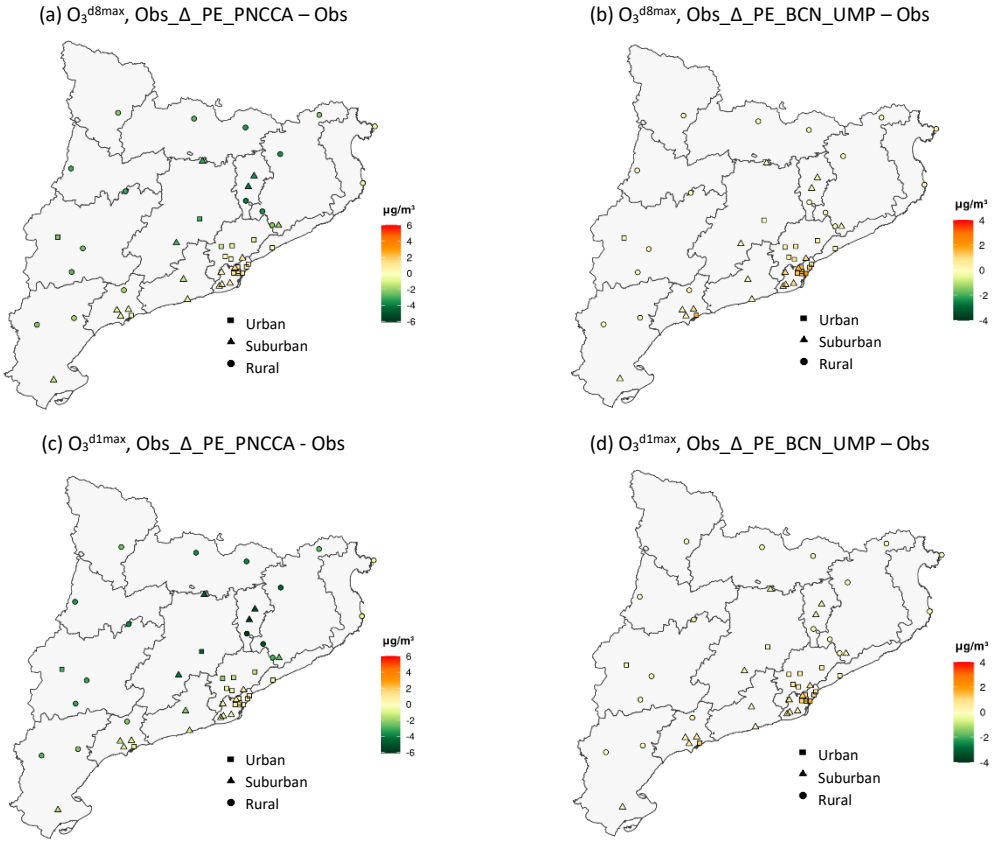

Results in Figure 38 are in line with the findings discussed in Section 6.3.1: in the case of PE_PNCCA, reductions of both O_3^{d8max} and O_3^{d1max} are observed in many of the air quality stations, reaching a maximum of around -4 and -6 µg/m^3 in the three sites of Plana de Vic, respectively, whereas some increases of about +2 and +1 µg/m^3 are seen in the BMA and Tarragona for O_3^{d8max} and O_3^{d1max} (Figure 38a-c).

As for the PE_BCN_UMP, the average O_3^{d8max} and O_3^{d1max} levels remain practically unchanged, with some minor reductions in inland Catalonia (of about -0.5 µg/m^3 for both metrics) and moderate increases between +1 and +2 µg/m^3 in Tarragona and Barcelona, respectively (Figure 38b and Figure 38d). In general, reductions are slightly more noticeable for O_3^{d1max} than for O_3^{d8max}, but a difference of <1 µg/m^3 among metrics is minimal considering that mean O_3 levels are on the order of 60-160 µg/m^3. Despite these minor differences, the trend for both O_3^{d1max} and O_3^{d8max} is practically equivalent.

Table 13 summarises this information per type of station (urban, suburban, rural), metric and scenario. Rural stations achieve the highest O_3^{d8max} and O_3^{d1max} reductions (e.g., -3.16 µg/m^3 in the PE_BCN_PNCAA for O_3^{d1max}), followed by suburban and urban sites. As previously mentioned, rural areas tend to be NO_x-limited since NO_x concentrations are low compared to VOCs levels, and subsequently, a reduction in NO_x leads to a significant decrease in O_3 concentrations. In contrast, urban areas are usually VOC-limited, where the contrary occurs: a decrease in NO_x levels entails an increase in O_3 concentrations (Massagué et al., 2022).

Table 13. Mean absolute difference [µg/m^3] between the estimated O_3^{d8max} and O_3^{d1max} observations for the abatement scenarios (PE_PNCCA and PE_BCN_UMP) and the O_3^{d8max} and O_3^{d1max} base case measured observations in the Catalan air quality stations from April to September 2019, according to station type.

	Station type	Obs_Δ_PE_PNCCA - Obs [µg/m^3]	Obs_Δ_PE_BCN_UMP - Obs [µg/m^3]
O_3^{d8max}	Rural	-2.52	-0.08
	Suburban	-1.05	+0.35
	Urban	-0.13	+0.81
	TOTAL	**-1.23**	**+0.36**
O_3^{d1max}	Rural	-3.16	-0.14
	Suburban	-1.85	+0.22
	Urban	-0.81	+0.68
	TOTAL	**-1.94**	**+0.25**

6.3.3. Impact on European standards and WHO recommendations

Table 14 shows the impact of the emission abatement scenarios on the exceedances of the European standards (240^h, 180^h and 120^{d8max}) and WHO guidelines (100^{d8max}) from April to September 2019, both in terms of number of exceedances and proportion of stations.

Table 14. Impact of the emission abatement scenarios PE_PNCCA and PE_BCN_UMP on European standards and WHO guidelines from April to September 2019: number of observed exceedances; proportion of stations with observed exceedances [%]; number of avoided and remaining exceedances in each scenario; proportion of stations with remaining exceedances [%]; and relative reduction of exceedances [%].

	Number of observed exceedances	Stations with observed exceedances [%]	Number of avoided exceedances	Number of remaining exceedances	Stations with remaining exceedances [%]	Relative reduction of exceedances [%]
	Observations			**PE_PNCCA scenario**		
240^h	7	14%	5	2 (*)	4% (*)	-71%
180^h	58	58%	22	36	50%	-38%
120^{d8max}	729	96%	197	532	94%	-27%
100^{d8max}	3301	100%	304	2297	100%	-9%
	Observations			**PE_BCN_UMP scenario**		
240^h	7	14%	2	5	10%	-29%
180^h	58	58%	3	55	58%	-5%
120^{d8max}	729	96%	15	714	96%	-2%
100^{d8max}	3301	100%	13	3288	100%	-0.4%

(*) See detailed discussions in Section 6.4.1.

A total of 7 (240^{h}), 58 (180^{h}), 729 (120^{d8max}) and 3301 (100^{d8max}) exceedances were observed across all the stations in Catalonia for the period of study. According to Table 14, the PE_PNCCA scenario would have reduced by -71%, -38%, -27% and -9% these exceedances, respectively, whereas these percentages would be -29%, -5%, -2% and -0.4% for the PE_BCN_UMP scenario. As expected, a larger impact is found in the PE_PNCCA scenario. Nevertheless, the reductions in the PE_BCN_UMP scenario are relevant considering that in this case the emission abatement measures only occur in the BMA and for a specific sector.

Despite the overall reduction of exceedances, there would still be a significant number of remaining exceedances both in the PE_PNCCA (e.g., 36 for 180^{h} and 532 for 120^{d8max}) and the PE_BCN_UMP (e.g., 55 for 180^{h} and 714 for 120^{d8ma}). Furthermore, a considerable number of stations would have remaining exceedances. For instance, the 120^{d8max} threshold would still be exceeded in the 94% (PE_PNCCA) and 96% (PE_BCN_UMP) of the air quality stations in Catalonia.

Regarding the $60^{peak\ season}$ threshold also established in the WHO guidelines, all the monitoring stations exceeded it from April to September 2019. This metric considers the six consecutive months with the highest six-month running average O_3 concentration. Considering that these six months are typically April-September and that this is the study period, we have considered this time frame to determine the $60^{peak\ season}$ threshold exceedances. For the PE_PNCCA and PE_BCN_UMP emission abatement scenarios, all stations would fail to meet with this recommendation in both cases. Therefore, in both scenarios, and based on the WHO recommendations, O_3 would continue to represent a major health problem.

On the other hand, despite the increase in O_3 levels in urban areas noted in Sections 6.3.1 and 6.3.2, especially in the BMA, the two emission abatement scenarios would not lead to further exceedances of the 240^{h}, 180^{h}, 120^{d8max}, 100^{d8max} and $60^{peak\ season}$ thresholds in April-September 2019.

6.4. Impact of the emission abatement scenarios on O_3 episodes

6.4.1. PE_PNCCA scenario

In this section, we assess the impact of the PE_PNCCA emission abatement scenario on Episodes A, B and C. Table 15 includes the measured and estimated O_3^{d1max} observations for the PE_PNCCA scenario, its relative differences (defined as Δ in Equation 6) and the relative difference between the BE1 modelled and measured observations at each station affected by the episodes.

According to the results, under the PE_PNCCA scenario, most of the alert threshold exceedances would be avoided, as the estimated O_3^{d1max} observations (Obs_Δ_PE_PNCCA in Table 15) would not exceed the limit of 240 µg/m^3. Specifically, the stations where the alert threshold would not be exceeded are 5: Sant Celoni, Santa Maria de Palautordera and Gavà in Episode A, and Manlleu and Vic in Episode B. According to the results, the exceedances in Montseny and Tarragona would still occur (they are highlighted in red in Table 15). Nevertheless, for these two stations, some considerations should be made:

- Regarding the Montseny station, the estimated O_3^{d1max} observation for 28 June is 240.05 µg/m^3 (Table 15), which is practically equal to the alert threshold (240 µg/m^3). Considering the model uncertainty, it could be that in this case this exceedance was

ultimately avoided. Furthermore, it should be noted that the measured observation value was 263.05 µg/m^3, which was the highest O_3 concentration registered from April to September 2019 in Catalonia, leading to the need for further efforts to reduce O_3 levels below 240 µg/m^3 compared with other peaks. In this context, the reduction under the PE_PNCCA scenario in Montseny is substantial (-8.74%).

- As shown in Section 5.2.3, the CALIOPE system failed to reproduce the stagnation situation and the breeze blockage that possibly led to the local accumulation of pollutants in Tarragona and, therefore, to the O_3 episode. Thus, in this case, we cannot rely on the relative difference of modelled O_3 levels between the PE_PNCCA and the BE1 scenarios (Δ), and subsequently, we are unable to confirm whether Episode C would still occur or not when implemented the PNCCAA emission reductions.

Nevertheless, as the model predicted Episodes A and B reasonably well, we can indeed have confidence in the Δ in this case and we can ensure that the alert threshold exceedances of these two episodes would probably not occur under the PE_PNCCA scenario (except the one in Montseny which is at the limit of 240 µg/m^3).

Regarding the sites where exceedances of the information threshold were recorded (180 µg/m^3), results indicate that the exceedances would still occur, although O_3 would be significantly reduced in most of the stations (i.e., between -6% and -10%). Exceptionally, modelling results highlight a slight increase of the estimated O_3^{d1max} in Vila-seca during Episode C. Nevertheless, the uncertainty of these results is very large since, as mentioned before, the CALIOPE system failed to capture Episode C.

Table 15. Summary of the PE_PNCCA scenario impact assessment on O_3 episodes according to O_3^{d1max}: measured observations (Obs, µg/m^3); estimated observations for the PE_PNCCA scenario (Obs_Δ_PE_PNCCA, µg/m^3); relative difference between the estimated observations for the PE_PNCCA scenario and the measured observations (Δ, defined in Equation 6, %); and relative difference between the modelled levels in the BE1 scenario and the measured observations (%). Stations with Obs_Δ_PE_PNCCA > 240 µg/m^3 are highlighted in red.

		Obs [µg/m^3]	Obs_Δ_PE_PNCCA [µg/m^3]	Δ [%]	Relative difference (Model_BE1-Obs) [%]
Alert threshold exceedances (240^h)					
28 June	Sant Celoni	245.04	232.02	-5.31	-16.82
	Montseny	263.05	240.05	-8.74	-19.28
	Santa Maria de Palautordera	248.04	234.84	-5.32	-17.67
29 June	Gavà	242.04	233.01	-3.73	-30.21
23 July	Vic	243.04	217.74	-10.41	-13.11
	Manlleu	240.04	215.49	-10.23	-10.15
18 September	Tarragona	248.04	245.69	-0.95	-54.60
Information threshold exceedances (180^h)					
28 June	Tona	223.04	201.77	-9.54	-6.78
	Vic	230.04	206.79	-10.11	-13.23
	Manlleu	204.04	182.15	-10.73	-2.12
23 July	Tona	235.04	220.18	-6.32	-7.93
18 September	Vila-seca	188.03	191.19	+1.68	-40.62

Figure 39 shows the relationship between Δ and the relative difference between the modelled levels in the BE1 scenario and the measured observations for Episodes A, B and C. The coefficient of determination (0.73) shows a reasonably strong linear relationship between the two variables. This means that the better the model represents the episode, which is related to the x-axis, the higher the relative reduction between the PE_PNCCA and the BE1 scenarios (y-axis).

Figure 39. Scatterplot of the relative difference of modelled levels between the PE_PNCCA scenario and the BE1 scenario (Δ, %) vs. the relative difference between the modelled levels in the BE1 scenario and the measured observations in Episodes A, B and C. It also includes the coefficient of determination R^2 and the linear regression equation.

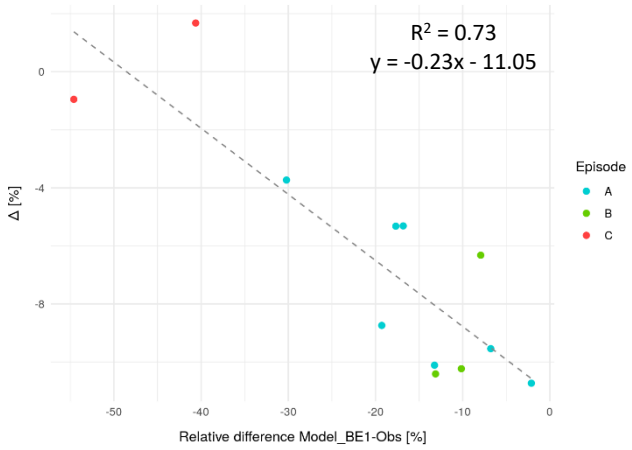

Figure 40 shows the spatial distribution of the modelled O_3^{d8max} absolute reductions during the 2019 O_3 episodes. Regarding Episodes A and B, the highest reductions would take place in Comarques de Girona (-25 µg/m^3 on 28 June) and in Plana de Vic, Catalunya Central and Pirineu Oriental (between -5 and -15 µg/m^3 each day). Nevertheless, some increases in O_3^{d8max} levels (around +10 µg/m^3 on 28 June) would occur in the BMA due to the local chemistry regime, as previously discussed in Section 6.3.1. Concerning Episode C, as expected there would not be reductions in O_3^{d8max} levels in Tarragona because the model failed to reproduce the local causes of the O_3 episode.

Figure 40. Difference between the modelled O_3^{d8max} levels in the PE_PNCCA and BE1 scenarios [µg/m^3], in absolute terms, during Episode A (28-29 June), Episode B (23 July) and Episode C (18 September).

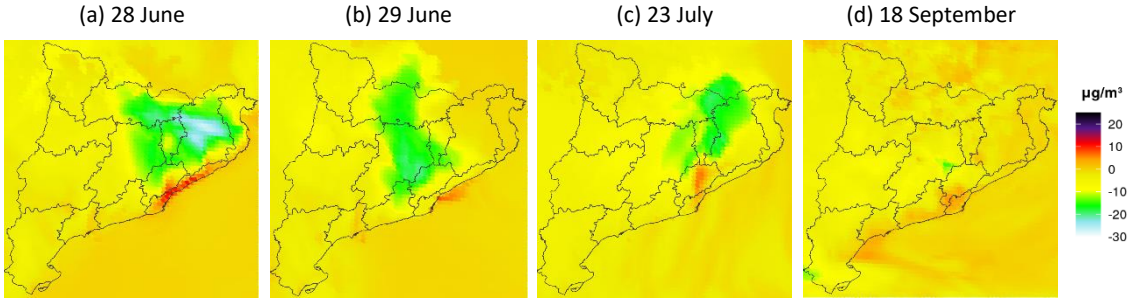

6.4.2. PE_BCN_UMP scenario

For the PE_BCN_UMP scenario, only two of the total exceedances of the alert threshold would be avoided: the ones from Episode B (23 July) in Vic and Manlleu (Table 16). These results are expected since in the PE_BCN_UMP only emissions from the BMA are reduced, and mainly from local road transport, whereas in the PE_PNCCA the emission abatement measures impact over all the study domain and several sources, including not only traffic but also industries, among

others. For this reason, the relative reductions (Δ, Table 16) would be lower in PE_BCN_UMP than in PE_PNCCA. In fact, in some cases there would even be slight increases in O_3^{d1max} levels, as in Santa Maria de Palautordera (+0.77%) or Gavà (+0.69%).

Despite the lower impact of the PE_BCN_UMP scenario, these results should not be downplayed because they indicate that emission abatement measures in the BMA would lead to a reduction in the frequency and severity of the classic O_3 episodes affecting Plana de Vic and Montseny. This is relevant as this region is one of the main O_3 hotspots in Spain, as previously mentioned. These results are in line with the conclusions of Valverde et al. (2016), which indicate a large contribution of the Barcelona urban emission plume to the O_3 peaks in the regions of Vic and Montseny.

Regarding the Episode C in Tarragona, the results obtained with the PE_BCN_UMP scenario (Table 16) are in line with those discussed for the PE_PNCCA scenario: the O_3^{d1max} levels would not be reduced and would actually increase around +4 µg/m^3. Nevertheless, considering that the model failed to predict this episode, we cannot rely on the relative difference of modelled O_3 levels between the PE_BCN_UMP and the BE2 scenarios (Δ).

Table 16. Summary of the PE_BCN_UMP scenario impact assessment on O_3 episodes according to O_3^{d1max}: measured observations (Obs, µg/m^3); estimated observations for the PE_BCN_UMP scenario (Obs_Δ_BCN_UMP, µg/m^3); relative difference between the estimated observations for the PE_BCN_UMP scenario and the measured observations (Δ, defined in Equation 6, %); and relative difference between the modelled levels in the BE2 scenario and the measured observations (%). Stations with Obs_Δ_PE_BCN_UMP > 240 µg/m^3 are highlighted in red.

		Obs [µg/m^3]	Obs_Δ_PE_BCN_UMP [µg/m^3]	Δ [%]	Relative difference (Model_BE2-Obs) [%]
Alert threshold exceedances (240^h)					
28 June	Sant Celoni	245.04	241.17	-1.58	-13.60
	Montseny	263.05	256.98	-2.31	-16.70
	Santa Maria de Palautordera	248.04	249.96	+0.77	-17.28
29 June	Gavà	242.04	243.71	+0.69	-24.23
23 July	Vic	243.04	237.08	-2.45	-24.62
	Manlleu	240.04	232.67	-3.07	-23.01
18 September	Tarragona	248.04	252.24	+1.69	-53.78
Information threshold exceedances (180^h)					
28 June	Tona	223.04	214.32	-3.91	-9.81
	Vic	230.04	221.06	-3.90	-12.25
	Manlleu	204.04	199.05	-2.45	-5.85
23 July	Tona	235.04	230.51	-1.93	-21.50
18 September	Vila-seca	188.03	193.22	+2.76	-47.04

7. Sustainability analysis and ethical implications

In this section we provide a sustainability analysis of the development of the final master's thesis and of the associated risks and constraints. In each part, we consider the three pillars of sustainability: environmental, economic and social.

7.1. Development of the final master's thesis

7.1.1. Environmental approach

From an environmental perspective, we calculated the carbon footprint related to the development of this final master's thesis. As this is a study, we did not consider the environmental impact of the implementation of the project. In this case, the environmental impact is mainly due to the energy consumption required by the MareNostrum 4 supercomputer to run the four HERMESv3 emission simulations that we executed in the framework of this study, in addition to the energy consumption associated with the use of computer and lighting.

Regarding the carbon footprint of the four simulations (5.06 kg CO_2e; Table 17), we used the Green Algorithms calculator (www.green-algorithms.org; Lannelongue et al., 2021), which enables to estimate and report the carbon footprint of computation based on several factors, such as the runtime of the simulations or the hardware requirements of MareNostrum 4 (included in Table S.6 from Supplementary Material).

In relation to the carbon footprint of computer energy consumption (3.21 kg CO_2e; Table 17), we estimated that the laptop has been connected to the electricity during 50% of the 750 hours dedicated to this thesis, and we assumed a mean consumption of 50 W (Energy Guide, 2021). Concerning the carbon footprint of lighting energy consumption (1.92 kg CO_2e; Table 17), we considered a linear LED lamp of 60 W and a factor of 0.25, to apportion the carbon footprint between the four people using it. Equations S.1 and S.2 in Supplementary Material provide the carbon footprint calculation of computer and lighting energy consumption, respectively. Supposing a carbon intensity of 171 g CO_2e/kWh (average data of the last 12 months in Spain; Electricity Maps, 2023), the total estimated carbon footprint is 10.19 kg CO_2e (Table 17).

Table 17. Carbon footprint associated with the development of this final master's thesis.

Carbon footprint of energy consumption associated to the four simulations	5.06 kg CO_2e
Carbon footprint of computer energy consumption	3.21 kg CO_2e
Carbon footprint of lighting energy consumption	1.92 kg CO_2e
Total estimated carbon footprint	**10.19 kg CO_2e**

7.1.2. Economic approach

Regarding the economic perspective, we estimated a hypothetical budget for the realisation of this document, considering the 750 hours dedicated to this thesis and the average salary of junior engineers in Spain (12.82 €/h; Talent, 2023). Furthermore, we included a 20 % cost overrun to account for the high-performance computing resources, the facilities and the energy consumption, among others. Overall, the total estimated cost of this study would be **11538.00 €.**

Table 18 includes a Gantt chart of the planning of this final master's thesis, which had a duration of seven and a half months.

Table 18. Gantt chart of the planning of this final master's thesis.

	March	April	May	June	July	August	September	October
Bibliographical review on O_3 and modelling techniques								
Analysis of O_3 precursor emissions, meteorology and O_3 levels								
Evaluation of the model in the base case emission scenarios								
Quantification of the impact of emission abatement scenarios								
Synthesis of results and preparation of the final document								
Preparation of the final exposition								
Follow-up meetings with the director of the final master's thesis and the AC-BSC team								

7.1.3. Social approach

This final master's thesis has impacted the author very positively. It has been really enriching to get familiar with a supercomputing environment and data analysis, using tools such as RStudio. This study has increased the author's awareness of the impact of air pollution on human health and the urgency of effective air quality management. Almost the entire global population breathes air that threatens their health. Therefore, it is necessary to tackle the problem of air pollution, both locally and globally. Another takeaway from this study is the fact that models are not perfect, although they can reproduce reality reasonably well and are essential for assessing the effectiveness of certain measures before their implementation.

On the other hand, this final master's thesis has provided the AC-BSC team with insights into the impact of the two emission abatement scenarios at a very local scale, since the analysis previously conducted was done on a more general scale and, for instances, without looking into the impact of the emission reductions on specific O_3 episodes. Furthermore, the team has received feedback that may be used in the future to improve the CALIOPE system. At the same time, the AC-BSC team has contributed to this final master's thesis with valuable comments and reflections, helping the author to improve the quality of the study. This interchange of information has occurred on a weekly basis with the director of the final master's thesis, and periodically with the rest of the team.

7.2. Risks and constraints

Here, we provide a sustainability analysis of the risks and constraints inherent to the final master's thesis. In this case, we consider all three approaches in the same section.

Regarding the environmental approach, the carbon footprint would be higher if the air quality modelling exercises regarding BE1, BE2, PE_PNCCA and PE_BCN_UMP scenarios were included in the scope of this study or if the evaluation works performed under this master's thesis would have indicated the need to re-run some of the simulations due to an issue with the setup of the modelling system.

In relation to the economic perspective, similarly to the environmental approach, the hypothetical invoice and the Gantt chart could differ if the study duration had been shorter or if the emissions and air quality modelling exercises had been included in the scope of the final master's thesis. Furthermore, the cost overrun could also vary if more details on actual energy consumption and other costs were available.

Concerning the social point of view, the main eventuality that could have caused the master's thesis to have a negative social impact on the author would be if the emission modelling exercise would not have been successfully completed. In this case, the author would have not been able to quantify the impact of the emission abatement scenarios on NO_x and NMVOC anthropogenic emissions over Catalonia.

8. Conclusions

Tropospheric O_3 is a secondary air pollutant detrimental for human health. It is primarily linked to warm climates with high temperatures and radiation levels, such as the Southern European regions. The present study analyses and discusses the trends of ozone O_3 concentrations in Catalonia and quantifies the potential impact of national and local emission abatement programs on its levels. To perform this work, we combined the use of air quality observations and numerical modelling outputs to determine the effectiveness of current air pollution control programmes and urban mobility plans that are being implemented at the Spanish and Barcelona city level, respectively. Air quality models are essential to quantify the impact of emission abatement measures prior to their implementation.

Observational data from the official EEA air quality monitoring network was compiled, processed and compared for the period 2000 to 2021 against current legal and recommended O_3 thresholds set up by the European Air Quality Directive (2008/50/EC) and the World Health Organisation (WHO), respectively. Trends in O_3 were discussed and linked to changes in primary precursor emissions (NO_x and NMVOC) and surface temperature levels.

The air quality modelling results considered in the study are based on high resolution numerical simulations (between 4km x 4km and 1km x 1km spatial resolution and hourly temporal resolution) that were performed by the Atmospheric Composition research team at the Barcelona Supercomputing Center (AC-BSC) making use of the CALIOPE system, a state-of-the-art air quality modelling system maintained and developed by the AC-BSC that is executed at the MareNostrum 4 supercomputer.

A total of four emission scenarios were simulated making use of the CALIOPE system: two emission abatement scenarios representing the expected changes in emissions linked to the implementation of the Spanish National Air Pollution Control Programme (PE_PNCCA) and the Barcelona Urban Mobility Plan (PE_BCN_UMP), respectively, and their respective base case scenario considering emissions in Spain for 2019 (BE1 and BE2). The modelled O_3 concentrations obtained for the base case scenarios were compared against measurements to assess the performance of the CALIOPE system in reproducing observed levels and specific episodes. The impact of the emission abatement scenarios was estimated considering the O_3 metrics that are used to define legal thresholds and recommendations set up by the European Air Quality Directive and WHO, respectively: hourly (O_3^h), daily mean (O_3^d), maximum daily 8-hour mean (O_3^{d8max}) and maximum daily 1-hour (O_3^{d1max}) concentrations. The impact of reducing emissions was also analysed for the three O_3 episodes that occurred in 2019.

The main findings and conclusions of this work are as follows:

- Concentrations of O_3 measured between 2000 and 2021 do not show a clear downward trend except for the years 2020 and 2021, when unusually low O_3 levels were recorded due to the impact of COVID-19 mobility restrictions on global-to-local anthropogenic emissions. Apart from these two years, O_3 concentrations have remained rather unaltered despite the significant reduction of NO_x and VOC precursor emissions (-51% and -38%, respectively), the largest O_3 levels being observed during the years with the highest summer mean temperature anomalies.

- The O_3 thresholds established by the European legislation and WHO have been persistently exceeded, especially in rural areas located downwind of the BMA (i.e., Plana de Vic and Montseny) and Tarragona. O_3 levels in urban and industrial areas are usually lower due to the consumption of O_3 through titration by NO and ozonolysis of VOCs.
- Overall, we proved that the CALIOPE system represents reasonably well the spatio-temporal variability of observed O_3 concentrations, although it has some difficulties in capturing very high O_3 peaks and night-time values, which is in agreement with previous evaluation works (e.g., Pay et al., 2019; Petetin et al., 2023). Out of the three O_3 episodes identified for 2019, the CALIOPE system was capable of capturing two of them with sufficient accuracy.
- Under the PE_PNCCA, NO_x and NMVOC anthropogenic emissions over Catalonia would decrease -36% and -4.19% (with respect to the BE1), respectively. For the PE_BCN_UMP, these rates would be -2.74% and -0.61%. O_3 precursor emissions are largely reduced in the PE_PNCCA than in the PE_BCN_UMP, as the latter only reduces emissions in the city of Barcelona, and mainly from local road transport, whereas in the PE_PNCCA the emission abatement measures impact over all the study domain and several sources.
- On average, we estimate that O_3^{d8max} mean levels in Catalonia from April to September 2019 would be reduced by -0.95 and -0.03 μg/m^3 in the PE_PNCCA and PE_BCN_UMP scenarios, respectively. The highest reductions (between -4 and -5 μg/m^3) would occur in the air quality zones of Plana de Vic, Catalunya Central and Comarques de Girona.
- According to both emission abatement scenarios, O_3 levels would slightly increase in the Barcelona Metropolitan Area (around +3 and +4 μg/m^3 for the PE_PNCCA and the PE_BCN_UMP, respectively) and in Tarragona (+1 and +3 μg/m^3 for the PE_PNCCA and the PE_BCN_UMP, respectively, at O_3^{d8max} scale), since the decrease of NO_x levels in VOCs-limited environments leads to rising O_3 concentrations. Nevertheless, as O_3 levels in these two regions are relatively low, there would not be further exceedances of any threshold.
- The number of exceedances of the target value of 120 μg/m^3 for the protection of human health across all monitoring stations in Catalonia would be reduced by -27% for the PE_PNCCA and -2% for the PE_BCN_UMP. Emission scenario impacts are higher when considering the information threshold of 180 μg/m^3 (-38% for the PE_PNCCA and -5% for the PE_BCN_UMP).
- The impact of the emission abatement scenarios is more noticeable during specific episodes (e.g., for the PE_PNCCA and on 28 June, -25 μg/m^3 in Comarques de Girona and between -5 and -15 μg/m^3 in Plana de Vic, Catalunya Central and Pirineu Oriental, on O_3^{d8max} terms). All in all, the O_3 episodes that occurred in 2019 would be avoided under the PE_PNCCA scenario, except Episode C in Tarragona. However, the model was not capable of reproducing this episode, and therefore we cannot ensure whether this episode would ultimately occur under this specific emission reduction scenario.
- The PE_BCN_UMP would not be sufficient to avoid all O_3 episodes, but it would lead to a reduction in the frequency and severity of the typical episodes affecting Plana de Vic

and Montseny. This result indicates that local measures can also help improve air quality levels beyond its administrative borders due to its transboundary effect.

- Despite the overall reduction of exceedances, there would still be a significant number of remaining exceedances of the 100^{d8max} threshold recommended by the WHO guidelines (2297 and 3288 exceedances, affecting 94% and 96% of the stations, in the PE_PNCCA and PE_BCN_scenarios, respectively), which are more restrictive than the European legislation. Similarly, all stations would still fail to meet the $60^{peak\ season}$ threshold recommended by WHO after applying the emission reductions in both scenarios.
- All these results are subordinated to the uncertainties and limitations of the CALIOPE system, including the representation of primary emissions, as well as specific meteorological conditions that influence the transport and stagnation of air pollution. To minimise this uncertainty, air quality models are being continuously refined.

The emission abatement scenarios considered in this study succeed in minimising O_3 episodes in one of the main O_3 hotspots in Spain (i.e., the northern regions of the BMA) and reducing the number of exceedances of the information threshold and the target value for the protection of human health. Nevertheless, they are insufficient to achieve significant reductions in O_3 background levels throughout Catalonia. The large contribution of imported O_3 to the ground-level O_3 concentration leaves very limited scope for reducing mean O_3 concentrations locally and confines it to specific episodes, when the local contribution becomes more significant. Therefore, comprehensive efforts must be undertaken both on a global and local scale to minimise O_3 levels and ensure proper air quality levels. The levels of O_3 recorded during 2020 are a clear proof that effective mitigation measures require a collective and coordinate effort across countries. Furthermore, the design of effective air quality strategies must be accompanied by the use of combined observations and numerical modelling techniques. It is fundamental to assess emission abatement measures in advance to avoid undesirable results, given the complex non-linear photochemical reactions involved in the formation of O_3.

The next steps that could be developed as a continuation of this study are as follows:

- Quantify the impact on O_3 levels of the emission abatement scenarios over a longer period of time (i.e., three years) to account for variability in meteorological variables that affect O_3 levels.
- Quantify the impact on O_3 levels of new emission abatement scenarios involving more ambitious reductions of NMVOC emissions.

References

Adame, J. A., Hernández-Ceballos, M. Á., Sorribas, M., Lozano, A., and De la Morena, B. A. (2014). Weekend-weekday effect assessment for O_3, NO_x, CO and PM_{10} in Andalusia, Spain (2003-2008). *Aerosol and Air Quality Research, 14*(7), 1862-1874. https://doi.org/10.4209/aaqr.2014.02.0026

Agència Catalana de Notícies (2015, 17 June). La xemeneia de la central tèrmica de Cubelles anirà a terra abans de quatre anys. *Ara.cat.* https://www.ara.cat/societat/central-termica-cubelles-endesa_1_1859539.html

Ajuntament de Barcelona (2022). *Pla de Mobilitat Urbana de Barcelona 2019-2024*. Retrieved 27 July, 2023, from https://www.barcelona.cat/mobilitat/ca/qui-som/pla-de-mobilitat-urbana-2024

Ajuntament de Tarragona (2019). *Santa Tecla 2019.* Retrieved 7 September, 2023, from https://www.tarragona.cat/cultura/noticies/noticies-2019/santa-tecla-2019-la-crida-dona-el-tret-de-sortida-a-les-festes

Badia, A., Vidal, V., Ventura, S., Curcoll, R., Segura, R., and Villalba, G. (2023). Modelling the impacts of emission changes on O_3 sensitivity, atmospheric oxidation capacity and pollution transport over the Catalonia region. *EGUsphere,* 1-38. https://doi.org/10.5194/egusphere-2023-160

Badia, A., Jorba, O., Voulgarakis, A., Dabdub, D., Pérez García-Pando, C., Hilboll, A., Gonçalves, M., and Janjic, Z. (2017). Description and evaluation of the Multiscale Online Nonhydrostatic AtmospheRe CHemistry model (NMMB-MONARCH) version 1.0: gas-phase chemistry at global scale. *Geoscientific Model Development, 10*(2), 609-638. https://doi.org/10.5194/gmd-10-609-2017

Badia, A., and Jorba, O. (2015). Gas-phase evaluation of the online NMMB/BSC-CTM model over Europe for 2010 in the framework of the AQMEII-Phase2 project. *Atmospheric Environment, 115*, 657-669. https://doi.org/10.1016/j.atmosenv.2014.05.055

Baldasano, J. M., Pay, M. T., Jorba, O., Gassó, S., and Jiménez-Guerrero, P. (2011). An annual assessment of air quality with the CALIOPE modeling system over Spain. *Science of the Total Environment, 409*(11), 2163-2178. https://doi.org/10.1016/j.scitotenv.2011.01.041

Baldasano, J. M., Jiménez-Guerrero, P., Jorba, O., Pérez García-Pando, C., López, E., Güereca, P., ... and Diéguez, J. J. (2008). Caliope: an operational air quality forecasting system for the Iberian Peninsula, Balearic Islands and Canary Islands–first annual evaluation and ongoing developments. *Advances in Science and Research, 2*(1), 89-98. https://doi.org/10.5194/asr-2-89-2008

Bowdalo, D., Basart, S., Guevara, M., Jorba, O., and Pérez García-Pando, C. (2023). GHOST: A globally harmonised dataset of surface atmospheric composition measurements. In *EGU General Assembly Conference Abstracts* (pp. EGU23-14689). https://doi.org/10.5194/egusphere-egu23-14689

BSC (2023). *CALIOPE System – Air quality forecast.* Retrieved 18 September, 2023, from http://www.bsc.es/caliope/en/forecasts?language=en

Byun, D., and Schere, K. L. (2006). Review of the governing equations, computational algorithms, and other components of the Models-3 Community Multiscale Air Quality (CMAQ) modeling system. *Applied mechanics reviews, 59*(2), 51-77. https://doi.org/10.1115/1.2128636

Copernicus Atmosphere Monitoring Service (2022). *Verification plots: documentation.* Retrieved 18 April, 2023, from http://macc-raq-int.meteo.fr/doc/USER_GUIDE_VERIFICATION_STATISTICS.pdf

Directive 2008/50/EC. *Directive 2008/50/EC of the European Parliament and of the Council of 21 May 2008 on ambient air quality and cleaner air for Europe.* https://eur-lex.europa.eu/legal-content/EN/TXT/PDF/?uri=CELEX:32008L0050

EMEP/EEA (2019). *EMEP/EEA Air Pollutant Emission Inventory Guidebook 2019: Technical Guidance to Prepare National Emission Inventories*. Publications Office of the European Union. https://doi.org/10.2800/293657

Energy Guide (2021). *Consumption and rates.* Retrieved 7 September, 2023, from https://www.energuide.be/en/questions-answers/how-much-power-does-a-computer-use-and-how-much-co2-does-that-represent/54/

European Environment Agency (2023a). *How air pollution affects our health.* Retrieved 14 August, 2023, from https://www.eea.europa.eu/en/topics/in-depth/air-pollution/eow-it-affects-our-health

European Environment Agency (2023b). *Europe's air quality status 2023.* Retrieved 13 September, 2023, from https://www.eea.europa.eu/publications/europes-air-quality-status-2023

European Environment Agency (2023c). *Classification of monitoring stations and criteria to include them in EEA's assessments products.* Retrieved 23 August, 2023, from https://www.eea.europa.eu/themes/air/air-quality-concentrations/classification-of-monitoring-stations-and

European Environment Agency (2023d). *Air Quality e-Reporting Database (AQ e-Reporting).* Retrieved 25 May, 2023, from https://www.eea.europa.eu/en/datahub/datahubitem-view/3b390c9c-f321-490a-b25a-ae93b2ed80c1

European Environment Agency (2023e). *[DEPRECATED] AirBase - The European air quality database.* Retrieved 25 May, 2023, from https://data.europa.eu/data/datasets/data_airbase-the-european-air-quality-database-7?locale=en

European Environment Agency (2020). *Air quality in Europe – 2020 report*. (EEA Report No 9/2020). https://doi.org/10.2800/786656

European Parliamentary Research Service (2023). *Revision of EU air quality legislation.* https://www.europarl.europa.eu/RegData/etudes/BRIE/2023/747087/EPRS_BRI(2023)747087_EN.pdf

Escudero, M., Querol, X., Ávila, A., and Cuevas, E. (2007). Origin of the exceedances of the European daily PM limit value in regional background areas of Spain. *Atmospheric Environment, 41*(4), 730-744. https://doi.org/10.1016/j.atmosenv.2006.09.014

Fleming, Z. L., Doherty, R. M., Von Schneidemesser, E., Malley, C. S., Cooper, O. R., Pinto, J. P., ... and Feng, Z. (2018). Tropospheric Ozone Assessment Report: Present-day ozone distribution and trends relevant to human health. *Elem Sci Anth, 6*, 12. https://doi.org/10.1525/elementa.273

Generalitat de Catalunya (2022). *Zones de Qualitat de l'Aire (ZQA)*. Departament de Territori i Sostenibilitat. Retrieved 28 March, 2023, from https://sig.gencat.cat/visors/hipermapa_antic.html#param=param&color=vermell&background=topo_ICC&BBOX=102248.358862,4485000,691751.641138,4752000&layers=ATMOSFERA_ZONES_QUALITAT_AIRE

Gorrochategui, E., Hernandez, I., Pérez-Gabucio, E., Lacorte, S., and Tauler, R. (2022). Temporal air quality (NO_2, O_3, and PM_{10}) changes in urban and rural stations in Catalonia during COVID-19 lockdown: An association with human mobility and satellite data. *Environmental Science and Pollution Research, 1-18*. https://doi.org/10.1007/s11356-021-17137-7

Guevara, M., Petetin, H., Jorba, O., Denier van der Gon, H., Kuenen, J., Super, I., ... and Pérez García-Pando, C. (2022). European primary emissions of criteria pollutants and greenhouse gases in 2020 modulated by the COVID-19 pandemic disruptions. *Earth System Science Data, 14*(6), 2521-2552. https://doi.org/10.5194/essd-14-2521-2022

Guevara, M., Tena, C., Porquet, M., Jorba, O., and Pérez García-Pando, C. (2020). HERMESv3, a stand-alone multi-scale atmospheric emission modelling framework–Part 2: The bottom–up module. *Geoscientific Model Development, 13*(3), 873-903. https://doi.org/10.5194/gmd-13-873-2020

Guevara, M., Tena, C., Porquet, M., Jorba, O., and Pérez García-Pando, C. (2019). HERMESv3, a stand-alone multi-scale atmospheric emission modelling framework–Part 1: global and regional module. *Geoscientific Model Development, 12*(5), 1885-1907. https://doi.org/10.5194/gmd-12-1885-2019

Guevara, M., Pay, M. T., Martínez, F., Soret, A., van der Gon, H. D., and Baldasano, J. M. (2014). Inter-comparison between HERMESv2. 0 and TNO-MACC-II emission data using the CALIOPE air quality system (Spain). *Atmospheric environment, 98*, 134-145. http://dx.doi.org/10.1016/j.atmosenv.2014.08.067

Im, U., Bianconi, R., Solazzo, E., Kioutsioukis, I., Badia, A., Balzarini, A., ... and Galmarini, S. (2015). Evaluation of operational on-line-coupled regional air quality models over Europe and North America in the context of AQMEII phase 2. Part I: Ozone. *Atmospheric environment, 115*, 404-420. https://doi.org/10.1016/j.atmosenv.2014.09.042

Jaén, C., Villasclaras, P., Fernández, P., Grimalt, J. O., Udina, M., Bedia, C., and van Drooge, B. L. (2021a). Source apportionment and toxicity of PM in urban, sub-urban, and rural air quality network stations in Catalonia. *Atmosphere, 12*(6), 744. https://doi.org/10.3390/atmos12060744

Jaén, C., Udina, M., and Bech, J. (2021b). Analysis of two heat wave driven ozone episodes in Barcelona and surrounding region: Meteorological and photochemical modeling. *Atmospheric Environment, 246*, 118037. https://doi.org/10.1016/j.atmosenv.2020.118037

Jaén, C. (2020). Ozone episodes in Catalonia during the summer of 2019. A meteorological and photochemical modeling analysis. *Dipòsit Digital de la Universitat de Barcelona*. Retrieved 26 May, 2023, from https://diposit.ub.edu/dspace/handle/2445/172706

Klose, M., Jorba, O., Gonçalves Ageitos, M., Escribano, J., Dawson, M. L., Obiso, V., ... and Pérez García-Pando, C. (2021). Mineral dust cycle in the Multiscale Online Nonhydrostatic AtmospheRe CHemistry model (MONARCH) version 2.0. *Geoscientific Model Development, 14*(10), 6403-6444. https://doi.org/10.5194/gmd-14-6403-2021

Lannelongue, L., Grealey, J., Inouye, M., Green Algorithms (2021): Quantifying the Carbon Footprint of Computation. *Adv. Sci*. 2100707. https://doi.org/10.1002/advs.202100707

Li, Q., Borge, R., de la Paz, D., Domingo, J., Cuevas, C., and Saiz-Lopez, A. (2019). Assessing the impact of halogen chemistry on air quality: application of CMAQ model in Europe. In *Geophysical Research Abstracts (Vol. 21)*. EGU General Assembly 2019. Retrieved 8 September, 2023, from https://digital.csic.es/bitstream/10261/210038/1/Assessing%20the%20impact.pdf

Malashock, D. A., DeLang, M. N., Becker, J. S., Serre, M. L., West, J. J., Chang, K. L., Cooper, O. R., and Anenberg, S. C. (2022). Estimates of ozone concentrations and attributable mortality in urban, peri-urban and rural areas worldwide in 2019. *Environmental Research Letters, 17*(5), 054023. https://doi.org/10.1088/1748-9326/ac66f3

Massagué, J., Escudero, M., Alastuey, A., Mantilla, E., Monfort, E., Gangoiti, G., Pérez García-Pando, C. and Querol, X. (2022). Contrasting 2008-2019 Trends in Tropospheric Ozone in Spain. *SSRN Electronic Journal.* http://dx.doi.org/10.2139/ssrn.4103368

Massagué, J., Carnerero, C., Escudero, M., Baldasano, J. M., Alastuey, A., and Querol, X. (2019). 2005–2017 ozone trends and potential benefits of local measures as deduced from air quality measurements in the north of the Barcelona metropolitan area. *Atmospheric Chemistry and Physics, 19*(11), 7445-7465. https://doi.org/10.5194/acp-19-7445-2019

MITECO (2023a). *Bases Científicas para un Plan Nacional de Ozono (2022).* Retrieved 21 August, 2023, from https://www.miteco.gob.es/es/calidad-y-evaluacion-ambiental/temas/atmosfera-y-calidad-del-aire/calidad-del-aire/documentacion-oficial/bct_plan_o3.html

MITECO (2023b). *Edición 2023 del Inventario Nacional de Contaminantes Atmosféricos (serie 1990-2021)*. Sistema Español de Inventario de Emisiones. Retrieved 5 June, 2023, from https://www.miteco.gob.es/es/calidad-y-evaluacion-ambiental/temas/sistema-espanol-de-inventario-sei-/inventario-contaminantes.html

MITECO (2023c). *Informe resumen del Inventario de emisiones de contaminantes atmosféricos.* Sistema Español de Inventario de Emisiones. Retrieved 9 June, 2023, from https://www.miteco.gob.es/es/calidad-y-evaluacion-ambiental/temas/sistema-espanol-de-inventario-sei-/inventario-contaminantes.html

MITECO (2020). *Plan Nacional Integrado de Energía y Clima 2021-2030.* Retrieved 21 July, 2023, from https://www.miteco.gob.es/content/dam/miteco/images/es/pnieccompleto_tcm30-508410.pdf

MITECO (2019). *I Programa Nacional de Control de la Contaminación Atmosférica*. Retrieved 21 July, 2023, from https://www.miteco.gob.es/content/dam/miteco/es/calidad-y-evaluacion-ambiental/temas/atmosfera-y-calidad-del-aire/primerpncca_2019_tcm30-502010.pdf

MITMA (2020). *Estadísticas tráfico portuario.* Puertos del Estado. Retrieved 6 September, 2023, from https://www.puertos.es/es-es/estadisticas/Paginas/estadistica_mensual.aspx

Oliveira, K., Guevara, M., Jorba, O., Querol, X., and Pérez García-Pando, C. (2023). A new NMVOC speciated inventory for a reactivity-based approach to support ozone control strategies in Spain. *Science of The Total Environment, 867*, 161449. https://doi.org/10.1016/j.scitotenv.2023.161449

OMIE (2023). *Mínimo, medio y máximo precio de la casación del mercado diario.* Retrieved 7 September, 2023, from https://www.omie.es/es/market-results/annual/daily-market/daily-prices?scope=annual&year=2023

Ortega, S., Soler, M. R., Beneito, J., and Pino, D. (2006). Numerical Modelling of Troposferic Ozone in Catalunya. *Journal edited by ACAM, Tethys, 3*, 25-36. DOI: 10.3369/tethys.2006.3.04https://doi.org/10.3369/tethys.2006.3.04

Pay, M. T., Gangoiti, G., Guevara, M., Napelenok, S., Querol, X., Jorba, O., and Pérez García-Pando, C. (2019). Ozone source apportionment during peak summer events over southwestern Europe. *Atmospheric chemistry and physics, 19*(8), 5467-5494. https://doi.org/10.5194/acp-19-5467-2019

Pay, M. T., Jiménez-Guerrero, P., Jorba, O., Basart, S., Querol, X., Pandolfi, M., and Baldasano, J. M. (2012). Spatio-temporal variability of concentrations and speciation of particulate matter across Spain in the CALIOPE modeling system. *Atmospheric Environment, 46*, 376-396. https://doi.org/10.1016/j.atmosenv.2011.09.049

Pay, M. T., Piot, M., Jorba, O., Gassó, S., Gonçalves, M., Basart, S., ... and Baldasano, J. M. (2010). A full year evaluation of the CALIOPE-EU air quality modeling system over Europe for 2004. *Atmospheric Environment, 44*(27), 3322-3342. https://doi.org/10.1016/j.atmosenv.2010.05.040

Pérez García-Pando, C., Haustein, K., Janjic, Z., Jorba, O., Huneeus, N., Baldasano, J. M., ... and Thomson, M. (2011). Atmospheric dust modeling from meso to global scales with the online NMMB/BSC-Dust model–Part 1: Model description, annual simulations and evaluation. *Atmospheric Chemistry and Physics, 11*(24), 13001-13027. https://doi.org/10.5194/acp-11-13001-2011

Petetin, H., Guevara, M., Garatachea, R., López, F., Oliveira, K., Enciso, S., Jorba, O., Querol, X., Massagué, A., Alastuey, A., and Pérez García-Pando, C. (2023). Assessing ozone abatement scenarios in the framework of the Spanish ozone mitigation plan. *Science of The Total Environment,* 165380. https://doi.org/10.1016/j.scitotenv.2023.165380

Port de Barcelona (2022). *Nexigen.* Retrieved 11 August, 2023, from https://www.portdebarcelona.cat/es/web/el-port/nexigen

Port Tarragona (2019a). *Setmana rècord de creuers al Port de Tarragona.* Retrieved 6 September, 2023, from https://www.porttarragona.cat/ca/autoritat-portuaria-tarragona/comunicacio-premsa/notes-premsa/item/2281-setmana-record-de-creuers-al-port-de-tarragona

Port Tarragona (2019b). *Tarragona acollirà la cimera mundial del transport de productes forestals.* Retrieved 6 September, 2023, from https://www.porttarragona.cat/ca/autoritat-portuaria-tarragona/comunicacio-premsa/notes-premsa/item/2273-tarragona-acollira-la-cimera-mundial-del-transport-de-productes-forestals

Querol, X., Massagué, J., Alastuey, A., Moreno, T., Gangoiti, G., Mantilla, E., Duéguez, J. J., Escudero, M., Monfort, E., Pérez García-Pando, C., Petetin, H., Jorba, O., Vázquez, V., de la Rosa, J., Campos, A., Muñóz, A., Monge, S., Hervás, M., Javato, R., Cornide, M. J. (2021). Lessons from the COVID-19 air pollution decrease in Spain: now what?. *Science of The Total Environment, 779*, 146380. https://doi.org/10.1016/j.scitotenv.2021.146380

Querol, X., Gangoiti, G., Mantilla, E., Alastuey, A., Minguillón, M. C., Amato, F., Reche, C., Viana, M., Moreno, T., Karanasiou, A., Rivas, I., Pérez, N., Ripoll, A., Brines, M., Ealo, M., Pandolfi, M., Lee, H., Eun, H., Ahn, K. H. (2017). Phenomenology of high-ozone episodes in NE Spain. *Atmospheric Chemistry and Physics, 17*(4), 2817-2838. https://doi.org/10.5194/acp-17-2817-2017

Querol, X., Alastuey, A., Reche, C., Orio, A., Pallares, M., Reina, F., Dieguez, J. J., Mantilla, E., Escudero, M., Alonso, L., Gangoiti, G., Millán, M. (2016). On the origin of the highest ozone episodes in Spain. *Science of the Total Environment, 572,* 379-389. https://doi.org/10.1016/j.scitotenv.2016.07.193

R Core Team (2021). R: A language and environment for statistical computing. R Foundation for Statistical Computing, Vienna, Austria. URL https://www.R-project.org/

RStudio Team (2020). RStudio: Integrated Development for R. RStudio, PBC, Boston, MA URL http://www.rstudio.com/

Rodriguez-Rey, D., Guevara, M., Armengol, J. M., Criado, A., Enciso, S., Tena, C., Benavides, J., Soret, A., Jorba, O., and Pérez García-Pando, C. (2023). Challenges for achieving clean air-The case of Barcelona (Spain) (No. EGU23-14487). Copernicus Meetings. https://doi.org/10.5194/egusphere-egu23-14487

Rodriguez-Rey, D., Guevara, M., Linares, M. P., Casanovas, J., Armengol, J. M., Benavides, J., Soret, A., Jorba, O., Tena, C., and Pérez García-Pando, C. (2022). To what extent the traffic restriction policies applied in Barcelona city can improve its air quality?. *Science of the Total Environment*, *807*, 150743. https://doi.org/10.1016/j.scitotenv.2021.150743

Rodriguez-Rey, D., Guevara, M., Linares, M. P., Casanovas, J., Salmerón, J., Soret, A., Jorba, O., Tena, C., and Pérez García-Pando, C. (2021). A coupled macroscopic traffic and pollutant emission modelling system for Barcelona. *Transportation Research Part D: Transport and Environment, 92*, 102725. https://doi.org/10.1016/j.trd.2021.102725

Rovira, J., Nadal, M., Schuhmacher, M., and Domingo, J. L. (2021). Environmental impact and human health risks of air pollutants near a large chemical/petrochemical complex: Case study in Tarragona, Spain. *Science of the Total Environment, 787,* 147550. https://doi.org/10.1016/j.scitotenv.2021.147550

Servei Meteorològic de Catalunya (2023a). *Històric de mapes de temperatura estacional.* Retrieved 26 May, 2023, from https://www.meteo.cat/wpweb/climatologia/butlletins-i-episodis-meteorologics/historic-de-cartografia-climatica/historic-de-mapes-de-temperatura-estacional/

Servei Meteorològic de Catalunya (2023b). *Mapa d'estacions automàtiques*. Retrieved 21 June, 2023, from https://www.meteo.cat/observacions/xema?dia=2019-06-29T00:00Z

Servei Meteorològic de Catalunya (2022a). *Butlletí anual d'indicadors climàtics.* Equip de Canvi Climàtic, Àrea de Climatologia. Retrieved 26 May, 2023, from https://static-m.meteo.cat/wordpressweb/wp-content/uploads/2023/04/06114859/BAIC-2021-2.pdf

Servei Meteorològic de Catalunya (2022b). *Evolució de la temperatura: la temperatura al conjunt de Catalunya.* Retrieved 26 May, 2023, from https://www.meteo.cat/wpweb/climatologia/evolucio-observada-del-clima/evolucio-observada-de-la-temperatura/

Servei Meteorològic de Catalunya (2021a). *Butlletí anual d'indicadors climàtics.* Equip de Canvi Climàtic, Àrea de Climatologia. Retrieved 26 May, 2023, from https://static-m.meteo.cat/wordpressweb/wp-content/uploads/2022/02/22062715/BAIC_2020_v2.pdf

Servei Meteorològic de Catalunya (2021b). *Butlletí climàtic anual del 2019.* Retrieved 16 May, 2023, from https://static-m.meteo.cat/wordpressweb/wp-content/uploads/2021/04/15125638/Butllet%C3%AD-clim%C3%A0tic-2019-v3.pdf

Servei Meteorològic de Catalunya (2021c). *La temperatura al conjunt de Catalunya.* Retrieved 30 May, 2023, from https://www.meteo.cat/wpweb/climatologia/evolucio-observada-del-clima/evolucio-observada-de-la-temperatura/

Servei Meteorològic de Catalunya (2013). *10 anys del tòrrid estiu del 2003.* Retrieved 16 May, 2023, from https://www.meteo.cat/wpweb/divulgacio/publicacions/efemerides/2003-06-01_10-anys-del-torrid-estiu-del-2003/

Servei Meteorològic de Catalunya (2011). *Butlletí climàtic de l'any 2010.* Retrieved 26 May, 2023, from https://static-m.meteo.cat/wordpressweb/wp-content/uploads/2014/11/18075144/Butlleti_climatic_2010.pdf

Sicard, P. (2021). Ground-level ozone over time: an observation-based global overview. *Current Opinion in Environmental Science & Health, 19*, 100226. https://doi.org/10.1016/j.coesh.2020.100226

Sicard, P., Paoletti, E., Agathokleous, E., Araminienė, V., Proietti, C., Coulibaly, F., and De Marco, A. (2020). Ozone weekend effect in cities: Deep insights for urban air pollution control. *Environmental Research, 191*, 110193. https://doi.org/10.1016/j.envres.2020.110193

Skamarock, W.C. and Klemp, J.B. (2008). A time-split nonhydrostatic atmospheric model for weather research and forecasting applications. *Journal of computational physics, 227*(7), 3465–3485. https://doi.org/10.1016/j.jcp.2007.01.037

Soret, A., Serradell, K., Guevara, M., Pérez García-Pando, C., Olid, M., Mateu, J., ... and Jorba, O. (2022). Status and Future Vision of the CALIOPE Air Quality Forecasting System: Support for Air Quality Policies. In *International Technical Meeting on Air Pollution Modelling and its Application* (pp. 167-174). Cham: Springer International Publishing. https://doi.org/10.1007/978-3-031-12786-1_23

Spada, M. (2015). Development and evaluation of an atmospheric aerosol module implemented within the NMMB/BSC-CTM, Ph.D. thesis, Universitat Politècnica de Catalunya, 2015. Retrieved from http://hdl.handle.net/2117/95991

Talent (2023). *Salario medio para Ingeniero Junior en España, 2023.* Retrieved 7 September, 2023, from https://es.talent.com/salary?job=ingeniero+junior

Tobías, A., Carnerero, C., Reche, C., Massagué, J., Via, M., Minguillón, M. C., Alastuey, A., and Querol, X. (2020). Changes in air quality during the lockdown in Barcelona (Spain) one month into the SARS-CoV-2 epidemic. *Science of the total environment, 726*, 138540. https://doi.org/10.1016/j.scitotenv.2020.138540

Turnock, S. T., Wild, O., Dentener, F. J., Davila, Y., Emmons, L. K., Flemming, J., ... and O'Connor, F. M. (2018). The impact of future emission policies on tropospheric ozone using a parameterised approach. *Atmospheric Chemistry and Physics, 18*(12), 8953-8978. https://doi.org/10.5194/acp-18-8953-2018

United Nations Economic Comission for Europe, 1979. *1979 Convention on Long-range Transboundary Air Pollution.* Retrieved 27 July, 2023, from https://unece.org/sites/default/files/2021-05/1979%20CLRTAP.e.pdf

Valverde, V., Pay, M. T., and Baldasano, J. M. (2016). Ozone attributed to Madrid and Barcelona on-road transport emissions: Characterization of plume dynamics over the Iberian Peninsula. *Science of the total environment, 543*, 670-682. http://dx.doi.org/10.1016/j.scitotenv.2015.11.070

Wetterzentrale (2023). *GFS. Maps based on Global Forecast System of the US weather service.* Retrieved 21 June, 2023, from https://www.wetterzentrale.de/de/topkarten.php?model=gfs&lid=OP

World Health Organisation (2022). *Billions of people still breathe unhealthy air: new WHO data.* Retrieved 14 August, 2023, from https://www.who.int/news/item/04-04-2022-billions-of-people-still-breathe-unhealthy-air-new-who-data

World Health Organisation (2021). *WHO global air quality guidelines: particulate matter (PM2.5 and PM10), ozone, nitrogen dioxide, sulfur dioxide and carbon monoxide.* https://www.who.int/publications/i/item/9789240034228

Ziemke, J. R., Kramarova, N. A., Frith, S. M., Huang, L. K., Haffner, D. P., Wargan, K., Lamsal, L. N., Labow, G. J., McPeters, R. D., and Bhartia, P. K. (2022). NASA Satellite Measurements Show Global-Scale Reductions in Free Tropospheric Ozone in 2020 and Again in 2021 During COVID-19. *Geophysical Research Letters, 49*(15), e2022GL098712. https://doi.org/10.1029/2022GL098712